SISSA, International School for Advanced Studies

PhD course in Statistical Physics

Academic Year 2011/2012

Superfluidity and localization in Bosonic glasses

Thesis submitted for the degree of

Doctor Philosophiae

Advisor:
Prof. Markus Müller

Candidate:
Xiaoquan Yu

November 20th, 2012

Contents

Chapter 1

Introduction

Disorder plays an important role in condensed matter systems. Since in practice impurities or defects are unavoidable, there are no perfect crystals in Nature. When the concentration of impurities is high, we have to face completely new situations, in the sense that the usual descriptions based on translational invariance break down.

A typical example of a disordered system is given by free electrons in a disordered potential. In a perfect crystal, free electrons are described by Bloch waves which extend through the whole crystal. When the disorder is weak, random scatterings on the impurities lead to diffusive behavior of electrons. Once the the mean free path l (the distance between two successive collisions with impurities) becomes shorter than the wavelength λ of the electron, transport breaks down and the electron wavefunctions get localized in real space. The existence of such a localized state in the disordered free fermions system was first predicted by Anderson [1]. The properties of such systems were extensively studied and are a well understood subject [2, 3, 4].

In high enough dimensions the single particle eigenfunctions undergo the Anderson localization transition from a metallic to an insulating phase upon increasing the disorder [1]. Recently, the question of what happens in such systems upon addition of weak repulsive short range interactions has attracted a lot of renewed interest. It is believed that 'many body'-localized phases with no intrinsic diffusion and transport may exist in sufficiently strong disorder, despite the presence of interactions [5, 6], which are commonly thought to induce thermalization in many body systems.

Among the simplest disordered and interacting systems are disordered boson systems. Studies of localization properties in disordered bosonic systems have less of a long history, despite the fact that Anderson's original work was actually motivated by the apparent absence of diffusion in (bosonic) spin systems. First interest in the question arose when Giamarchi and Schultz [7] showed that bosons in 1d can undergo a delocalization transition (unlike fermions). The notion of a transition between "Bose glasses" (insulating, disordered states of bosons) and superfluids of bosons, driven by disorder was then generalized to higher dimensions by M. P. A. Fisher [8], motivated by experiments by Hebbard and Paalanen [9] on Indium oxide films, which suggested that the SI transition in those systems might be of bosonic nature, i.e., due to the loss of phase coherence of paired electrons, instead of the destruction of pairing amplitude as in the standard BCS mechanism.

More recent realizations of disordered bosons in optical lattices [10, 11, 12] and spin ladders [13] have spurred renewed interest in questions regarding localization of disordered bosonic systems [7, 14, 15, 16, 17, 18], some of which have arisen previously in the context of the above mentioned dirty superconductors [19, 20, 21], or in studies of ^{4}He in porous media [22, 23, 24].

In all these examples, interactions between the bosons are, however, essential to prevent a collapse into the lowest-lying single particle eigenstate. Consequently, the problem of bosonic localization is inherently an interacting problem, which requires a many body approach. However, in contrast to repulsive fermions, bosons can condense into a superfluid state with long range order and perfect transport. Nevertheless, when subjected to too strong disorder, global phase coherence is suppressed and the bosons localize into an insulating Bose glass state [7, 8, 25]. It is intuitive to consider the related disorder-driven quantum phase transition as a kind of "collective boson delocalization" transition, but the precise differences and similarities between this phenomenon and single particle Anderson transition is not well understood [26]. While certain qualitative features may carry over from the single particle case, one should also expect significant differences due to the quantum statistics of repulsive bosons (as opposed to that of non-interacting fermions) and the incipient long range order.

1.1 Main questions addressed in this thesis

1.1.1 Non-frustrated Bose glasses

Bosonic excitations *within* long-range ordered, but strongly inhomogeneous phases have been studied in quite some detail by Chalker and Gurarie [27]. A good part of my thesis focuses instead on understanding the insulating, localized phase of disordered bosonic systems. In particular I study localization properties of strongly interacting bosons and spin systems in a disorder potential at zero temperature. I focus on simple, prototypical spin models (Ising model and XY model) in random fields on a Cayley tree with large connectivity. Regarding the nature of the quantum phase transition in strong disorder I find the following results: i) With a uniformly distributed disorder non-extensive excitations in the disordered phase are all localized. ii)Moreover, I find that the order arises due to a collective condensation, which is qualitatively distinct from a Bose Einstein condensation of single particle excitations into a delocalized state. In particular, in non-frustrated Bose glasses, I do not find evidence for a boson mobility edge in the Bose glass. These results are qualitatively different from claims in the recent literatures [28, 29].

Considering that (many body) localization of bosons is a kind of quantum glass transition, it is an interesting question to ask what phenomena occur, if the ingredients for more conventional (classical) glassy physics are added to a disordered bosons system, namely: random, frustrated interactions between the bosons. One can still think about such a system as bosons in a disordered potential, where the disordered potential is, at least partly, self-generated by random frustrated interactions between

the bosons. This question takes us to the study of another type of disordered systems: —glassy systems. Those are typically characterized by low temperature phases with an inhomogeneous density or magnetization pattern, which is extremely long-lived due to the occurrence of non-trivial ergodicity breaking.

1.1.2 Superglasses

Because of the interplay of superfluidity and glassy ordering, such a system of bosons with random and frustrated interactions might in fact exhibit a rather intricate coexistence phase —a superglass phase, which is characterized both by nonvanishing superfluid order and glassy order (an amorphous frozen density pattern).

The question as to the existence of such a phase of coexistence is not just a purely academic question. In recent years, supersolidity in crystalline ^{4}He [23, 30] has been reported. It soon became clear that defects of the crystalline order and amorphous solids sustain more robust supersolidity, spurring the idea that disorder, or even glassy order, may be a crucial element in understanding the superfluid part of those systems [31, 32, 33, 34, 35]. A recent experiment [36] reported indeed that the supersolidity in ^{4}He is accompanied by the onset of very slow glassy relaxation. This suggested that an amorphous glass with a superfluid component is forming, the novel state of matter —sometimes referred to as "superglass". These experimental results have motivated several theoretical investigations into the possibility and nature of such amorphously ordered and yet supersolid systems [37, 38, 39, 40, 41, 42]. These studies also stimulate anew the question of how the delocalization transition in interacting fermionic systems occurs: Is the interacting and disordered metal-insulator transition a single phase transition, or does it split into a glass transition within the metallic phase and a subsequent localization transition [43, 44]? While answers for fermionic systems are very hard to obtain due to the notorious sign problem for Monte Carlo simulations, and due to technical difficulties in analytical appraoches that go beyond mean field theory, that latter question remains open as of now. In contrast the bosonic analogue of the question is amenable to theoretical progress, to which this thesis contributes, especially in Chapter V.

Similar questions as to the coexistence and interplay of glassy density ordering and superfluidity arise in disordered superconducting films, which feature disorder- or field-driven superconductor-to-insulator quantum phase transitions [21]. In several experimental materials, this transition appears to be driven by phase fluctuations of the order parameter rather than by the depairing of electrons, suggesting that the transition can be described in terms of bosonic degrees of freedom only [9]. This had lead to the dirty boson model [8] and the notion of the Bose glass [7], in which disorder and interactions lead to the localization of the bosons, while the system remains compressible [20, 45]. In this context, the term "glass" refers mostly to the amorphous nature of the state rather than to the presence of slow relaxation and out-of equilibrium phenomena. However, if superconductivity develops in a highly disordered environment, such frustration may add in the form of Coulomb interactions between the charged carriers, which may become important, as screening is not very effective. It is well known that in more insulating regimes, strong disorder and Coulomb interactions may

induce a glassy state of electrons (the Coulomb glass) [46, 47, 48]. It is therefore an interesting question whether such glassy effects can persist within the superconducting state of disordered films.

The recent developments in ultra cold atoms [49] open new ways to studying bosonic atoms in the presence of both interactions and disorder. Those can exhibit superfluid or localized, and potentially also glassy phases, especially if the interactions are sufficiently long ranged and frustrated, as is possibly the case for dipolar interactions.

The above motivated my study, reported in Chapter V of such a a random frustrated interacting boson system. I study a solvable model of hard core bosons (pseudospins) subject to disorder and frustrating interactions, as proposed previously in Ref. [39]. This solvable model provides insight into the possibility of coexistence of superfluidity and glassy density order, as well as into the nature of the coexistence phase (the superglass). In particular, for the considered mean field model I prove the existence of a superglass phase. This complements the numerical evidence for such phases provided by quantum Monte Carlo investigations in finite dimensions [39] and on random graphs [40]. Those were, however, limited to finite temperature, and could thus not fully elucidate the structure of the phases at $T = 0$. In contrast, my analytical approach allows one to understand the quantum phase transition between glassy superfluid and insulator, and the non-trivial role played by glassy correlations.

I should point out that the glassy, amorphous supersolid, which the superglass phase constitutes, is quite different from the type of supersolids proposed theoretically in the early seventies [50]. In that scenario the bosons organize spontaneously on a lattice, which breaks translational symmetry, but is incommensurate with the boson density, allowing for vacancies to move through the solid. The model I study considers instead bosons on a predefined lattice, on which an inhomogeneous density pattern establishes within the glass phase.

1.1.3 Frustrated Bose glasses and the mobility edge

When the frustrated interactions are strong enough, the superfluid order may be destroyed. As I will show in a specific meanfield model, this happens within the glass phase of the system, where a disorder induced superfluid-insulator phase transition takes place to give way to a frustrated Bose glass. The glassy background on top of which this happens leads to many interesting phenomena which seem not to have been noticed before. To understand the nature of the glassy superfluid-insulator quantum phase transition at zero temperature and the transport properties on the insulating, Bose glass side of the transition is the goal of the third part of my thesis.

To address the above questions, I studied an exactly solvable model of a glassy superfluid-insulator quantum phase transition on a Bethe lattice geometry with high connectivity. My main results can be summarized as follows: i) I found that the superfluid-insulator transition is significantly shifted to stronger hopping. This is a result of the pseudo gap in the density of states of the glass state, which tends to strongly disfavor the onset of superfluidity. ii) In the glassy insulator, the discrete local energy levels become broadened due to the quantum fluctuations.The level-broadening process appears as a phase transition which has strong similarities with an Anderson

localization transition, and has implications on many body localization. By using the locator expansion for bosons [51] I found that, the glassy insulator has a finite mobility edge for the bosonic excitations, which, however, does not close upon approaching the SI quantum phase transition point. This finding helps to understand the nature of the superfluid-to-frustrated Bose glass transition: the superfluid emerges as a collective phase ordering phenomenon at zero temperature, and not as a condensation in to a single particle delocalized state, in contrast to opposite predictions in the recent literature [28, 29, 52].

The existence of a mobility edge in the insulator suggests the possibility of phononless, activated transport in the bosonic insulator [53], which might be a candidate explanation for the experimentally seen activated transport, which has remained a mystery for a long time.

1.2 The structure of this thesis

The remaining chapters of this thesis are organized as follows: In Chapter II I will review basics of Anderson localization, discussing and reviewing in detail Anderson's original work on localization, as well as single particle localization on the Cayley tree (or Bethe lattice). This will provide important material, especially for Chapters IV and VI. An introduction to spin glasses is the main content of Chapter III, which provides background material to understand the technical and conceptual parts of Chapter V where frustrated bosons will be discussed. Chapters IV, V, and VI contain my three original works: on localization in non-frustrated Bose glasses, a mean field model of superglasses, and the superfluid-insulator transition in this same model of frustrated bosons. I conclude with a summary and discussion in Chapter VII.

Chapter 2

Anderson localization

After a short introduction on Anderson localization, I will review Anderson's original work on localization [1]. This work not only contains many key points and insights about localization, but is also a guide for my research work that I will describe in Chapters IV and VI. At the end of this chapter, I will show an exactly solvable case —Anderson localization on a Bethe lattice. This is also a guide for the studies in Chapters IV and VI, where I will focus on the localization/delocalization properties of bosonic excitations of disorderd interacting bosons on a Bethe lattice.

2.1 Disordered, non-interacting fermions and Anderson localization

In a perfect crystal, free electrons' wave functions extend over the whole crystal due to the discrete translation symmetry. They are described by the Bloch waves. In a disordered material (e.g., due to impurities or defects), we would expect that random scatterings on the impurities lead to diffusive behavior in the electrons' motion, similar to the Brownian motion of classical particles. Upon coarsegraining, the probability density of such an electron at position r and at time $t > 0$ is

$$|\psi(r,t)|^2 = \frac{\exp(-r^2/2Dt)}{(2\pi Dt)^{d/2}} \tag{2.1}$$

with the diffusion coefficient $D = \hbar k_F l/2m$. Here k_F is the Fermi momentum, m is the electron effective mass, and l is the mean free path which is determined by the disorder strength. It is clear that this wave function still extends over the whole crystal. It leads to Drude conductivity according to the Einstein relation:

$$\sigma_0 = e^2 N(E_F) D = \frac{ne^2\tau}{m} = \frac{e^2}{2\pi\hbar} k_F l \tag{2.2}$$

where $N(E_F) = dn/dE$ is the density of states at the Fermi energy, n is the electron density, e is the electron charge, and $\tau = l/v_F = ml/\hbar k_F$ is the mean free time between two successive elastic collisions with impurities.

However, this is valid only when the electron wavelength $\lambda_F = 2\pi/k_F$ is much smaller than the mean free path $l = v_F\tau$, namely

$$k_F l \gg 1; \quad \text{or} \quad E_F\tau \gg 1. \tag{2.3}$$

Once the above condition is violated by strong disorder, namely when $k_F l \leqslant 1$, things will change dramatically, and the above picture breaks down. The diffusion coefficient turns to zero, and transport disappears. The wave function is localized with an exponentially decreasing envelope

$$\psi_{\rm loc}(r) \sim A\exp(-|r - r_a|/\xi), \tag{2.4}$$

where ξ is called localization length. In three dimensions it occurs at sufficiently strong disorder or near the band edges. In one dimension, all states are localized by an arbitrarily weak disorder.

Now let us understand why transport disappears when wave functions are localized. Suppose at $t = 0$ the electron is at the position $r = 0$, namely $\psi(r, t = 0) = \delta_{r,0} = \sum_\alpha c_\alpha\psi^\alpha(r)$, where $\psi^\alpha(r)$ is the eigenstate of the system. At time $t > 0$,

$$\psi(r, t) = \sum_\alpha c_\alpha e^{-iE_\alpha t}\psi^\alpha(r). \tag{2.5}$$

With the Eq. (2.4), it is easy to obtain

$$|\psi(r, t)|^2 \leq e^{-2r/\xi} \quad \text{for} \quad r \gg \xi \tag{2.6}$$

for any t. This implies $D = 0$, and so the conductivity vanishes, too, due to the Einstein relation $\sigma = e^2N(E_F)D$. We can see from Eq. (2.5) that the probability of staying at the initial site (the long time average of $|\psi(0, t)|^2$) is given by $\sum_\alpha |\langle\psi^\alpha|\psi(0)\rangle|^4$. This is often referred to as the "inverse participation ratio" (IPR). With the normalization condition $\sum_\alpha |\langle\psi^\alpha|\psi(0)\rangle|^2 = \sum_\alpha |c_\alpha|^2 = 1$, it is easy to show that IPR $= \sum_\alpha |\langle\psi^\alpha|\psi(0)\rangle|^4 \sim \sum_\alpha 1/\xi^{2d} \sim 1/\xi^d$. Therefore the IPR is a good indicator for localization: IPR$(\psi) > 0$ if $\psi(r)$ is localized and IPR$(\psi) = 0$ [1] if $\psi(r)$ is delocalized.

Whether a state with definite energy is localized or delcoalized is determined by the competition between energy mismatching (due to disorder) and delocalization channels (number of neighbors $\times$ density of states)^2 . In high dimensions (d$>$2), the localization starts from the band edges by turning on the disorder. There exists a critical energy E_c, the mobility edge, which separates the localized states (regime of low density of states) from the extended states (regime of high density of states) (see Fig. 2.1) . The delocalization/localization (Anderson) transition happens in metals when $E_F = E_c$.

We should emphasize that Anderson localization is an effect of quantum interference. The propagation is stopped even in the classically allowed region (see Fig.2.2). For an electron with energy $E > E_0$, the repeated scattering at the disordered potential may eventually lead to a superposition of interfering waves and become localized even if classically it should be extended [3].

[1] For the finite system, this should be proportional to the inverse of the system volume.

[2] This is true only for high dimensions $d > 2$, in low dimensions disorder always wins due to proliferation of weak localization effects.

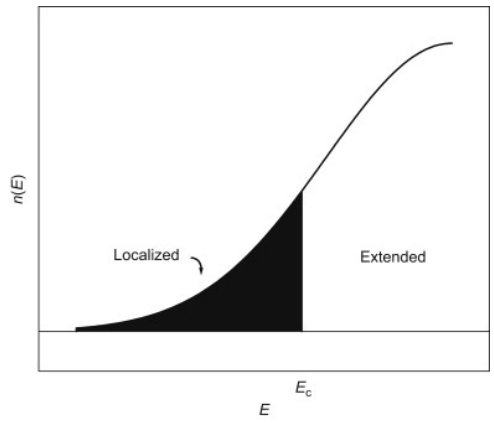

Figure 2.1: The mobility edge separates the localized states from the extended states. If the Fermi energy lies in the region of the localized states, the system is insulating at $T = 0$. If it is in the extended states region, the system is metallic.

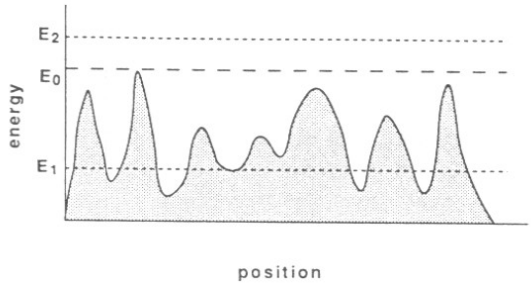

Figure 2.2: Classical particle in a 1D random potential. The motion of the particle is confined to finite intervals for $E_1 < E_0$. For $E_2 > E_0$ the motion is unrestricted.

2.2 Thermally activated conduction in the localized regime

When $E_F < E_c$, the states at the Fermi energy are localized. The conductivity at $T = 0$ is zero. However, at low but finite temperatures the electron can gain thermal energy to perform various transport processes, which we are particularly interested in.

Before discussing these transport behaviors, let us first have a look at several relevant energy scales in the problem. Denoting ν the density of states (DOS) at the Fermi level, the typical energy separation between the localized states inside the localization volume is $\Delta_\xi \sim (\nu\xi^d)^{-1}$ (mean level spacing), where d is the dimension of the system. The corresponding characteristic temperature is $T_0 \sim \Delta_\xi/k_B$. $\tau_\phi \propto T^{-p}$ is the characteristic time between two successive inelastic scatterings (scattering with phnons). By lowering the temperature, we have [54]

(1) Activation to the mobility edge.

$$\sigma \propto e^{-(E_c - E_F)/k_B T}. \tag{2.7}$$

If there is no phonon bath, the conductivity shows simple activated behavior.

2) Activation to a neighboring localized states (phonon assisted processes).

$$\sigma \propto T^p, \tag{2.8}$$

if $\tau_\phi > \xi^2/D$ or $T < T_\xi$, where T_ξ is the crossover temperature such that $\tau_\phi \sim \xi^2/D$, the electron processes a random walk with a step ξ and time τ_ϕ, thus $D \sim \xi^2/\tau_\phi$ and so $\sigma \propto \tau_\phi^{-1} \propto T^p$. The inelastic scattering provides the electron enough energy to move from one block of size ξ to the next, this requires $T > T_0$.

3) Variable range hopping (VRH)(phonon assisted processes).

If $T \ll T_0$, from the energy conservation point of view the electrons are not able to hop inside the localization volume but can hop further (see Fig. 2.3). On the other hand, the overlap matrix element between the states which are far away from each other is exponentially small, $e^{-L/\xi}$, where $L \gg \xi$ is the spatial distance between these states.

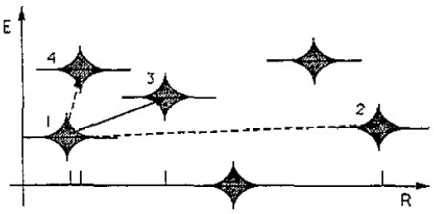

Figure 2.3: Hopping between states localized at different sites R. States that are inside the localization volume (1 and 4) are separated by Δ_ξ. On the other hand, states at almost the same energies are far from each other in real space.

The energy needed now, Δ_L, is obtained as

$$\Delta_L \sim (\nu L^d)^{-1} \sim \Delta_\xi (\xi/L)^d \quad (L \gg \xi). \tag{2.9}$$

Therefore the hopping over a length L is controlled by $e^{-2L/\xi} e^{-\Delta_L/k_B T}$, where the Boltzmann factor $e^{-\Delta_L/k_B T}$ comes from the exponentially small occupation number of bosonic bath modes (phonons). The optimal L for such jumps is given by minimizing the exponent

$$L_{\rm opt} \sim \left(\frac{\xi}{\nu k_B T}\right)^{1/(d+1)}. \tag{2.10}$$

This mechanism is relevant as long as $L_{\rm opt} > \xi$. That is when the temperature is low enough so that $T \ll T_0$. At such low temperatures, the VRH conductivity is given by[3]

$$\sigma \propto e^{-C(T_0/T)^{1/(d+1)}}. \tag{2.11}$$

[3]If Coulomb interactions are taken into account, due to the Coulomb gap in the DOS, the exponent changes from $1/(d+1)$ to $1/2$ [55].

2.3 Anderson's reasoning for localization

Consider spinless non-interacting fermions in a disorder potential

$$H = \sum_i \epsilon_i n_i - \sum_{\langle ij \rangle} V_{ij} \left(c_i^\dagger c_j + c_j^\dagger c_i \right), \tag{2.12}$$

where ϵ_i is a random onsite potential, V_{ij} is the hopping strength and $\langle ... \rangle$ means nearest neighbor pairs. For simplicity we assume the site energies $\{\epsilon_i\}$ are uniformly distributed in the range from $-W/2$ to $W/2$. The operators c_i ($c_i^\dagger$) create or annihilate a fermion at the lattice site i.

Anderson studied this problem by considering a large value of W/V_{ij}, and analyzing how much the ratio could be reduced before the localized states became unstable. The instability of the localized states was argued for via the failure of a perturbation series in powers of V_{ij}/W to converge.

Consider the zero temperature retarded Green's function

$$G_{ik}(t) = -i\Theta(t)\langle \mathrm{GS}|\{c_i(t), c_k^\dagger\}|\mathrm{GS}\rangle, \tag{2.13}$$

where $|\mathrm{GS}\rangle$ is the ground state of the Hamiltonian (2.12) and $c_i(t) = e^{iHt} c_i e^{-iHt}$. Note that $G_{ik}(t = 0^+) = -i\delta_{ik}$, which means that at $t = 0$ the electron (wave function) is localized at site i. We now ask how the wave function varies with time. In particular, we are interested in the behavior as $t \to \infty$. This requires us to study the time evolution of the Green's function $G_{ik}(t)$:

$$i\frac{dG_{ik}(t)}{dt} = \delta(t)\langle \mathrm{GS}|\{c_i(t), c_k^\dagger\}|\mathrm{GS}\rangle - i\Theta(t)\langle \mathrm{GS}|\{i\dot{c}_i(t), c_k^\dagger\}|\mathrm{GS}\rangle \tag{2.14}$$

with

$$i\dot{c}_i(t) = [c_i(t), H] = \epsilon_i c_i - \sum_{j \neq i} V_{ij} c_j. \tag{2.15}$$

We study the Fourier transformation of the Eq. (2.14). Let

$$G_{ik}(E) = \int_{-\infty}^{\infty} dt G_{ik}(t) \exp\left[i(E + i\epsilon)t\right] \quad \text{with} \quad \epsilon \to 0^+. \tag{2.16}$$

Plugging it into Eq.(2.14) we have

$$G_{ik}(E) \;=\; \frac{\delta_{ik}}{E - \epsilon_i + i\epsilon} - \sum_j \frac{V_{ij}}{E - \epsilon_i + i\epsilon} G_{jk}. \tag{2.17}$$

This equation can be solved formally by iteration, namely

$$
\begin{aligned}
G_{ik}(E) = \frac{\delta_{ik}}{E-\epsilon_i+i\epsilon} &- \sum_j \frac{V_{ij}}{E-\epsilon_i+i\epsilon} G_{jk} \\
= \frac{\delta_{ik}}{E-\epsilon_i+i\epsilon} &- \sum_j \frac{V_{ij}\delta_{jk}}{(E-\epsilon_i+i\epsilon)(E-\epsilon_j+i\epsilon)} \\
&+ \sum_{j,l} \frac{V_{ij}V_{jl}}{(E-\epsilon_i+i\epsilon)(E-\epsilon_j+i\epsilon)} G_{lk} \quad \text{etc.} \qquad (2.18)
\end{aligned}
$$

where $\frac{\delta_{ik}}{E-\epsilon_i+i\epsilon}$ is the bare propagator.

The the local Green's function

$$
G_{ii}(E) = \left[E - \epsilon_i - S_i(E)\right]^{-1}, \qquad (2.19)
$$

where we have defined the local self-energy

$$
S_i(E) = \sum_{j\neq i} V_{ij} \frac{1}{E-\epsilon_j+i\epsilon} V_{ji} + \sum_{j,l\neq i} V_{ij} \frac{1}{E-\epsilon_j+i\epsilon} V_{jl} \frac{1}{E-\epsilon_l+i\epsilon} V_{li} + ... \qquad (2.20)
$$

Since $V_{ij}/W \ll 1$, we study the leading order term

$$
\begin{aligned}
S_i^{(1)}(E) &= \sum_{j\neq i} \frac{V_{ij}^2}{E-\epsilon_j+i\epsilon} \\
&= \sum_{j\neq i,\epsilon_j\neq E} \frac{V_{ij}^2}{E-\epsilon_j} - i\pi \sum_{j\neq i,\epsilon_j=E} \delta(E-\epsilon_j) V_{ij}^2 - i\epsilon \sum_{j\neq i,\epsilon_j\neq E} \frac{V_{ij}^2}{(E-\epsilon_j)^2} \\
&= \Delta E^{(2)} - \frac{i}{\tau} - i\epsilon k_i^{(1)}, \qquad (2.21)
\end{aligned}
$$

where $\Delta E^{(2)} = \sum_{j\neq i,\epsilon_j\neq E} \frac{V_{ij}^2}{E-\epsilon_j}$ is the second order perturbation correction of the energy, $1/\tau = \pi \sum_{\epsilon_j=E} \delta(E-\epsilon_j) V_{ij}^2$ is the decay rate which controls the state of perturbed energy $E + \Delta E^{(2)}$ decaying at a rate $e^{-t/\tau}$, and $k_i^{(1)} = \sum_{j\neq i,\epsilon_j\neq E} \frac{V_{ij}^2}{(E-\epsilon_j)^2}$.

If τ were finite, the state of energy $E + \Delta E^{(2)} \sim E$ at site i would simply decay exponentially in time. However, a simple consideration shows [4] that $1/\tau = 0$ for the short range hopping ($V_{ij} \sim 1/r_{ij}^{\alpha}$ with $\alpha > d$). In this case, $k_i^{(1)}$ becomes important in Eq. (2.21). It can be shown that for the short range hopping $k_i^{(1)} = \sum_{j\neq i,\epsilon_j\neq E} \frac{V_{ij}^2}{(E-\epsilon_j)^2}$ converges in the sense that the probability distribution of $k_i^{(1)}$ has a distribution with a finite most probable value [1]. So $\mathrm{Im}S_i^{(1)}(E) = -\epsilon k_i^{(1)} \to 0$ as $\epsilon \to 0$. Thus, if delocalization is to appear it must arise from higher order terms. It turns out that

[4] Denoting the average level distance in the volume R_{hop}^d by $\Delta\epsilon$ and the density of states by ν, we have $\Delta\epsilon = \frac{1}{\nu R_{hop}^d}$ and so $R_{hop} \sim \frac{1}{(\Delta\epsilon)^{1/d}}$. Then the effective hopping $V_{hop} \sim \frac{1}{R_{hop}^{\alpha}} \sim (\Delta\epsilon)^{\alpha/d} \ll \Delta\epsilon$ if $\alpha > d$.

Anderson has explained somewhere else that for any finite order perturbation k_i always converges. Therefore we have to study the whole series:

$$\begin{aligned} S_i(E) &= \Delta E_i - i\epsilon k_i \\ &= \left(\sum_{j \neq i, \epsilon_j \neq E} \frac{V_{ij}^2}{E - \epsilon_j} + ... \right) - i\epsilon \left(\sum_{j \neq i, \epsilon_j \neq E} \frac{V_{ij}^2}{(E - \epsilon_j)^2} + ... \right). \end{aligned} \tag{2.22}$$

Note that the terms containing δ functions which require exact energy conservation occur with vanishing probability in a discrete energy system. If the perturbation expansion $S_i(E)$ converges, k_i must converge as well. Then $\mathrm{Im}S_i(E) = -\epsilon k_i \to 0$ as $\epsilon \to 0$. Thus delocalization, i.e. the emergence of a finite decay rate can come about only through a divergence of the whole series for $S_i(E)$. The non-convergence of $S_i(E)$ then leaves open the possibility that k_i diverges[5] . In this case, it may happen that

$$\lim_{\epsilon \to 0} \mathrm{Im}S_i(E) = \lim_{\epsilon \to 0} -\epsilon k_i = \text{a finite value.} \tag{2.23}$$

The complete series for $S_i(E)$ is given by the sum of the contributions from all paths which start from the site i and return to it without passing through i at any intermediate stage. This perturbation series breaks down if there are paths which repeatedly visit a site with energy arbitrarily close to E, so that the denominators are very small. For instance, if ϵ_j is very close to E, such a term $\left(\frac{V_{jl}}{E-\epsilon_j} \frac{V_{lj}}{E-\epsilon_l} \right)^n > 1$ would be very large for $n \gg 1$ (see Fig. 2.4). However, this problem does not really indicate a breakdown of the localized state yet. Rather it reflects that this kind of series diverges whenever the energy level under consideration attempts to cross another level as V is varied. This must happen frequently if there are many close levels in a system [2] .

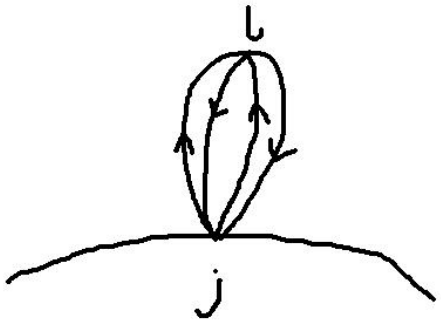

Figure 2.4: Sketch of repeated paths between site j and l.

[5]The divergence of the series is promoted especially by energy resonances. Resonances are on site energies ϵ_j close to the energy E. As one can see, k_i is more singular than ΔE_i when a resonance occurs.

The way out from this problematics consists in taking into account the repeated paths self-consistently. This leads to a renormalized perturbation theory [56, 57]. In this theory the sum over paths is restricted to those nonrepeating paths which do not pass through the same site more than once. Thus, we have (see Fig. 2.5)

$$\begin{aligned} S_i(E) = \quad & \sum_{j\neq i} V_{ij}\{E-\epsilon_j - S_j^{(i)}(E)\}^{-1}V_{ji} - \sum_{j\neq i}\sum_{k\neq i,j} V_{ik}\{E-\epsilon_k - S_k^{(ij)}(E)\}^{-1} \\ & \times V_{kj}\{E-\epsilon_j - S_j^{(i)}(E)\}^{-1}V_{ji} + \sum_{j\neq i}\sum_{k\neq i}\sum_{l\neq i,j,k} V_{il}\{E-\epsilon_l - S_{ijk}^{(l)}(E)\}^{-1}V_{lk}... \end{aligned} \tag{2.24}$$

where the energy denominator is changed from $E-\epsilon_i$ to $E-\epsilon_i - S_i^{(...)}$ and the self energy $S_i^{(...)}$ is defined in terms of noninteracting paths that do not pass through any of the sites (...) already visited. For example

$$S_j^{(i)} = \sum_{k\neq i,j} V_{jk}\{E-\epsilon_k - S_k^{(ij)}(E)\}^{-1}V_{kj} - \sum_{k\neq i,j}\sum_{l\neq i,j,k} V_{il}... \tag{2.25}$$

Anderson's analysis was based on a study of the probability distribution of the individual terms of the series (2.24). The number of nonrepeating paths which return to their starting point after L steps is of order K^L. K is the connective constant and $Z-2 < K < Z-1$, where Z is the number of nearest neighbors. The main assumption underlying his argument is: Each of the K^L paths of length L from a point makes a contribution which is statistically independent of the other contributions [6] .

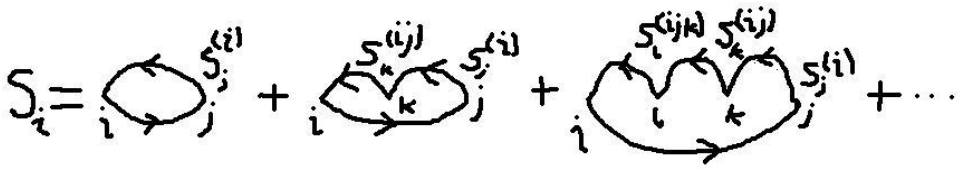

Figure 2.5: Sketch of the series expansion of the self-energy on site i. Each term can be interpreted as a loop with fixed starting point and ending point. S_i is then just a sum of all these paths/loops.

[7] For simplicity we choose $W=2$ and $V_{ij}=V$. We consider the Lth term in the perturbation series for $S_i(E=0)$[8]. This is a sum of approximately K^L terms, each of which is of the form

[6] This assumption was criticized by Thouless [58] and many other people, see the review paper by Thouless [2] and also the references therein. Because different paths may have sites in common, it is certainly not so that all paths are statistically independent. Here we just treat this assumption as an approximation.

[7] In the following I will closely follow the arguments of the review by Thouless [58].

[8] The reason for choosing the band center is to find the convergence limit of the series for $S_i(E)$. Since the density of states has the highest value in the band center, the states there are most prone to become unstable as the hopping V is increased.

$$V^{L+1}\prod_{i=1}^{L}\left(\frac{1}{e_i}\right), \tag{2.26}$$

where $e_i \equiv E-\epsilon_i - S_i^{(\ldots)}$, then e_1, for instance, is given by $e_1 = E-\epsilon_1 - S_1^{(0)}$. Suppose that the self energy $S_i^{(\ldots)}$ is small, then the locators $1/e_i$ in the product are nearly independent of one another[9], and the distribution of e_i can be approximated as the same as ϵ_i's.

The probability for $l = \log(1/|e_i|)$ is $\exp(-l)$ [10] . So the probability density for $y = \sum_{i=1}^{L}\log(1/|e_i|)$ is easy to obtain by considering the Laplace transform

$$f(s) = \int_0^\infty P(y)\exp(-ys)dy = \prod_{i=1}^{L}\left[\int_0^\infty P(l)\exp(-ls)dl\right] = \frac{1}{(s+1)^L}. \tag{2.27}$$

Then we have

$$P(y) = \frac{1}{2\pi i}\int_{-i\infty}^{i\infty} f(s)\exp(ys)ds = \frac{1}{(L-1)!}y^{L-1}\exp(-y). \tag{2.28}$$

Therefore the probability density for

$$|x| = \left|\prod_{i=1}^{L}\left(\frac{1}{e_i}\right)\right| \tag{2.29}$$

is

$$P(x) = \frac{1}{(L-1)!}\frac{1}{x^2}\left(\log|x|\right)^{L-1} \quad \text{for} \quad |x|>1. \tag{2.30}$$

Note that this probability distribution has a long tail, so that the first moment $\langle x\rangle$ and the second moment $\langle(x-\langle x\rangle)^2\rangle$ do not exist. Assuming that all the K^L terms are independent, the sum of a number of terms of this sort, where the individual terms have a long-tailed distributed function, is dominated by the largest term in this sum [11]. If the K^L terms are independent, the probability that $|x|$ is less than X for all the terms is

[9] This is not precise, we will come back to this point later.

[10] Suppose x is uniformly distributed in the range $[0,1]$ and $y = \log\left(\frac{1}{x}\right)$. The probability that y is less than Y is $P(y<Y) = \int_{-\infty}^{Y}P(y)dy = P(x>e^{-Y}) = \int_{e^{-Y}}^{1}P(x)dx = 1-e^{-Y}$. So the probability density is $P(y) = e^{-y}$.

[11] Consider the sum of independent and identically distributed variables $S_N = \sum_i^N X_i$. Suppose $\langle x\rangle = \infty$ and $\langle(x-\langle x\rangle)^2\rangle = \infty$, which occurs, e.g., if $P(x)\sim 1/x^{\alpha+1}$ for $x\gg 1$, with $\alpha\leq 1$. The sum is dominated by the largest term in the sum. In this case the sum of N elements grows faster than N. This can only occur if the sum is dominated by the largest element which is itself of order $x_{\max}\sim N^{1/\alpha}$ [59].

$$\left(1-\int_X^\infty P(x)dx\right)^{K^L} \tag{2.31}$$

and so the probability density is

$$K^L P(X)\left(1-\int_X^\infty P(x)dx\right)^{K^L-1} \simeq K^L P(X), \tag{2.32}$$

where the last step is obtained by considering $K^L\int_X^\infty P(x)dx$ is small, since we focus on the tail of this distribution.

Finally, it has to be shown that the series whose terms are given by the equation (2.26) has high probability of being bounded by a certain geometric series. The probability that the Lth order term will exceed $V^{L+1}x^{L-1}$[12] is approximately

$$\begin{aligned} P\left(\text{the } L\text{th order term} > V^{L+1}x^{L-1}\right) &= K^L\int_{x^{L-1}}^\infty P(x')dx' \\ &= \frac{1}{(L-1)!}\frac{K^L}{x^{L-1}}\left[(L-1)\log x\right]^{L-1} \\ &\simeq \left(\frac{eK\log x}{x}\right)^{L-1}\frac{K}{\sqrt{L-1}}. \end{aligned} \tag{2.33}$$

The probability that none of the terms beyond the Nth one exceed $V^{L+1}x^{L-1}$ is

$$\prod_{L=N+1}^\infty\left\{1-\left(\frac{eK\log x}{x}\right)^{L-1}\frac{K}{\sqrt{L-1}}\right\}. \tag{2.34}$$

This tends to unity as $N\to\infty$ provided that

$$\frac{eK\log x}{x} < 1. \tag{2.35}$$

Therefore the series has a high probability to converge if

$$eKV\log\left(\frac{1}{V}\right) < 1. \tag{2.36}$$

By putting back the disorder strength W, we find the condition

$$W > 2eKV\log(W/2V) \tag{2.37}$$

and the critical condition is given by

$$\frac{2eKV_c}{W}\log\left(\frac{W}{2V_c}\right) = 1. \tag{2.38}$$

[12] $\sum_L V^{L+1}x^{L-1}$ converges if $x < \frac{1}{V}$.

Note that this estimation is based on neglecting the correlations among $1/e_i$, and therefore is an upper limit on $(W/V)_c$.

Above we assumed that the locators $1/e_i$ in the product (2.26) are independent of one another by neglecting the self energy $S_i^{(...)}$. However, this is of course not precise. The locators $1/e_i$ in the product have very important correlations. Namely, for instance, suppose the locater $1/e_k^{(ij)}$ in the product

$$V_{ik}\frac{1}{e_k^{(ij)}}V_{kj}\frac{1}{e_j^{(i)}}V_{ji} \tag{2.39}$$

is very large. Then $1/e_j^{(i)} = \left(E-\epsilon_j - S_j^{(i)}\right)^{-1}$ will be very small, because

$$S_j^{(i)} = \sum_{k\neq i,j} V_{jk}\frac{1}{e_k^{(ij)}}V_{kj} - \sum_{k\neq i}\sum_{l\neq i,j,k} V_{il}... \tag{2.40}$$

contains the term $|V_{ij}|^2/e_k^{(ij)}$. So the term $1/e_j^{(i)}$ will compensate the previous large factor. The product (2.26) with correlated terms is very difficlut to deal with. However, Anderson had noticed that the main effect of the self-energy is to reduce the effect of small energy denominators. This can be effectively accounted for by ignoring all denominators e_i less than a certain cut-off value. Apart from that all the terms $1/e_i$ are considered to be independent. Anderson suggested that the cut-off value $\Delta = 4V^2/W$ for $E=0$ [13] . Under this approximation, we modify the uniform distribution to

$$\begin{aligned} P(e_j) &= \frac{1}{W-\Delta}, \quad \frac{\Delta}{2} < |e_j| < \frac{W}{2}; \\ P(e_j) &= 0, \quad |e_j| < \frac{\Delta}{2} \quad \text{or} \quad |e_j| > \frac{W}{2}. \end{aligned} \tag{2.41}$$

In this case, one can obtain the critical condition [1]

$$\frac{4KV_c}{W}\log(W/2V_c) = 1. \tag{2.42}$$

Note that in this case $(W/V)_c$ is smaller than the previous one given by (2.38).

At the end of this section I would like to emphasize an important point. It has been shown that the Lth term in the perturbation series for $S_i(E=0)$ which is the sum of approximately K^L terms is dominated by the largest term in the sum. This means that in this approximation, the main contribution to the self energy, or the decay rate, comes from a single path. Here we want to argue this from the opposite

[13] The idea is the following: in the original term, if $1/e_k^{(ij)}$ is very large, $1/e_j^{(i)}$ will be very small and so $1/e_k^{(ij)} \gg 1/e_j^{(i)}$. In order to capture this effect in the approximated product, we must neglect all the terms which satisfy $2|e_i| < \Delta$. So the condition $1/e_k^{(ij)} \sim 1/e_j^{(i)} \sim e_k^{(ij)}/V^2$ should give a good estimation of Δ. Since $|e_k^{(ij)}|$ can not be larger than $W/2$, namely, $2/W < 1/|e_k^{(ij)}|$, we obtain $2/W < |e_k^{(ij)}|/V^2 < \Delta/(2V^2)$.

side [2]. Suppose every path in the sum has more or less the same weight, then the Lth order term in the perturbation series should therefore have magnitude

$$K^L \left(\frac{V}{E - \tilde{\epsilon}} \right)^L , \tag{2.43}$$

where $E - \tilde{\epsilon}$ is some typical value of the denominator. If E is zero and ϵ is uniformly distributed between $-\frac{W}{2}$ and $\frac{W}{2}$, a typical value of the denominator is its average $\overline{|\epsilon|} = \frac{W}{4}$, and so the condition for the convergence of the series would be

$$W > 4KV. \tag{2.44}$$

From this we can see that the localized states are much less stable according to Anderson's argument (for $K \geq 2$). This suggests that the electrons escape from localized states by particularly favorable paths, rather than by typical paths. One may think that it is a precursor of fractality at the Anderson transition! The similar situation will occur again on the Bathe lattice. It has been pointed out that the fractality appears also in the disorder induced SI transition, which I will discuss in Chapter IV. Further more in Chapter VII, I will discuss the effect of the "Coulomb gap" on the fractality at the SI transition.

2.4 Anderson localization on a Bethe lattice

1D Anderson model (2.12) and the Anderson model on a Bethe lattice can be exactly solved. In this section I will mainly focus on the later case. The Bethe lattice (see Fig.2.6) is characterized by the root i and the connectivity $K = Z - 1$, where Z is the number of nearest neighbors of a given site. There are approximately K^L nonintersecting paths connecting a given site to the sites L steps further down in the tree. On a Bethe lattice, since there are no loops, the only non-repeating path that returns to an initial site is a path of two steps from a site to its neighbor and back, so the second order term in the perturbation series (2.24) is the only term remaining. In this case, the stability of localized states can be examined by looking for a solution of the selfconsistency equation in which $\mathrm{Im}S_i(E)$ is proportional to ϵ. Where such a solution exists the states are localized, and where no such solution exists the states are delocalized [60].

The second order term in the series (2.24) is

$$S_i(E) = \sum_{j \neq i} V_{ij} (E - \epsilon_j - S_j^{(i)}(E))^{-1} V_{ji} \tag{2.45}$$

with

$$S_j^{(i)}(E) = \sum_{k \neq i,j} V_{jk} (E - \epsilon_k - S_k^{(ij)}(E))^{-1} V_{kj}, \text{etc.} \tag{2.46}$$

Notice that $S_k^{(ij)} = S_k^{(j)}$ due to the absence of loops, we consider the equation

$$S_i(E) = \sum_j V_{ij}(E - \epsilon_j - S_j(E))^{-1} V_{ji}. \tag{2.47}$$

The distribution of the self-energy will be treated self-consistently. The probability distribution for S_i generated by the probability distribution for ϵ_j and S_j should reproduce the same distribution as the one for sites on the previous generation on the tree, S_j.

By writing

$$E = R + i\epsilon \quad S_i(R + i\epsilon) = E_i - i\Delta \tag{2.48}$$

with $\epsilon > 0$, we separate Eq.(2.47) into its real part and imaginary part

$$\begin{aligned} E_i &= \sum_j \frac{|V_{ij}|^2 (R - \epsilon_j - E_j)}{(R - \epsilon_j - E_j)^2 + (\epsilon + \Delta_j)^2} \\ \Delta_i &= \sum_j \frac{|V_{ij}|^2 (\epsilon + \Delta_j)}{(R - \epsilon_j - E_j)^2 + (\epsilon + \Delta_j)^2}. \end{aligned} \tag{2.49}$$

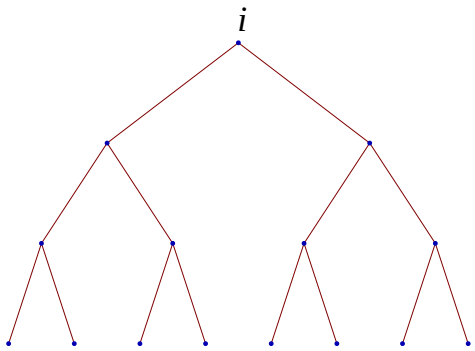

Figure 2.6: A part of a Bethe lattice with connectivity $K = 2$.

We assume the states are localized, so Δ_j should be proportional to ϵ. In the limit of small ϵ, the linearized form of Eqs. (2.49) is

$$\begin{aligned} E_i &= \sum_j \frac{V_{ij}^2}{R - \epsilon_i - E_j}, \\ \Delta_i &= \sum_j \frac{V_{ij}^2 (\epsilon + \Delta_j)}{(R - \epsilon_i - E_j)^2}. \end{aligned} \tag{2.50}$$

Note that the equation for E_i does not involve Δ_i, and the equation for Δ_i is a linear inhomogeneous equation.

An approximation (upper limit) for the stability condition (2.50) can be made by neglecting the real part of the self-energy E_i [14] . And so the equation for the imaginary part of the self energy in this approximation is

$$\Delta_i = \sum_j \frac{V_{ij}^2(\epsilon + \Delta_j)}{(R - \epsilon_i)^2}. \tag{2.51}$$

The Laplace transform of its probability density satisfies the equation

$$f(s) = \left\{ \int dx P(R-x) f\left(\frac{sV^2}{x^2}\right) \exp\left(-\frac{sV^2\epsilon}{x^2}\right) \right\}^K. \tag{2.52}$$

The stability of localized states requires the existence of a solution of this integral equation. If there is a solution, there must be a solution for small s. From Eq.(2.52), it is clear that $f(s=0) = 1$ and $f(s>0) < 1$, so a natural guess of the form of $f(s)$ for small s is

$$f(s) \approx 1 - As^\beta. \tag{2.53}$$

Substitution of this ansatz on the right hand side of the Eq.(2.52) gives

$$\begin{aligned} f(s) &= \{1 - A\int dx P(R-x)\frac{sV^{2\beta}}{x^2\beta}s^\beta + O(s^{1/2})\}^K & (2.54)\\ &= 1 - As^\beta KV^{2\beta}\int dx \frac{P(R-x)}{x^{2\beta}} + O(s^{1/2}, s^{2\beta}) & (2.55) \end{aligned}$$

with β between 0 and 1/2 [15] . Then we obtain

$$KV^{2\beta}\int \frac{P(R-x)}{x^{2\beta}}dx = 1. \tag{2.56}$$

This equation has a solution only for V less than some critical value V_c. V_c can be found by differentiating Eq.(2.56) with respect to β:

$$\log V = KV^{2\beta}\int dx P(R-x)|x|^{-2\beta}\log|x|. \tag{2.57}$$

We consider the center of the band, $R = 0$. The Eqs. (2.56) and (2.57) yield

$$\begin{aligned} \frac{K}{1-2\beta}\left(\frac{2V}{W}\right)^{2\beta} &= 1 \\ \log V = \log\left(\frac{W}{2}\right) - (1-2\beta)^{-1} & \quad (2.58) \end{aligned}$$

[14] The main effect of the real part of the self energy is to reduce the effect of small denominators as we have argued in the previous section. Here this can be traced precisely in principle.

[15] This means the probability distribution for very large Δ_i is $P(\Delta_i) \sim |\Delta_i|^{-\alpha}$ with $1 < \alpha < 3/2$, which implies that the average of Δ_i do not exist. This is an indicator of that the delocalization is dominated by rare events. We will come to this point in Chapter IV.

By eliminating β from the equations, we obtain

$$\frac{2eKV_c}{W}\log\left(\frac{W}{2V_c}\right)=1 \tag{2.59}$$

with $\beta_c < 1/2$, which is the same as (2.38). The approach here is rather different from the Anderson's reasoning, where the convergence of the whole series of the self-energy was considered, but gives results very like those of Anderson and the upper limit is just the same. This is not so surprising. Consider the propagation of an electron on the Cayley tree from the root i to the boundary which is L steps further. There are K^L paths connecting the root i to the boundary which can be treated independently. By neglecting the self energy in the locators, the propagator along one of the K^L paths is nothing but $V^{L+1}\prod_{i=1}^{L}\left(\frac{1}{E-\epsilon_i}\right)$ which is one element of the Lth term in the series expansion of the self energy (2.24) . The point is, the assumption that the K^L terms are statistically independent in the Anderson's reasoning is true on the Cayley tree. In Chapter IV I will discuss in detail the propagation of disordered hard-core bosons on a Cayley tree and compare with the results for noninteracting fermions.

In order to restore the effect of the real part of the self energy, we introduce the cut-off $\Delta=\frac{4V^2}{W}$ into the onsite energy distribution:

$$\begin{aligned} P(\epsilon_j) &= \frac{1}{W-\Delta}, \quad \frac{\Delta}{2}<|\epsilon_j|<\frac{W}{2}; \\ P(\epsilon_j) &= 0, \quad |\epsilon_j|<\frac{\Delta}{2} \quad \text{or} \quad |\epsilon_j|>\frac{W}{2}. \end{aligned} \tag{2.60}$$

With this modified distribution, for E in the center of the band, the Eqs. (2.56) and (2.57) give

$$\frac{2KV_c}{W}\log\frac{W^2}{4V^2}=1 \tag{2.61}$$

with $\beta_c = 1/2$ [2].

The probability distributions of the real part and imaginary part of the self energy can be obtained exactly by solving the integral equations about the Fourier transformation of these probability distributions [60]. It turns out that in the exact solution the critical exponent β_c is 1/2 and the critical hopping V_c agrees with the upper limit quite well when the connectivity is large $K >> 1$. The later can be seen from the fact that the cut-off $\Delta=\frac{4V^2}{W}\sim 1/(K\log K)^2$ becomes very small for large K, which means the effect of the real part of the self energy is very weak and so the upper limit is a quite good approximation for large connectivity.

Chapter 3

Spin glasses

In this Chapter, I will give an introduction on spin glasses. As another important type of disordered systems, spin glasses exhibit nontrivial ergodicity breaking and the low temperature phase is rather complex. There are still many open problems in this field. The main topic of this thesis is about disorderd bosons. The simplest model for interacting bosonic systems is the hard-core boson model which is equivalent to the pseudo spin model. A random frustrated hard-core boson system which will be discussed in Chapters V and VI, is nothing but a quantum spin glass. So first of all it is important to understand the basic concepts in classical spin glasses.

3.1 Basic properties of spin glasses

A spin glass is a collection of spins, i.e. magnetic moments, whose low temperature phase is a frozen, but disordered state, rather than the uniform or periodic pattern we usually find in conventional magnets. Two ingredients are necessary to produce such a state. One is frustration, namely no single configuration of spins is uniquely favored by all the interactions due to the competition among them. The other one is that these interactions should be random. Fig. 3.1 shows a cartoon of such a system.

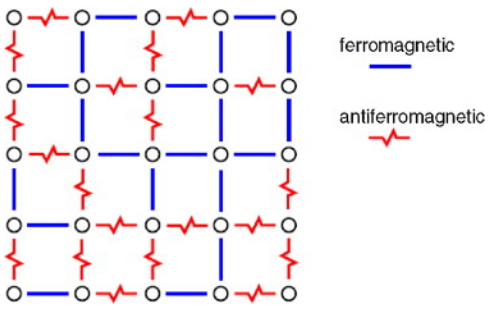

Figure 3.1: Sketch of a random, frustrated spin system with mixed ferromagnetic and antiferromagnetic couplings.

There are many materials that satisfy these requirements. For instance, some metallic materials hosting magnetic impurities located at random positions. Because

each magnetic impurity polarizes the surrounding conduction electrons, the impurities moments interact with each other effectively. It turns out that these induced interactions are oscillating in sign at large distance [1] . Also in some magnetic insulators and amorphous alloys, there exist random, competing interactions [61, 62].

An important question is how to observe such a frozen, but disordered glass state. There are at least two experimental characteristics of spin glasses[2] : 1) A frequency dependent cusp in ac-susceptibility (see Fig. 3.2); 2) A difference between field cooled (FC) and zero field cooled (ZFC) susceptibility (see Fig. 3.4).

The difference between the measured susceptibility and the extrapolation of the high-temperature form indicates that some degrees of freedom are frozen. This effect is known from antiferromagnets (see Fig. 3.3), where a reduction in the susceptibility from its extrapolated high temperature form signals the onset of antiferromagnetic order. In spin glasses, the local spontaneous magnetization $m_i = \langle s_i \rangle$ is nonzero while the average magnetization $N^{-1}\sum_i m_i$, as well as any 'staggered 'magnetization $N^{-1}\sum_i e^{-i\vec{K}\cdot\vec{r}_i} m_i$ vanishes because of the presence of quenched disorder.

The connection between the reduction of the susceptibility and the existence of frozen magnetic moments is the following. Consider the single-site susceptibility

$$\chi_{ii} = \frac{\partial m_i}{\partial h_i} = \beta \left\langle (s_i - \langle s_i \rangle)^2 \right\rangle = \beta(1 - m_i^2). \tag{3.1}$$

Averaging over all the sites in the system gives $\chi_{loc} = N^{-1}\sum_i \chi_{ii} = \beta(1 - q_{\rm EA})$, where

$$q_{\rm EA} \equiv N^{-1} \sum_i m_i^2 \tag{3.2}$$

is the Edwards-Anderson order parameter. It is clear that the onset of the local magnetic order reduces the susceptibility. If $m_i = 0$, Eq. (3.1) recovers the Curie law. So the experiment of Fig. 3.2 really does indicate the existence of a nonzero frozen spontaneous magnetization[3] . Another important feature in this experiment is the frequency dependent freezing temperature T_f, which suggests that the energy landscape of glasses is complex, namely there are many metastable spin configurations with a distribution of energy barriers separating them.

The FC susceptibility is obtained by applying the field above T_c and then subsequently cooling the sample in this field below T_f. The ZFC susceptibility $\chi_{\rm zfc}$ is obtained by cooling the sample below T_f in zero field and then applying the field. If there is only a single phase at low temperature, the two procedures would not yield different results. The difference between FC and zero field cooled ZFC susceptibility in the experiment Fig. 3.4 suggests that there are many states/metalstable states at low temperature. In the field-cooling procedure, since the field is applied at the high

[1] This interaction was first studied by Ruderman and Kittel and latter by Kasuya and Yosida. It is therefore known as the RKKY interaction.

[2] Aging dynamics is of course another very important characteristic of spin glasses. Here we are only focusing on the static, quasi-equilibrium properties of spin glasses.

[3] The experiments do not measure $\chi_{\rm loc}$ but the uniform susceptibility $\chi = N^{-1}\sum_{ij}\chi_{ij}$. If the disorder is not biased, $\overline{\chi}_{i\neq j}$=0. So the uniform χ will have a cusp if χ_{loc} does.

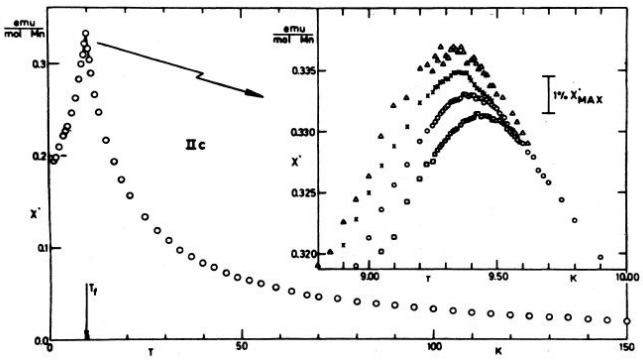

Figure 3.2: Real part of the complex susceptibility $\chi(\omega)$ as a function of temperature. The inset shows the frequency dependence [61, 62].

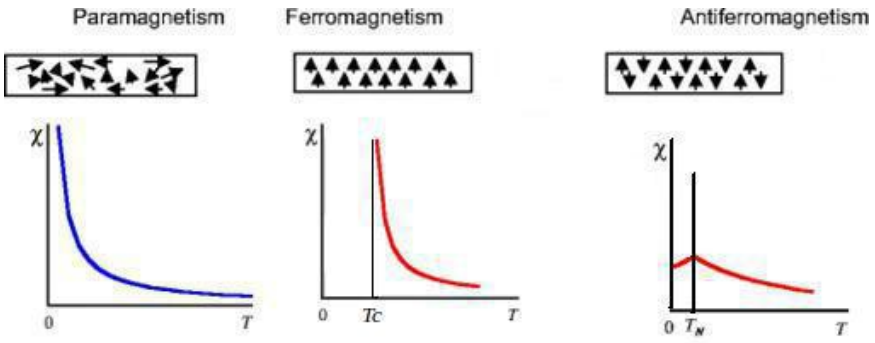

Figure 3.3: Temperature dependence of the magnetic susceptibility of paramagnetic, ferromagnetic, and antiferromagnetic systems. T_c is the Curie temperature, below which the ferromagnetic order emerges. T_N is the Néel temperature, below which the antiferromagnetic order emerges.

temperature, all the states will respond to the field even below the freezing temperature. In the zero-field-cooling procedure, below the freezing temperature T_f, only some of the states can contribute to the field response. So one expects in general that $\chi_{\text{zfc}} < \chi_{\text{fc}}$, which is indeed seen in the experiments, cf. Fig. 3.4.

We have already seen some characteristics of spin glasses which set them apart from conventional magnets. On the other hand, in some aspects, the glass transition behaves like a standard second order phase transition, as it can be characterized by critical exponents and the divergence of certain response functions at the transition point due to onset of infinitely long ranged correlations. However, unlike in ferromagnets, in spin glasses, the linear response does not diverge at the transition point because on average the correlation could not extend so long distance due to the randomness.

Instead the correlation square $\frac{1}{N}\sum_{i\neq j}\overline{\langle s_i s_j\rangle^2}$ could be a relevant quantity which signals that fluctuations of magnetization (instead of expectation values) start proliferating spontaneously. Also this correlation square is related to the higher order response function:

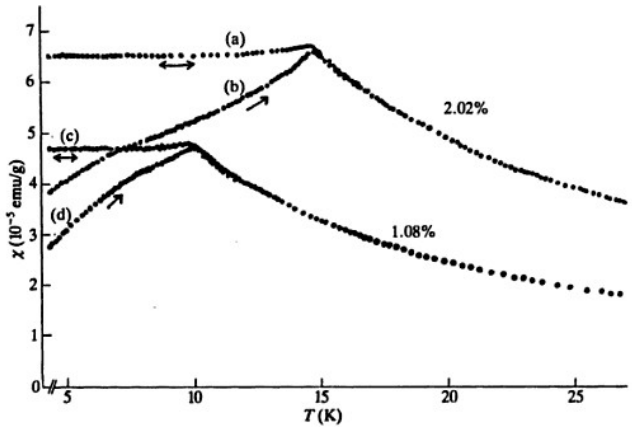

Figure 3.4: After zero-field cooling ($H < 0.05$ Oe), initial susceptibilities (b) and (d) were taken for increasing temperature in a field of $H = 5.90$ Oe. The susceptibility (a) and (c) were obtained in the field $H = 5.90$ Oe, which was applied above T_f before cooling the samples [61].

$$m(h) = \chi h - h^3 \chi_{nl} + o(h^5), \tag{3.3}$$

where χ_{nl} is the non-linear susceptibility. From the fluctuation-dissipation relation we have

$$\begin{aligned} \chi_{nl} = -\frac{\beta^3}{3!N}\left\langle \left(\sum_i s_i\right)^4 \right\rangle_c &= -\frac{\beta^3}{3!}\frac{1}{N}\sum_{ijkl}\left(\langle s_i s_j s_k s_l\rangle - 3\langle s_i s_j\rangle\langle s_k s_l\rangle\right) \\ &= -\frac{\beta^3}{6N}\left(4N - 6\sum_{ij}\langle s_i s_j\rangle^2\right) \\ &= \beta(\chi_{\rm SG} - \frac{2}{3}\beta^2), \end{aligned} \tag{3.4}$$

where $\chi_{\rm SG} \equiv \frac{1}{N}\sum_{i\neq j}\overline{\langle s_i s_j\rangle^2}$. χ_{nl} can be measured in experiments [61], and it turns out that χ_{nl} indeed diverges at $T = T_f$.

Below T_f, it is generally accepted that a spin glass has many metastable states and the low temperature free energy landscape is rather complex (see Fig. 3.5). Next we will review some models which exhibit the freezing transition and complex low temperature phases.

3.2 Fully connected spin glasses models

Some spin glass models with infinitely long range interactions (fully connected) can be solved exactly. For such systems, a thermodynamically stable state is fully characterized by the local magnetizations $\{m_i\}$, where the fluctuation correlations $\langle \delta s_i \delta s_j\rangle = \langle (s_i - m_i)(s_j - m_j)\rangle$ can be neglected in the thermodynamic limit $N \to \infty$.

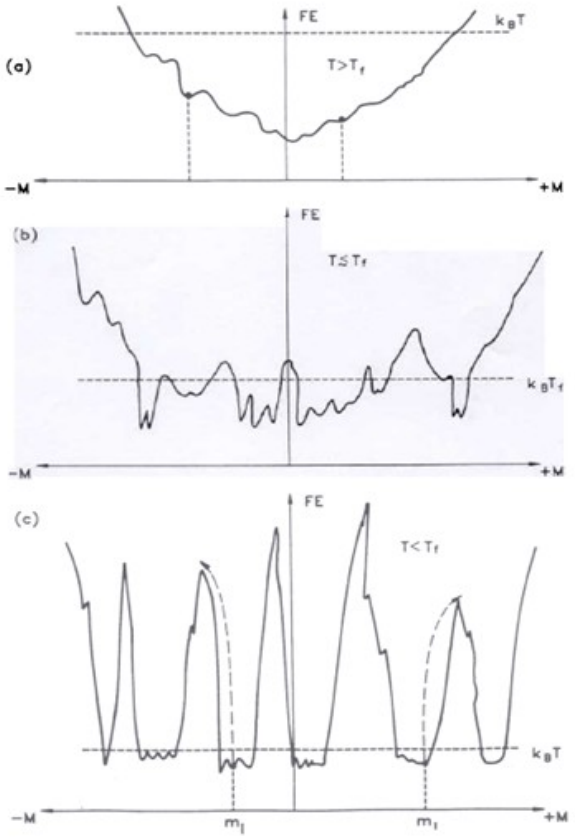

Figure 3.5: Sketch of the multi-valley landscape of free energy as a function of temperature for a spin glass.

A well studied fully connected model is the Sherrington-Kirkpatrick model (SK model) [63]:

$$H = -\frac{1}{2}\sum_{i\neq j} J_{ij}s_i s_j, \tag{3.5}$$

where the random coupling J_{ij} is Gaussian distributed: $P(J_{ij}) = \sqrt{\frac{N}{2\pi J^2}}\exp\left(-\frac{N}{2J^2}J_{ij}^2\right)$ with $\overline{J_{ij}} = 0$ and $\overline{J_{ij}^2} = \frac{J^2}{N}$. The scaling of J_{ij} is chosen such that the Hamiltonian is an extensive quantity in the thermodynamic limit $N \to \infty$. This model exhibits a freezing transition, accompanied by non-trivial ergodicity breaking at low temperature. "Non trivial" here means that there are many phases at low temperature and the ergodicity breaking does not associate with the symmetry spontaneously breaking [4] . This transition can also be seen as a continuous phase transition, in the sense that the order parameter $q_{\rm EA}$ becomes finite in a continuous way upon crossing the transition

[4]For the Ising model (has Z_2 symmetry), there are two ergodicity broken phases at low temperature which are connected by the symmetry group Z_2. The SK model also has the Z_2 symmetry, while the low temperature phases are not connected by Z_2.

point. Moreover, the spin glass susceptibility $\chi_{\rm SG}$ diverges at the transition point. In the Sec. 3.3 and 3.4 we will mainly discuss this model.

Another exactly solvable spin glass model is the p-spin model

$$H = -\sum_{1\le i_1\le i_2..\le i_p\le N} J_{i_1\ldots i_p} s_{i_1}\ldots s_{i_p}, \tag{3.6}$$

where $J_{i_1\ldots i_p}$ is Gaussian random variable with $\overline{J}=0$, and $\overline{J^2_{i_1\ldots i_p}} = \frac{J^2 p!}{2N^{p-1}}$. For $p=2$, this is just the SK model. For $p>2$, this model is more interesting in the context of dynamics [64] which we will not study here. The random energy model is obtained by taking the limit $p\to\infty$ [65].

The random energy model [65] is the simplest spin glass model displaying non-trivial broken ergodicity. We consider the probability distribution of the energy of a spin configuration:

$$P(E) = \overline{\delta\left(E - H[\{s_i\}]\right)}. \tag{3.7}$$

One can easily get the probability distribution of the total energy as a Gaussian:

$$P(E) = \frac{1}{\sqrt{\pi J^2 N}} \exp\left(-\frac{E^2}{NJ^2}\right). \tag{3.8}$$

Then the number of the states with energy E is

$$\langle n(E)\rangle = 2^N P(E) = \frac{1}{\sqrt{\pi J^2 N}} \exp\left[N\left(\log 2 - \left(\frac{E}{NJ}\right)^2\right)\right]. \tag{3.9}$$

For $|E| < E_0 = NJ\sqrt{\log 2}$, there is an exponentially large number of levels, and therefore a finite entropy,

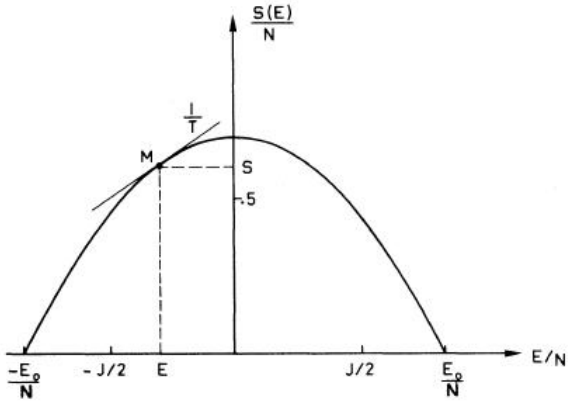

Figure 3.6: Entropy for the random energy model [65].

$$S(E) = \log n(E) = N\left[\log 2 - \left(\frac{E}{NJ}\right)^2\right]\Theta(E_0 - |E|). \tag{3.10}$$

On the other hand, for $|E| > E_0$, there are no levels left in the thermodynamic limit, and therefore no entropy. This situation is illustrated in Fig. 3.6.

Using $T^{-1} = \frac{\partial S}{\partial E}$, one finds the freezing temperature is $T_f = \frac{J}{2\sqrt{\log 2}}$. Below T_f, the entropy vanishes. Physically, it means that the system freezes into the last available state at $|E| = E_0$.

3.3 Thouless-Anderson-Palmer (TAP) equations

For a generic fully connected Ising model

$$H = -\frac{1}{2}\sum_{i\neq j} J_{ij}s_i s_j + \sum_i h_i s_i, \tag{3.11}$$

where h_i is the external magnetic field on site i, the local magnetization m_i can be easily obtained:

$$m_i = \frac{\sum_{\{s_i\}} s_i \exp\left[\beta s_i(y_i + h_i)\right]}{\sum_{\{s_i\}} \exp\left[\beta s_i(y_i + h_i)\right]} = \tanh\left[\beta(y_i + h_i)\right] \tag{3.12}$$

with

$$y_i \;\; = \;\; \sum_j J_{ij} m_j^{(i)}, \tag{3.13}$$

where $m_j^{(i)}$ is the local magnetization on site j in the absence of spin s_i. The shift of the magnetization m_j by adding back the spin s_i is

$$\Delta m_j = m_j - m_j^{(i)} = \chi_{jj} J_{ij} m_i, \tag{3.14}$$

where the local susceptibility

$$\chi_{jj} = \left.\frac{\partial m_j}{\partial h_j}\right|_{h_j=0} = \beta(1 - m_j^2). \tag{3.15}$$

At the end, we obtain

$$y_i = \sum_j J_{ij} m_j - \beta \sum_j J_{ij}^2 (1 - m_j^2) m_i, \tag{3.16}$$

where $\beta \sum_j J_{ij}^2 (1 - m_j^2) m_i$ is called Onsager term.

The Eqs. (3.12) are called Thouless-Anderson-Palmer (TAP) equations [66]. Note that for the fully connected ferromagnetic model where $J_{ij} = J/N$, the Onsager term vanishes for the thermodynamic limit $N \to \infty$. For the SK model where $J_{ij} \sim J/\sqrt{N}$, the Onsager term survives as $N \to \infty$.

3.3.1 High temperature expansion

In this section we derive the TAP equations (3.12) by the high temperature expansion (Georges-Yedidia expansion) [67].

Consider a spins system with an external magnetic field h_i acting on the spin s_i, the free energy is

$$-\beta F[\{h_i\}] = \log \sum_{\{s_i\}} \exp\left(-\beta H[\{s_i\}] + \beta \sum_i h_i s_i\right). \tag{3.17}$$

The local magnetization is

$$m_i[h] = \langle s_i \rangle_h = -\frac{\partial F[\{h_i\}]}{\partial h_i} \tag{3.18}$$

and the susceptibility is

$$\chi_{ij} = \frac{\partial m_i}{\partial h_j} = -\frac{\partial^2 F[\{h_i\}]}{\partial h_i \partial h_j} = \beta \langle (s_i - m_i)(s_j - m_j) \rangle, \tag{3.19}$$

which is positive definite.

We introduce the free energy $\Gamma[\{m_i\}]$ according to the *Legendre transformation* [5] :

$$\begin{aligned} -\beta\Gamma[\{m_i\}] &= -\beta\left(\sum_i h_i m_i + F[\{h_i\}]\right) \\ &= \log \sum_{\{s_i\}} \exp\left[-\beta H[\{s_i\}] + \beta \sum_i h_i (s_i - m_i)\right] \end{aligned} \tag{3.20}$$

where $h_i[\{m_i\}] = \frac{\partial \Gamma[\{m_i\}]}{\partial m_i}$.

To simplify the notation we introduce $A^\beta[\{m_i\}] = -\beta\Gamma[\{m_i\}]$ and $\lambda_i^\beta = \beta h_i$, and then

$$A^\beta[\{m_i\}] = \log \sum_{\{s_i\}} \exp\left[-\beta H[\{s_i\}] + \sum_i \lambda_i^\beta (s_i - m_i)\right]. \tag{3.21}$$

We would like to expand $A^\beta[\{m_i\}]$ at $\beta = 0$. The derivatives of $A^\beta[\{m_i\}]$ with respect to β are

[5] If we defined $-\beta\Gamma[\{m_i\}] = -\beta \max_{\{h_i\}} \left(\sum_i h_i m_i + F[\{h_i\}]\right)$, $\Gamma[\{m_i\}]$ would be a convex function which cannot have many local minima.

$$\left.\frac{\partial A^\beta}{\partial \beta}\right|_{\beta=0} = -\langle H\rangle_0 + \sum_i \left.\frac{\partial \lambda_i^\beta}{\partial \beta}\right|_{\beta=0} \langle s_i - m_i\rangle_0 = -\langle H\rangle_0 \tag{3.22}$$

$$\left.\frac{\partial^2 A^\beta}{\partial \beta^2}\right|_{\beta=0} = \left\langle \left(H - \langle H\rangle - \sum_i \left.\frac{\partial \lambda_i^\beta}{\partial \beta}\right|_{\beta=0} (s_i - m_i)\right)^2 \right\rangle_0 \tag{3.23}$$

...

with

$$\left.\frac{\partial \lambda_i^\beta}{\partial \beta}\right|_{\beta=0} = \frac{\partial}{\partial \beta}\left(-\frac{\partial A^\beta}{\partial m_i}\right)\Big|_{\beta=0} = -\frac{\partial}{\partial m_i}\left(\frac{\partial A^\beta}{\partial \beta}\right)\Big|_{\beta=0} = \frac{\partial \langle H\rangle_0}{\partial m_i}, \tag{3.24}$$

where $\langle ...\rangle_0$ means the thermodynamic average at $\beta = 0$.

We now consider a generic Ising model with out external magnetic fields

$$H = -\frac{1}{2}\sum_{i\neq j} J_{ij} s_i s_j. \tag{3.25}$$

The zeroth order term can be easily obtained:

$$A^0[\{m_i\}] = \log \sum_{s_i} \exp\left(\sum_i \lambda_i^0 (s_i - m_i)\right) = -\sum_i \lambda_i^0 m_i + \log 2\cosh \lambda_i^0, \tag{3.26}$$

with

$$\frac{\partial A^0}{\partial \lambda_i^0} = \langle s_i - m_i\rangle_0 = \tanh(\lambda_i^0) - m_i = 0. \tag{3.27}$$

Expressing λ_i^0 as a function of m_i we get

$$A^0[\{m_i\}] = \sum_i S^0(m_i) = -\sum_i \left(\frac{1+m_i}{2}\log\frac{1+m_i}{2} + \frac{1-m_i}{2}\log\frac{1-m_i}{2}\right), \tag{3.28}$$

which is the entropy of model (3.25) at infinite temperature.

The first and second derivatives of A^β are:

$$\left.\frac{\partial A^\beta}{\partial \beta}\right|_{\beta=0} = -\langle H\rangle_0 = \frac{1}{2}\sum_{i\neq j} J_{ij} m_i m_j + \sum_i h_i m_i, \tag{3.29}$$

$$\left.\frac{\partial \lambda_i^\beta}{\partial \beta}\right|_{\beta=0} = \frac{\partial \langle H\rangle_0}{\partial m_i} = -\sum_{j\neq i} J_{ij} m_j - h_i,$$

$$\left.\frac{\partial^2 A^\beta}{\partial \beta^2}\right|_{\beta=0} = \frac{1}{2}\sum_{i\neq j} J_{ij}^2 (1-m_i^2)(1-m_j^2). \tag{3.30}$$

Finally we obtain

$$-\beta\Gamma[\{m_i\}] = \frac{\beta}{2}\sum_{i\neq j} J_{ij}m_i m_j + \beta\sum_i h_i m_i + \frac{\beta^2}{4}\sum_{i\neq j} J_{ij}^2(1-m_i^2)(1-m_j^2) - \sum_i \left(\frac{1+m_i}{2}\log\frac{1+m_i}{2} + \frac{1-m_i}{2}\log\frac{1-m_i}{2}\right) + o(\beta^2). \quad (3.31)$$

Notice that for the fully connected ferromagnetic model where $J_{ij} = J/N$ and $h_i = h$, the terms of order β^2 and all the other higher order terms in the expansion vanish as $N \to \infty$. In this case, the TAP equations simplify to the mean field self-consistent equation

$$m_i = \tanh[\beta(Jm_i + h_i)]. \quad (3.32)$$

For the SK model, the terms $O(\beta^2)$ are relevant, however. If the condition

$$\frac{J^2}{N}\sum_i \beta^2(1-m_i^2)^2 = J^2\overline{\chi_{ii}^2} \leqslant 1 \quad (3.33)$$

is satisfied, the higher order terms vanish for $N \to \infty$. Supposing this is the case, we obtain the TAP equations (3.12) by minimizing the free energy (3.31) in the absence of external fields $h_i = 0$

$$0 = \left.\frac{\partial\Gamma[\{m_i\}]}{\partial m_i}\right|_{m_i=\tanh\left(\beta\sum_j J_{ij}m_j - \beta^2\sum_j J_{ij}^2(1-m_j^2)m_i\right)}. \quad (3.34)$$

At high temperature the TAP equations (3.34) have only the paramagnetic solution $m_i = 0$. We study the stability of this solution by considering the response of the magnetization around $m_i = 0$ to the infinitesimal external magnetic field. The linearized TAP equation is

$$\delta m_i = \beta\left(\delta h_i + \sum_{j\neq i} J_{ij}\delta m_j - \delta m_i \beta J^2\right). \quad (3.35)$$

We define

$$\delta m_\lambda \equiv \sum_i \phi_i^{(\lambda)}\delta m_i, \quad \delta h \equiv \sum_i \phi_i^{(\lambda)}\delta h_i, \quad (3.36)$$

where $\{\phi_i^{(\lambda)}\}$ is the eigenvector of the random matrix J_{ij}

$$\sum_j J_{ij}\phi_j^{(\lambda)} = \lambda\phi_i^{(\lambda)}. \quad (3.37)$$

The distribution of the spectrum of the random matrix J_{ij} is the Wigner semicircle: $\rho(\lambda) = (2\pi J^2)^{-1}\sqrt{4J^2 - \lambda^2}$. From this, we can read off the largest eigenvalue of the random matrix J_{ij} to be $\max|\lambda| = 2J$.

The response to an infinitesimal external magnetic field

$$\frac{\delta m_\lambda}{\delta h} = \frac{\beta}{1 + (\beta J)^2 - \beta\lambda} \tag{3.38}$$

is finite if $1 + (\beta J)^2 - \beta\lambda > 0$. The transition occurs when $1 + (\beta_c J)^2 - \beta_c \lambda_{\max} = 1 + (\beta_c J)^2 - 2\beta_c J = 0$. This gives $T_c = J$[6].

We can understand this result qualitatively in the following way. The energy cost due to one spin flip $\sim y_i = \sum_{j\neq i} J_{ij} m_j - m_i \beta \sum_j J_{ij}^2 (1 - m_j^2)$. The transition happens when $T \sim y_i^{\text{typ}}$. Near the transition point $\sum_{j\neq i} J_{ij} m_j$ is Gaussian distributed, $y_i^{\text{typ}} \sim m_i \beta \sum_j J_{ij}^2 (1 - m_j^2)$ can be approximated by $m_i J^2 \beta$. So we obtain $T_c \sim J$.

The paramagnetic solution $m_i = 0$ is stable for high temperature $T > T_c$. For $T < T_c$, $1 + (\beta J)^2 - \beta\lambda > 0$ holds again. It thus looks as if the paramagnetic solution $m_i = 0$ is also stable for low temperature. Actually this is not true, the paramagnetic phase is unstable for $T \leq T_c$. We consider the free energy $f_{para} = \Gamma[m_i = 0]/N = -\beta J^2/4 - T\log 2$. The entropy $s_{para} = -df_{para}/dT = \log 2 - \beta^2 J^2/4$ becomes negtive for $T < J/(2\sqrt{2}) \sim 0.91J$. This means $m_i = 0$ cannot be the physical thermodynamic state at low temperature. It is missed by the TAP equations. The reason is the condition (3.33) is not satisfied for $m_i = 0$ at $T < T_c = J$. The resummation of the higher order terms in the high temperature expansion is divergent when $\frac{J^2}{N}\sum_i \beta^2 (1 - m_i^2)^2 > 1$.

For the fully connected ferromagnetic model, the TAP equation (3.32) has only two stable nonzero solutions at low temperature in the absent of external field h. At low temperature the TAP equations (3.34) of the SK model have many solutions with $m_i \neq 0$. We interpret these solutions as stable or metastable thermodynamic states. Local minima of $\Gamma[\{m_i\}]$ correspond to locally stable magnetization configurations. If, in the large N limit, some of the barriers between these minima become infinite, we can partition the entire state space into mutually inaccessible 'valleys'. Each of these valley corresponds to a thermodynamic phase. Within such a state or valley, there can be several sub-valley which are local minima of $\Gamma[\{m_i\}]$, but with finite barriers separating them. All but the lowest of these correspond to metastable states. We label these separated by infinite barriers states by an index α running from 1 to the number N_s of states and denote their local magnetizations by m_i^α. The number of such states is given by

$$N_s = \sum_{\{s_i\}} \prod_i \Theta\left(s_i \sum_j J_{ij} s_j\right) = \sum_{\{s_i\}} \prod_i \int_0^\infty d\epsilon_i \delta\left(\epsilon_i - s_i \sum_j J_{ij} s_j\right). \tag{3.39}$$

[6] A dual way is to look at the Hessian matrix $\chi_{ij}^{-1} = \frac{\partial^2 \Gamma[\{m_i\}]}{\partial m_i \partial m_j}\Big|_{m_i=0} = (1 + (\beta J)^2)\delta_{ij} - \beta J_{ij}$. The solutions of the TAP equations are stable only if the Hessian matrix is positive. For $T > J$, we have $1 + (\beta J)^2 > \beta\lambda_{\max} = 2\beta J$, and the paramagnetic phase is stable. At $T = J$, the spectrum of the Hessian matrix $\frac{\partial^2 \Gamma[\{m_i\}]}{\partial m_i \partial m_j}$ touches zero, hence below $T = J$ the paramagnetic phase becomes unstable.

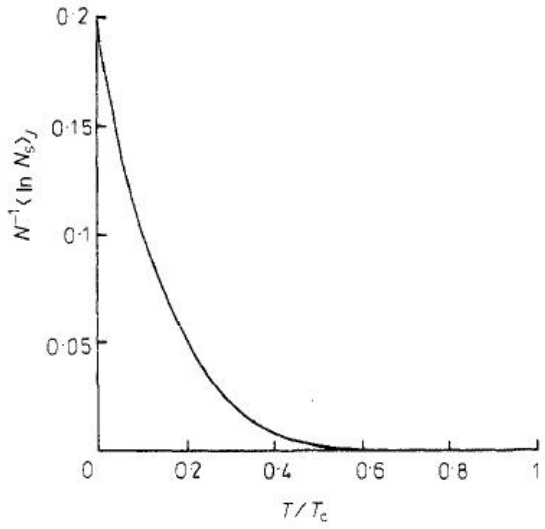

Figure 3.7: Logarithm of the total number of TAP solutions, divided by N, as a function of temperature.[68]

It turns out that N_s increases exponentially with the number N of spins at low temperature [61]. Namely $N^{-1}\overline{\log(N_s)} \equiv \Sigma(T) > 0$ for $T < T_c$. This is case of nontrivial broken ergodicity. Due to this reason, T_c is called freezing temperature. In clean systems, the broken ergodicity is usually accompanied by the symmetry spontaneously broken. For instance, the two low temperature phases of the ferromagnetic Ising model associate with the Z_2 symmetry. In this case, we can select a phase by adding an infinitesimal external field which breaks the symmetry in a certain way. But in a spin glass, we can not apply the external fields h_i^α proportional to the m_i^α to select this phase becuase we do not know these conjugate fields m_i^α a priori.

The total number of solutions as a function of temperature is shown in Fig. 3.7.

3.3.2 The local field distribution at zero temperature

The TAP equations without external magnetic fields are

$$m_i = \tanh(\beta y_i). \tag{3.40}$$

The local field $y_i = \sum_j J_{ij} m_j - \beta \sum_j J_{ij}^2 (1 - m_j^2) m_i$ is the effective field created by the other spins acting on the site i in the absence of spin s_i. Its distribution is defined as

$$P(y) = \frac{1}{N} \sum_i \delta(y - y_i). \tag{3.41}$$

At $T = 0$, the solutions of TAP equations (3.40) are

$$m_i = \mathrm{sign}(y_i), \quad y_i = \sum_{j \neq i} J_{ij} m_j. \tag{3.42}$$

The stability of such solutions requires that $P(y)$ must be zero at $y = 0$. Consider the subset of spins $\{s_i, i \in \Gamma\}$ with $|y_i| < \delta y \ll J$. Suppose there are n of these spins and the total number of spins is N, the ratio is given by $\frac{n}{N} = \int_{-\delta y}^{\delta y} P(y)dy$.

In order to check the stability of this state, we should flip at least two spins simultaneously. By rearranging these spins $\{s_i, i \in \Gamma\} \to \{-s_i, i \in \Gamma\}$, the energy change is

$$\Delta E = \Delta E(\Delta s y) + \Delta E(s \Delta y), \tag{3.43}$$

where

$$\Delta E(\Delta s y) = \sum_{i \in \Gamma(\delta y)} \Delta s_i y_i = \sum_{i \in \Gamma(\delta y)} 2 s_i y_i, \tag{3.44}$$

$$\begin{aligned} \Delta E(s \Delta y) = \sum_{i \in \Gamma(\delta y)} s_i \Delta y_i &= -\sum_{i \in \Gamma(\delta y)} s_i \sum_{j \neq i, j \in \Gamma(\delta y)} 2 J_{ij} s_j \\ &= -\sum_{i \neq j \in \Gamma(\delta y)} 2 J_{ij} s_i s_j. \end{aligned} \tag{3.45}$$

$\Delta E(\Delta s y)$ is the energy cost due to the rearrangement of these spins but without changing the local fields $\{y_i\}$. $\Delta E(s \Delta y)$ is the energy cost due to the shift of their local fields. $\Delta E(\Delta s y)$ is positive, and its variance is $\overline{(\Delta E(s \Delta y))^2} \propto \frac{J^2}{N} n = J^2 \int_{-\delta y}^{\delta y} P(y) dy$.

The stability condition of Eqs. (3.42) requires $0 \leq \Delta E = \Delta E(\Delta s y) + \Delta E(s \Delta y) \sim \delta y - \left[\overline{(\Delta E(s \Delta y))^2}\right]^{1/2} \sim \delta y - J \left[\int_{-\delta y}^{\delta y} P(y) dy\right]^{1/2}$. This gives that $P(y) \sim |y|^\alpha$ with $\alpha \geq 1$.[7] Numerical simulations [66, 69] and the more sophisticated analysis [70] shows that $\alpha = 1$. This means the TAP solutions (3.42) are on the stability boundary, in other words, the zero temperature states for the SK model are critical. We will see in the next section that the TAP solutions below the freezing temperature T_c are all critical!

The ZFC suseptbility can be obtained

$$\chi \equiv \frac{1}{N} \sum_i \chi_{ii} = \frac{1}{N} \sum_i \frac{\partial m_i}{\partial h_i} = \beta \frac{1}{N} \sum_i (1 - m_i^2) = \beta (1 - q_{\rm EA}). \tag{3.46}$$

The existence of the linear pseudo gap in the local field distribution leads to the linear temperature dependence of χ at low temperature:

$$\begin{aligned} \chi &= \beta \int dy P(y) \left[1 - \tanh^2(\beta y)\right] \\ &\overset{\beta y = \widetilde{y}}{=} \int d\widetilde{y} \frac{P(\widetilde{y}/\beta)}{\cosh^2(\widetilde{y})} = \int_{-\beta J}^{\beta J} d\widetilde{y} \frac{P(\widetilde{y}/\beta)}{\cosh^2(\widetilde{y})} + O(e^{-\beta J}), \quad T \to 0. \end{aligned} \tag{3.47}$$

[7] There is another similar argument: Assume $P(y) \sim |y|^\alpha$ for $y \ll J$. $y_{\rm min} = \min_i |y_i|$, and the probability $P(y > y_{\rm min})$ can be estimated as $P(y > y_{\rm min}) \simeq \left(1 - \int_{-y_{\rm min}}^{y_{\rm min}} P(y) dy\right)^N$ which would be O(1). This gives $y_{\rm min} \sim N^{\frac{-1}{1+\alpha}}$. The energy cost due to two spins flip is $\Delta E = |y_1| + |y_2| - N^{-1/2} \sim N^{\frac{-1}{1+\alpha}} - N^{-\frac{1}{2}} > 0$. This requires $\alpha \geq 1$.

The distribution $P(y)$ is linear in y for $y \ll J$. So $P(\widetilde{y}/\beta) \sim T|\widetilde{y}|$ as $T \to 0$ and we obtain $\chi \sim T$ as $T \to 0$. This also means that the Onsager term vanishes linearly in T as $T \to 0$.

The linear temperature dependence of the susceptibility $\chi(T)$ as $T \to 0$ can also be obtained from the entropy

$$\begin{aligned} S(T) = -\frac{\partial \Gamma[\{m_i\}]}{\partial T} &= -\frac{\beta^2}{4} \sum_{i \neq j} J_{ij}^2 (1 - m_i^2)(1 - m_j^2) \\ &\quad - \sum_i \left(\frac{1+m_i}{2} \log \frac{1+m_i}{2} + \frac{1-m_i}{2} \log \frac{1-m_i}{2} \right). \end{aligned} \tag{3.48}$$

In the limit $T \to 0$ one has $m_i \to \pm 1$ and the second term in (3.48) vanishes. This leads to

$$S(T=0) = -\frac{1}{2} N J^2 \lim_{T \to 0} \beta^2 (1 - q_{\rm EA}). \tag{3.49}$$

The condition of a vanishing entropy at $T = 0$ is therefore that $1 - q_{\rm EA}$ vanishes faster than T as $T \to 0$. It turns out that the "edge behavior" shows again [70]:

$$1 - q_{\rm EA}(T) \sim \left(\frac{T}{T_c} \right)^2, \tag{3.50}$$

consistent with $\chi \sim T$ as $T \to 0$.

3.3.3 Marginal stability of TAP equations

In this section, we study the stability of TAP solutions below the freezing temperature T_c. The TAP equations (3.12) with $h_i = 0$ can be derived by a variational principle from the TAP free energy (3.31)

$$\begin{aligned} \beta \Gamma[\{m_i\}] = -\frac{\beta}{2} \sum_{i \neq j} J_{ij} m_i m_j - \beta \sum_i h_i m_i + \frac{\beta^2}{4} \sum_{i \neq j} J_{ij}^2 (1 - m_i^2)(1 - m_j^2) \\ + \sum_i \left(\frac{1+m_i}{2} \log \frac{1+m_i}{2} + \frac{1-m_i}{2} \log \frac{1-m_i}{2} \right). \end{aligned} \tag{3.51}$$

The stability of these solutions is governed by the Hessian matrix

$$A_{ij} = \frac{\partial^2 (\beta \Gamma)}{\partial m_i \partial m_j}. \tag{3.52}$$

A locally stable solution must be a local minimum of the free energy and this requires that all eigenvalues of matrix A are positive. Note that A_{ij} is related to the spin correlations in the system. We introduce the susceptibility matrix $\chi_{ij} = \partial m_i / \partial h_j$. One can easily get

$$\beta \delta_{i,k} = \sum_j A_{ij} \chi_{ij}, \quad A_{ij}^{-1} = \beta^{-1} \chi_{ij} = \langle s_i s_j \rangle_c, \tag{3.53}$$

where $\langle s_i s_j\rangle_c = \langle s_i s_j\rangle - \langle s_i\rangle\langle s_j\rangle$. We introduce the eigenvalue density $\rho(\lambda) = N^{-1}\sum_i \delta(\lambda - \lambda_i)$, where λ_i are the eigenvalues of the matrix A_{ij}. It can easily be shown that $\rho(0)$ must itself vanish. To do this we calculate the trace of the inverse of the matrix A_{ij}:

$$\begin{aligned} N^{-1}\mathrm{Tr}A^{-1} &= N^{-1}\sum_i \frac{1}{\lambda_i} \overset{N\to\infty}{=} \int_0^\infty d\lambda \frac{\rho(\lambda)}{\lambda} \\ &= N^{-1}\sum_i \langle s_i s_i\rangle_c = N^{-1}\sum_i (1 - m_i^2) = 1 - q_{\mathrm{EA}}. \end{aligned} \tag{3.54}$$

$1 - q_{\mathrm{EA}}$ is finite. This implies $\rho(0) = 0$, since otherwise the integral $\int_0^\infty d\lambda \frac{\rho(\lambda)}{\lambda}$ would be logarithmically divergent at $\lambda = 0$. Further more, it can be shown that $\rho(\lambda) \propto \lambda^{1/2}$ for small λ[70]. The eigenvalue spectrum of A_{ij} can be arbitrarily small for all $T \le T_c$ but with vanishing density. This means the solutions below $T = T_c$ are marginally stable or the low temperature phases are critical.

As a consequence of the marginal stability of the low temperature phase

$$\chi_{\mathrm{SG}} \equiv N^{-1}\sum_{i,j} \chi_{ij}^2 = (\beta^2/N)\mathrm{Tr}(A^{-2}) = (\beta^2/N)\int_0^\infty \frac{\rho(\lambda)}{\lambda^2} \to \infty. \tag{3.55}$$

χ_{SG} always diverges when $T < T_c$. Also we recover the linear behavior of the zero field cooled suseptbility in T at low temperature

$$\chi_{\mathrm{zfc}} = N^{-1}\sum_i \chi_{ii} = \beta\int_0^\infty d\lambda \frac{\rho(\lambda)}{\lambda} = \beta(1 - q_{\mathrm{EA}}) \sim T. \tag{3.56}$$

3.4 The order parameter of spin glasses

As we have learned from the SK model, certain spin glasses have many states. The existence of many phases implies that a spin glass cannot be fully described by a single order parameter. It is useful to introduce the correlation between these states, i.e the overlap:

$$q_{\alpha\beta} = \frac{1}{N}\sum_i m_i^\alpha m_i^\beta. \tag{3.57}$$

Since α and β range over a large number of phases, $q_{\alpha\beta}$ could have many values between -1 and 1. It is therefore better to consider its distribution

$$P(q) = \overline{P_J(q)} = \sum_{\alpha\beta} \overline{P_\alpha P_\beta \delta(q - q_{\alpha\beta})}, \tag{3.58}$$

where $\overline{(...)}$ denotes the average over random couplings J_{ij} and $P_\alpha = \frac{e^{-\beta\Gamma_\alpha}}{\sum_\alpha e^{-\beta\Gamma_\alpha}}$ is the weight of the state α.

$P(q)$ is the fundamental quantity to capture non-trivially broken ergodicity. For a system with just two phases, $P(q)$ is just the sum of a pair of delta functions. If there

is strong broken ergodicity, $P(q)$ may have a continuous part, indicating the possibility of a continuum of possible overlaps between various phases. We can distinguish the systems with conventional broken symmetry from those with nontrivial broken ergodicity by the form of $P(q)$. Any moment of $P(q)$ can be obtained by using the clustering property of pure states:

$$\begin{aligned} q^{(1)} = \int dq P(q) q &= \int dq \sum_{\alpha\beta} \overline{P_\alpha P_\beta \delta(q - q_{\alpha\beta})} q \\ &= \frac{1}{N} \sum_i \sum_{\alpha\beta} \overline{P_\alpha P_\beta \langle s_i \rangle_\alpha \langle s_i \rangle_\beta} = \frac{1}{N} \sum_i \overline{\langle s_i \rangle^2}. \end{aligned} \tag{3.59}$$

$$\begin{aligned} q^{(k)} = \int dq P(q) q^k &= \int dq \sum_{\alpha\beta} \overline{P_\alpha P_\beta \delta(q - q_{\alpha\beta})} q^k \\ &= \frac{1}{N^k} \sum_{i_1 \ldots i_k} \sum_{\alpha\beta} \overline{P_\alpha P_\beta \langle s_{i_1 \ldots s_{i_k}} \rangle_\alpha \langle s_{i_1} \ldots s_{i_k} \rangle_\beta} \\ &= \frac{1}{N^k} \sum_{i_1 \ldots i_k} \sum_{\alpha\beta} \overline{P_\alpha P_\beta \langle s_{i_1} \rangle_\alpha \ldots \langle s_{i_k} \rangle_\alpha \langle s_{i_1} \rangle_\beta \ldots \langle s_{i_k} \rangle_\beta} \\ &= \frac{1}{N^k} \sum_{i_1 \ldots i_k} \overline{\langle s_{i_1 \ldots s_{i_k}} \rangle^2}. \end{aligned} \tag{3.60}$$

The self overlap $q_{\alpha\alpha} = \frac{1}{N} \sum_i \langle s_i \rangle_\alpha^2$ measures the mean square single-valley local magnetization. Since we are not able to identify any single-valley, it is convenient to average over all possible states. This gives the Edwards-Anderson order parameter

$$q_{\mathrm{EA}} = \frac{1}{N} \sum_\alpha P_\alpha \sum_i \langle s_i \rangle_\alpha^2. \tag{3.61}$$

Note that $q_{\mathrm{EA}} \geq q^{(1)}$. The equality is attained when there is just a single phase.

3.4.1 Replica method

In mean field models, the physically relevant quantities which we introduced in the last section can be computed using so called replica method. The replica are introduced when we average the logarithm of the partition function:

$$F \equiv \overline{F_J} = -\frac{1}{\beta} \overline{\log(Z_J)}. \tag{3.62}$$

The partition function

$$Z_J = \sum_{\{s_i\}} \exp(-\beta H_J[\{s_i\}]). \tag{3.63}$$

To perform this averaging procedure, we consider the integer power n of the partition function (3.64). This quantity is the partition function of the n non-interacting identical replica of the original system:

$$Z_J^n = \prod_{a=1}^{n} \sum_{\{s_i^a\}} \exp(-\beta \sum_{a=1}^{n} H_J[\{s_i^a\}]). \tag{3.64}$$

The index a labels the replica. Formally taking the limit $n \to 0$, we obtain

$$\overline{\log Z_J} = \lim_{n\to 0} \frac{\overline{Z_J^n} - 1}{n}. \tag{3.65}$$

Now we consider the SK model. We first calculate the average of the n-th power of the partition function:

$$\begin{aligned}
\overline{Z_J^n} &= \overline{\sum_{\{s_i^a\}} \exp\left(\beta \sum_a \sum_{i<j} J_{ij} s_i^a s_j^a + \beta h \sum_\alpha \sum_i s_i^\alpha\right)} \\
&= \sum_{\{s_i^a\}} \exp\left[\frac{J^2}{2N} \sum_{i<j} \beta^2 (\sum_{a,b=1}^{n} s_i^a s_i^b s_j^a s_j^b) + \beta h \sum_{a,i} s_i^a\right] \\
&= \sum_{\{s_i^a\}} \exp\left[\frac{\beta^2 J^2}{2N}\left(n\frac{N(N-1)}{2} + \sum_{a<b}\left(\sum_i s_i^a s_i^b\right)^2 + \beta h \sum_{i,a} s_i^a\right)\right] \\
&= \exp\left[nN\left(\frac{\beta J}{2}\right)^2\right] \int \prod_{a<b} dQ_{ab} \frac{\beta J N^{1/2}}{\sqrt{2\pi}} \exp\left[-\frac{1}{2} N (\beta J)^2 \sum_{a<b} Q_{ab}^2\right] \\
&\quad \sum_{\{s_i^a\}} \exp\left[(\beta J)^2 \sum_i \sum_{a,b} Q_{ab} s_i^a s_i^b + \beta h \sum_{i,a} s_i^\alpha\right] \\
&= \int \prod_{a<b} dQ_{ab} \frac{\beta J N^{1/2}}{\sqrt{2\pi}} \exp(-Nn\beta f_n[Q]),
\end{aligned} \tag{3.66}$$

with

$$\begin{aligned}
f_n[Q] &= -\frac{J^2\beta}{4} + \frac{\beta J^2}{2n} \sum_{a<b} Q_{ab}^2 - \frac{1}{\beta n} \log \sum_{\{s^a\}} \exp\left[(\beta J)^2 \sum_{a<b} Q_{ab} s^a s^b + \beta h \sum_a s^a\right] \\
&= -\frac{J^2\beta}{4} + \frac{\beta J^2}{2n} \sum_{a<b} Q_{ab}^2 - \frac{1}{\beta n} \log \sum_{\{s^a\}} \exp\left[H_{\text{eff}}\right] \\
&= -\frac{J^2\beta}{4} + \frac{\beta J^2}{2n} \sum_{a<b} Q_{ab}^2 - \frac{1}{\beta n} \log Z[Q],
\end{aligned} \tag{3.67}$$

where $H_{\rm eff} = (\beta J)^2 \sum_{a<b} Q_{ab} s^a s^b + \beta h \sum_a s^a$ and $Z[Q] = \sum_{\{s_a\}} \exp(H_{\rm eff})$. Note that the disorder averaging introduces attractive interactions between replica, which were previously uncorrelated. In the thermodynamic limit $N \to \infty$, $\overline{Z_J^n}$ is governed by the saddle point of $f_n[Q]$:

$$\frac{\delta f_n[Q^\star]}{\delta Q_{ab}} = 0 \Rightarrow Q^\star_{ab} = \langle s^a s^b \rangle \equiv \frac{\sum_{s^a=\pm 1} s^a s^b e^{H_{\rm eff}}}{\sum_{s^a=\pm 1} e^{H_{\rm eff}}}. \tag{3.68}$$

Now by taking the limit $n \to 0$, we obtain the free energy per spin

$$F/N = f = \lim_{n\to 0} f_n[Q^\star]. \tag{3.69}$$

The crucial point is that we can compute the physically relevant quantities using this replica trick. In particular,

$$\begin{aligned} q^{(1)} = \frac{1}{N}\sum_i \overline{\langle s_i \rangle^2} &= \overline{\frac{1}{Z^2}\sum_{s^1,s^2} e^{-\beta(H[s^1]+H[s^2])} \frac{1}{N}\sum_i s_i^1 s_i^2} \\ &= \lim_{n\to 0} \overline{\frac{1}{N}\sum_i \sum_{s^a} \; s_i^1 s_i^2 \; e^{-\beta \sum_a H(s^a)}}, \end{aligned} \tag{3.70}$$

where the last equation is obtained writing $Z^{-2} = \lim_{n\to 0} Z^{n-2}$. By introducing the Q matrix after disorder averaging, we get

$$\overline{\sum_{s_i^a} s_i^1 s_i^2 e^{-\beta \sum_a H[\{s_i^a\}]}} = \int \prod_{a<b} dQ_{ab} \frac{\beta J N^{1/2}}{\sqrt{2\pi}} \exp(-N\beta C_n[Q]), \tag{3.71}$$

where

$$\begin{aligned} C_n[Q] &= -n\frac{J^2\beta}{4} + \frac{\beta J^2}{2}\sum_{a<b} Q_{ab}^2 \\ &\quad -\frac{1}{\beta}\log \frac{1}{N}\sum_{\{s^a\}} s_i^1 s_i^2 \exp\left[(\beta J)^2 \sum_{a<b} Q_{ab} s^a s^b + n\beta h \sum_a s^a\right]. \end{aligned} \tag{3.72}$$

In the large N limit, the integral (3.71) is governed by the saddle point of C_n:

$$\begin{aligned} C_n[Q^\star] &= -n\frac{J^2\beta}{4} + \frac{\beta J^2}{2}\sum_{a<b}(Q^\star_{ab})^2 - \frac{1}{\beta}\log\left[\frac{1}{N}\langle s_i^1 s_i^2\rangle Z[Q^\star]\right] \\ &= -\frac{1}{\beta}\log\left[\frac{1}{N}\langle s_i^1 s_i^2\rangle\right] + n f_n[Q^\star]. \end{aligned} \tag{3.73}$$

At the end, we obtain

$$q^{(1)} = \lim_{n\to 0}\frac{1}{N}\sum_i \langle s_i^1 s_i^2\rangle e^{n f_n[Q^\star]} = \frac{1}{N}\sum_i \langle s_i^1 s_i^2\rangle = \langle s^1 s^2\rangle = Q_{12}. \tag{3.74}$$

Of course, $q^{(1)}$ should not depend on the replica indices. Namely $q^{(1)}$ should not change under permutation group S_n acting on $\{s^a\}$. We must therefore average over all different saddle points Q^*, which is equivalent to symmetrizing the equation (3.74):

$$\int P(q)qdq = q^{(1)} = \lim_{n\to 0} \frac{1}{n(n-1)} \sum_{a\neq b} Q_{ab}. \tag{3.75}$$

This result is already telling us that there is a connection between $q^{(1)}$ and the matrix of the overlap among replica Q_{ab}. To go further, we can generalize (3.75) to get

$$\int P(q)q^k dq = q^{(k)} = \lim_{n\to 0} \frac{1}{n(n-1)} \sum_{a\neq b} Q_{ab}^k. \tag{3.76}$$

Comparing with equation (3.76) gives that for a generic function $f(q)$

$$\int dq f(q)P(q) = \lim_{n\to 0} \frac{1}{n(n-1)} \sum_{a\neq b} f(Q_{ab}), \tag{3.77}$$

which, in particular, for $f(q) = \delta(q-q')$ finally provides the crucial equation connecting physics to replica,

$$P(q) = \lim_{n\to 0} \frac{1}{n(n-1)} \sum_{a\neq b} \delta(q - Q_{ab}). \tag{3.78}$$

This equation shows that the average probability that two pure states of the system have overlap q is equal to the fraction of elements of the overlap matrix Q_{ab} equal to q. In other words, *the elements of the overlap matrix (in the saddle point) are the physical values of the overlap among pure states, and the number of elements of Q_{ab} equal to q is related to the probability of q.*

The field cooled susceptibility can also be derived easily:

$$\begin{aligned} \chi &= \left.\frac{\partial^2 f}{\partial h^2}\right|_{h=0} = \frac{1}{\beta}\left[\beta^2 \lim_{n\to 0}\frac{1}{n}\sum_{a,b=1}^{n}\langle s^a s^b\rangle - \langle s^a\rangle\langle s^b\rangle\right] \\ &= \beta\left(1 + \lim_{n\to 0}\frac{1}{n}\sum_{a\neq b} Q_{ab}\right) \\ &= \beta(1-q^{(1)}), \end{aligned} \tag{3.79}$$

where we use $-\left.\frac{\partial f}{\partial h}\right|_{h=o} = \beta\langle s^a\rangle_{h=0} = 0$ in the third step.

Finally, it is useful to define the function

$$x(q) = \int_0^q P(q')dq' \in [0,1]\ , \qquad\qquad \frac{dx}{dq} = P(q)\ . \tag{3.80}$$

As $P(q)$ is positive, $x(q)$ is a monotonically increasing function and so we can define its inverse $q(x)$. In particular we can write

$$q^{(1)} = \int_0^1 qP(q)dq = \int_0^1 q\frac{dx}{dq}dq = \int_0^1 q(x)dx\ . \tag{3.81}$$

Now the problem is that for an arbitrary Q matrix the replica free energy (5.8) can not be calculated. So we have to propose an ansatz for the Q matrix. The simplest one is the replica symmetry (RS) ansatz: $Q_{ab} = q_0$ for $a \neq b$. Here the replica symmetry means that the replica Hamiltonian H_{eff} does not change under permutation group S_n acting on $\{s_a\}$. In this case, we have

$$P(q) = \delta(q - q_{\alpha\beta}) = \delta(q - q_0). \tag{3.82}$$

As we pointed out, if there is a strong broken ergodicity, which indeed is the case of the SK model, $P(q)$ should have a continuous part. So the delta function form of $P(q)$ indicates that this RS solution cannot describe this SK glass. The replica symmetry free energy can be easily obtained:

$$\beta f_{\text{RS}} = -\left(\frac{\beta J}{2}\right)^2 (1 - q_0)^2 - \int dz \frac{e^{-z^2/2}}{\sqrt{2\pi}} \log\left[2\cosh(\beta(J\sqrt{q_0}z + h))\right], \tag{3.83}$$

with the saddle point equation

$$q_0 = \int dz \frac{e^{-z^2/2}}{\sqrt{2\pi}} \tanh^2\left[\beta(J\sqrt{q_0}z + h)\right]. \tag{3.84}$$

However, this RS solution leads to a negative entropy at zero temperature, $S(T = 0) = -1/2\pi \simeq -0.17$, which is physically unacceptable.

The way out is to break the replica symmetry. The difficulty is that there are infinite ways to do this! The Parisi's ansatz [71] has been physically argued and now mathematically proven to be the correct ansatz describing the replica symmetry breaking (RSB). The idea is the following: Let us introduce a series of integers: $\{m_i\}$ $(i = 0, 1, ..., K)$ such that $m_0 = n$, $m_{K+1} = 1$ and all m_i/m_{i+1} are integers. Next, we divide n replica into n/m_1 groups such that each group would consist of m_1 replica; each group of m_1 replica divided into m_1/m_2 subgroups, so that each subgroup would consist of m_2 replica; and so on. Finally let us define the Q matrix as

$$\begin{aligned} &Q_{ab} = q_i, \quad \text{for} \quad I(a/m_i) \neq I(b/m_i) \quad \text{and} \\ &I(a/m_{i+1}) = I(b/m_{i+1}); \quad i = 0, 1, ..., K, \end{aligned} \tag{3.85}$$

where $I(x)$ is the integer valued function, which is equal to the smallest integer larger than or equal to x.

We now take an example of 1-step RSB ansatz $K = 1$. The structure of the Q matrix for $K = 1$ is shown in the following:

$$Q = \begin{pmatrix} 1 & q_1 & q_1 & q_0 & q_0 & q_0 \\ q_1 & 1 & q_1 & q_0 & q_0 & q_0 \\ q_1 & q_1 & 1 & q_0 & q_0 & q_0 \\ q_0 & q_0 & q_0 & 1 & q_1 & q_1 \\ q_0 & q_0 & q_0 & q_1 & 1 & q_1 \\ q_0 & q_0 & q_0 & q_1 & q_1 & 1 \end{pmatrix}. \tag{3.86}$$

The distribution of the overlap between different phases in the 1-step RSB case is

$$\begin{aligned} P(q) &= \lim_{n\to 0}\frac{1}{n(n-1)}\sum_{a\neq b}\delta(q-Q_{ab}) \\ &= \lim_{n\to 0}\frac{1}{n-1}\left[(m_1-1)\delta(q-q_1)+(n-m_1)\delta(q-q_0)\right] \\ &= (1-m_1)\delta(q-q_1)+m_1\delta(q-q_0). \end{aligned} \tag{3.87}$$

Note that after taking the limit $n\to 0$, $0\leq m_1\leq 1$ is not anymore an integer. $P(q)$ now is the sum of two delta functions, which indeed improved comparing to the replica symmetry case. But the continuum part is still missing. With this 1-step RSB ansatz, the replica patition function $Z[Q]$ can be written as

$$\begin{aligned} Z[Q] &= \sum_{\{s_a\}}\exp(H_{\text{eff}}) = \sum_{\{s^a\}}\exp\left[\frac{(\beta J)^2}{2}\sum_{a\neq b}Q_{ab}+\beta h\sum_a s^a\right] \\ &= \sum_{\{s^a\}}\exp\left\{\frac{(\beta J)^2}{2}\left[q_0\left(\sum_a s^a\right)^2+(q-q_0)\sum_{block}\left(\sum_{a\in block}\right)^2-nq_0\right]\right\} \end{aligned} \tag{3.88}$$

By introducing a Hubbard-Stratonovich transformation, we get

$$\begin{aligned} Z[Q] &= \exp\left(-\frac{(\beta J)^2}{2}nq_0\right)\int dP_{q_0}(z)\prod_{k\in block,k=1}^{n/m_1}dP_{q_1-q_0}(y_k)\times \\ &\quad \sum_{\{s^a\}}\exp\left[\beta(h+z)\sum_a s^a-\sum_{k=1}^{n/m_1}y_k\left(\sum_{a\in block}s^a\right)\right] \\ &= \exp\left(-\frac{(\beta J)^2}{2}nq_0\right)\times \\ &\quad \int dP_{q_0}(z)\left\{\int dP_{q_1-q_0}(y)\left[2\cosh(\beta(z+h+y))\right]^{m_1}\right\}^{n/m_1}, \end{aligned} \tag{3.89}$$

where

$$dP_q(z) = \frac{1}{\sqrt{2\pi qJ^2}}\exp\left(-\frac{z^2}{2qJ^2}\right)dz. \tag{3.90}$$

Taking the limit $n\to 0$, we obtain

$$\begin{aligned} \beta f_{1-step} &= -\frac{(\beta J)^2}{4}-\lim_{n\to 0}\frac{(\beta J)^2}{4n}\sum_{a\neq b}Q_{ab}^2+\lim_{n\to 0}\frac{1}{n}\log Z[Q] \\ &= -\frac{(\beta J)^2}{4}\left[1+m_1q_0^2+(1-m_1)q_1^2\right]-\frac{(\beta J)^2q_0}{2} \\ &\quad +\frac{1}{m_1}\int dP_{q_0}(z)\log\left\{\int dP_{q_1-q_0}(y)\left[2\cosh(\beta(h+z+y))\right]^{m_1}\right\}. \end{aligned} \tag{3.91}$$

In this case, one gets the entropy at zero temperature $S(T=0) \simeq -0.01$. It is still negative but improved a lot comparing to the RS case. As one may expect, the entropy becomes less and less negative as we go to further steps of RSB, and the exact solution is approached when $K \to \infty$.

3.4.2 Sommers-Dupont recursions for discrete RSB and the continuum limit

In this section we will present an elegant way to go to arbitrary steps of RSB. Let us consider the replica Hamiltonian

$$-\beta H[\{s_a\}] = \frac{\beta^2 J^2}{2} \sum_{a \neq b} s_a Q_{ab} s_b. \tag{3.92}$$

We write a generic Parisi matrix Q_{ab} with K steps in the form

$$Q_{ab} = (\widetilde{q} - q_K)\delta_{ab} + \sum_{k=1}^{K} \Delta q_k \mathcal{R}^{(k)}_{ab} + q_0 \mathcal{R}^{(0)}_{ab} \tag{3.93}$$

where $\widetilde{q}$ is the diagonal entry and $\Delta q_k \equiv q_k - q_{k-1}$ with q_k being the entries for replica at distance $x_k < x < x_{k+1}$. $\mathcal{R}^{(k)}$ are $n \times n$ matrices having (n/x_k) $x_k \times x_k$-matrices with all entries equal to 1 along the diagnoal, and with vanishing entries elsewhere.

Let us also introduce the notation $Q^{(l)} = (\widetilde{q} - q_K)\mathcal{R}^{(m)} + \sum_{k=l}^{K} \Delta q_k \mathcal{R}^{(k)}$.[8] In the following we will restrict certain sums over spins to the subclusters $\mathcal{C}_k$ of x_k spins that correspond to a single block in $\mathcal{R}^{(k)}$ in the above decomposition. In this context, a matrix $Q^{(k)}$ is always understood to be restricted to one single cluster $\mathcal{C}_k$. Let us define the scale and field dependent free energy for per spin, $\phi(y; x_k)$, as

$$\exp[x_k \phi(y, x_k)] = \sum_{s_a = \pm 1, a \in \mathcal{C}_k} \exp\left[\frac{\beta^2 J^2}{2} \sum_{a,b \in \mathcal{C}_k} s_a Q^k_{ab} s_b - \beta y \sum_a s_a \right]. \tag{3.97}$$

We can easily obtain a recursion relation between $\phi(y, x_k)$ and $\phi(y', x_{k+1})$ by writing $Q^k = (Q^{k+1})^{\otimes (x_k/x_{k+1})} + \mathcal{R}^{(k)} \Delta q_k$, breaking up the coupling introduced by Δq_k by a Hubbard-Stratonovich transformation. One finds

$$\exp[x_k \phi(y, x_k)] = \int dz \frac{\exp[-\frac{z^2}{2\Delta q_k J^2}]}{\sqrt{2\pi \Delta q_k J^2}} \exp[x_k \phi(y + z, x_{k+1})], \tag{3.98}$$

which allows for a recursive calculation of $\phi(y; x_k)$, using the initial condition

[8] Here is an example of the decomposition (3.93) and $Q^{(l)}$ with $K = 2$:

$$\phi(y, x_{K+1} \equiv 1) = \log[\cosh(\beta y)] + \frac{\beta^2 J^2}{2}(\widetilde{q} - q_K). \tag{3.99}$$

Taking the continuous limit in (3.97) one finds the Sommers-Dupont equation

$$\begin{aligned}
Q \;=\; & \begin{pmatrix}
1 & q_2 & q_1 & q_1 & q_0 & q_0 & q_0 & q_0 \\
q_2 & 1 & q_1 & q_1 & q_0 & q_0 & q_0 & q_0 \\
q_1 & q_1 & 1 & q_2 & q_0 & q_0 & q_0 & q_0 \\
q_1 & q_1 & q_2 & 1 & q_0 & q_0 & q_0 & q_0 \\
q_0 & q_0 & q_0 & q_0 & 1 & q_2 & q_1 & q_1 \\
q_0 & q_0 & q_0 & q_0 & q_2 & 1 & q_1 & q_1 \\
q_0 & q_0 & q_0 & q_0 & q_1 & q_1 & 1 & q_2 \\
q_0 & q_0 & q_0 & q_0 & q_1 & q_1 & q_2 & 1
\end{pmatrix} = \begin{pmatrix}
q_0 & q_0 & q_0 & q_0 & q_0 & q_0 & q_0 & q_0 \\
q_0 & q_0 & q_0 & q_0 & q_0 & q_0 & q_0 & q_0 \\
q_0 & q_0 & q_0 & q_0 & q_0 & q_0 & q_0 & q_0 \\
q_0 & q_0 & q_0 & q_0 & q_0 & q_0 & q_0 & q_0 \\
q_0 & q_0 & q_0 & q_0 & q_0 & q_0 & q_0 & q_0 \\
q_0 & q_0 & q_0 & q_0 & q_0 & q_0 & q_0 & q_0 \\
q_0 & q_0 & q_0 & q_0 & q_0 & q_0 & q_0 & q_0 \\
q_0 & q_0 & q_0 & q_0 & q_0 & q_0 & q_0 & q_0
\end{pmatrix} \\
& + \begin{pmatrix}
q_1 - q_0 & q_1 - q_0 & q_1 - q_0 & q_1 - q_0 & & & & \\
q_1 - q_0 & q_1 - q_0 & q_1 - q_0 & q_1 - q_0 & & & & \\
q_1 - q_0 & q_1 - q_0 & q_1 - q_0 & q_1 - q_0 & & & & \\
q_1 - q_0 & q_1 - q_0 & q_1 - q_0 & q_1 - q_0 & & & & \\
& & & & & 0 & & \\
& & & & & & & \\
& & 0 & & q_1 - q_0 & q_1 - q_0 & q_1 - q_0 & q_1 - q_0 \\
& & & & q_1 - q_0 & q_1 - q_0 & q_1 - q_0 & q_1 - q_0 \\
& & & & q_1 - q_0 & q_1 - q_0 & q_1 - q_0 & q_1 - q_0 \\
& & & & q_1 - q_0 & q_1 - q_0 & q_1 - q_0 & q_1 - q_0
\end{pmatrix} \\
& + \begin{pmatrix}
q_2 - q_1 & q_2 - q_1 & 0 & 0 & & & & \\
q_2 - q_1 & q_2 - q_1 & 0 & 0 & & & & \\
0 & 0 & q_2 - q_1 & q_2 - q_1 & & & & \\
0 & 0 & q_2 - q_1 & q_2 - q_1 & & & & \\
& & & & & 0 & & \\
& & & & & & & \\
& & 0 & & q_2 - q_1 & q_2 - q_1 & 0 & 0 \\
& & & & q_2 - q_1 & q_2 - q_1 & 0 & 0 \\
& & & & 0 & 0 & q_2 - q_1 & q_2 - q_1 \\
& & & & 0 & 0 & q_2 - q_1 & q_2 - q_1
\end{pmatrix} \\
& + \begin{pmatrix}
1 - q_2 & 0 & 0 & 0 & & & & \\
0 & 1 - q_2 & 0 & 0 & & & & \\
0 & 0 & 1 - q_2 & 0 & & & & \\
0 & 0 & 0 & 1 - q_2 & & & & \\
& & & & & 0 & & \\
& & & & & & & \\
& & 0 & & 1 - q_2 & 0 & 0 & 0 \\
& & & & 0 & 1 - q_2 & 0 & 0 \\
& & & & 0 & 0 & 1 - q_2 & 0 \\
& & & & 0 & 0 & 0 & 1 - q_2
\end{pmatrix}.
\end{aligned} \tag{3.94}$$

$$Q^{(1)} = \begin{pmatrix}
1 - q_0 & q_2 - q_0 & q_1 - q_0 & q_1 - q_0 & & & & \\
q_2 - q_0 & 1 - q_0 & q_1 - q_0 & q_1 - q_0 & & & & \\
q_1 - q_0 & q_1 - q_0 & 1 - q_0 & q_2 - q_0 & & & & \\
q_1 - q_0 & q_1 - q_0 & q_2 - q_0 & 1 - q_0 & & & & \\
& & & & & 0 & & \\
& & & & & & & \\
& & 0 & & 1 - q_0 & q_2 - q_0 & q_1 - q_0 & q_1 - q_0 \\
& & & & q_2 - q_0 & 1 - q_0 & q_1 - q_0 & q_1 - q_0 \\
& & & & q_1 - q_0 & q_1 - q_0 & 1 - q_0 & q_2 - q_0 \\
& & & & q_1 - q_0 & q_1 - q_0 & q_2 - q_0 & 1 - q_0
\end{pmatrix}. \tag{3.95}$$

$$\dot{\phi}(y,x) = -\frac{\dot{q}(x)}{2}(\phi''(y,x) + x\phi'(y,x)^2), \tag{3.100}$$

with

$$q(x) \equiv \sum_{i=0}^{K} q_i \Theta(x_i < x < x_{i+1}), \tag{3.101}$$

where the dot and prime are derivatives with respect to x and y variables, correspondingly. The local magnetization in the presence of the frozen field is $m(y,x) = \frac{1}{\beta}\frac{\partial\phi(y,x)}{\partial y}$.

We also introduce a scale-dependent distribution of fields, $P(y,x_k)$, defined implicitly via all its moments: For every product of spins belonging to a cluster $\mathcal{C}_k$, we require the identity

$$\begin{aligned}\langle s_{a_1}...s_{a_r}\rangle &= \int dy P(y;x_k)\left[\sum_{s_a=\pm 1, a\in\mathcal{C}_k}(s_{a_1}...s_{a_r})\times\right. \\ &\left.\frac{\exp\left(\frac{\beta^2J^2}{2}\sum_{a,b\in\mathcal{C}_k}s_aQ^k_{ab}s_b - \beta y\sum_{a\in\mathcal{C}_k}s_a\right)}{\exp(x_k\phi(y;x_k))}\right].\end{aligned} \tag{3.102}$$

Note that the Boltzmann weight within the bracket is normalized for any value of y. The physically interesting object is the distribution of fields on shortest time scales, $P(y,x_K)$.

For the field distribution $P(y,x_k)$ we can derive a recursion relation as well. Let us consider expectation values of spins belonging to a cluster $\mathcal{C}_{k+1} \subset \mathcal{C}_k$. In (3.102) we break up the coupling due to Δq_k via a Hubbard Stratonovich transformation and perform the sum over all spins in $\mathcal{C}_k \backslash \mathcal{C}_{k+1}$. Casting this back into the form (3.102) but for x_{k+1} we find the recursion

$$P(y,x_{k+1}) = \int dz \frac{\exp\left(-\frac{z^2}{2\Delta q_k J^2}\right)}{\sqrt{2\pi\Delta q_k J^2}} \exp\left[x_k(\phi(y,x_{k+1}) - \phi(y-z,x_k))\right], \tag{3.103}$$

$$Q^{(2)} = \begin{pmatrix} 1-q_1 & q_2-q_1 & 0 & 0 & & \\ q_2-q_1 & 1-q_1 & 0 & 0 & & \\ 0 & 0 & 1-q_1 & q_2-q_1 & & 0 \\ 0 & 0 & q_2-q_1 & 1-q_1 & & \\ & & & & 1-q_1 & q_2-q_1 & 0 & 0 \\ & 0 & & & q_2-q_1 & 1-q_1 & 0 & 0 \\ & & & & 0 & 0 & 1-q_1 & q_2-q_1 \\ & & & & 0 & 0 & q_2-q_1 & 1-q_1 \end{pmatrix}. \tag{3.96}$$

with the initial condition

$$P(y, x_0 \equiv 0) = \delta(y). \tag{3.104}$$

Taking the continuum limit, and using (3.97), one derives the second Sommers-Dupont equation

$$\dot{P}(y,x) = \dot{q}(x)\left[\frac{P''(y,x)}{2} - x(\phi'(y,x)P(y,x))'\right]. \tag{3.105}$$

At very low temperature $T \ll J$, a full replica symmetry breaking solution of the SK model in the low energy sector has been found [71, 72]. In the following I will illustrate the basic idea of Ref. [72]. We again write the Parisi infinite RSB scheme equations —Sommers-Dupont equations:

$$\dot{m}(y,x) = -\frac{\dot{q}(x)}{2}\left[m''(y,x) + 2\beta x m(y,x)m'(y,x)\right], \tag{3.106}$$

$$\dot{P}(y,x) = \frac{\dot{q}(x)}{2}\left\{P''(y,x) - 2\beta x\left[m(y,x)P(y,x)\right]'\right\}, \tag{3.107}$$

with the initial conditions: $m(y,1) = \tanh(\beta y)$ and $P(y,0) = \delta(y)$. In principle, these equations can be solved iteratively. One can compute $m(y,x)$ and $P(y,x)$ for a given order parameter $q(x)$, which is computed from $m(y,x)$ and $P(y,x)$:

$$q(x) = \int dy P(y,x) m^2(y,x). \tag{3.108}$$

By introducing new notations: $m(y,x) = \tilde{m}(z,x)$, $P(y,x) = (\beta x)^{-1}\tilde{p}(z,x)$, $\dot{q}(x) = 2\beta(\beta x)^{-3}c(x)$, where $z = \beta x y$, Eqs. (3.106,3.107) become:

$$x\dot{\tilde{m}} = -c\left(\tilde{m}'' + 2\tilde{m}\tilde{m}'\right) - z\tilde{m}', \tag{3.109}$$

$$x\dot{\tilde{p}} = c\left[\tilde{p}'' - 2(\tilde{p}\tilde{m})'\right] - z\tilde{p}' + \tilde{p}, \tag{3.110}$$

where the dot and prime are now derivatives with respect to x and z variables, correspondingly. Pankov's scaling ansatz assumes that $\tilde{m}$ and $\tilde{p}$ become functions of the scaling variable z only, and c is a constant. Under this assumption, we obtain the scaling equations

$$0 = -c\left(\tilde{m}'' + 2\tilde{m}\tilde{m}'\right) - z\tilde{m}', \tag{3.111}$$

$$0 = c\left[\tilde{p}'' - 2(\tilde{p}\tilde{m})'\right] - z\tilde{p}' + \tilde{p}. \tag{3.112}$$

It is can be demonstrated that the ansatz becomes asymptotically exact in the scaling regime described above. In the large z limit, from the scaling equations (3.111,3.112), one finds that the field distribution is asymptotically linear:

$$|z| \gg 1, \quad \tilde{m} = \ \mathrm{sign}(z), \quad \tilde{p} = \gamma(|z| + 2c). \tag{3.113}$$

The local field distribution $P(y,x)$ develops a linear gap at zero temperature, which is consistent with the previous analysis in the section 1.3.2. The scaling ansatz also allows us to compute the slope of $P(y,1)$ in the low temperature limit. Because the scaling equations can be easily integrated numerically, one can obtain the value of the slope with arbitrary precision. With a fixed constant c the function $\tilde{p}$ enters the equations linearly, therefore one can set $\gamma = 1$ when solving for c, and then compute the slope as $\gamma = c[\int dz \tilde{p}_{\gamma=1}(z)(1-\tilde{m}^2(z))]^{-1}$. Up to ten digits of precision one found $c = 0.4108020997$, $\gamma = 0.3010464715$.

At the end of this Chapter I would like to comment on broken ergodicity and broken replica symmetry in spin glasses: as far as we know, the broken replica symmetry in real three-dimensional spin glasses is doubtful. Nevertheless, the nontrivial broken ergodicity does persist in real systems, especially in their dynamics. That is, even though there are not infinitely many thermodynamically stable phases, there do appear to be many metastable states. Thus broken ergodicity on a given timescale remains an important concept in real spin glasses, even if strict thermodynamic broken ergodicity is not.

3.5 Conclusion

In this chapter I reviewed some basic aspects of the mean field theory of spin glasses. I mainly focused on the SK model which exhibits nontrivial broken ergodicity and broken replica symmetry. The technique I presented here can be also extended to quantum systems which I will study in Chapter V.

Chapter 4

Non-frustrated Bose glasses-Energy localization

In this Chapter I study localization properties of strongly interacting bosons and spin systems in a disordered potential at zero temperature. Disordered hard-core bosons and a closely related XY ferromagnet in a transverse field are analyzed on a Cayley tree with large connectivity K which allows us to approach the quantum phase transition to an ordered (superfluid or ferromagnetic) phase. I find that with a uniformly distributed disorder non-extensive excitations in the disordered phase are all localized. Moreover, I find that the order arises due to a collective condensation, which is qualitatively distinct from a Bose Einstein condensation of single particle excitations into a delocalized state. In particular, in non-frustrated Bose glasses, I do not find evidence for a boson mobility edge in the Bose glass.

4.1 Models

The phenomenon of Anderson localization is well epitomized by the model of a spinless quantum particle hopping on a lattice [1], as it arises e.g. in the impurity band of a semiconductor if interactions are neglected:

$$H = -\sum_i \epsilon_i n_i - \sum_{\langle i,j \rangle} t_{ij} \left(c_i^\dagger c_j + c_j^\dagger c_i \right). \tag{4.1}$$

Here ϵ_i is a random onsite potential and t_{ij} is the hopping strength. For simplicity we will take ϵ_i to be uniformly distributed in $[-W, W]$, and choose energy units such that $W = 1$. The operators $c_i(c_i^\dagger)$ create or annihilate a fermion at the lattice site i. This model has been extensively studied numerically. In 3d, at weak disorder, most eigenstates are delocalized, apart from the band edges which are separated from the continuum of extended states by the mobility edge. Upon increase of the disorder the mobility edges progress toward the bulk of the spectrum. The states in the middle of the band ($E = 0$) are the last to become localized. On a 3d cubic lattice, this happens when the hopping becomes weaker than $t_c \approx 0.12$. [73] The single particle

wavefunctions at the mobility edge are neither fully delocalized (space-filling) nor fully localized, but exhibit interesting multifractal properties [5].

Given the canonical model (4.1) of localization of free fermions, it is interesting to ask how a canonic model of bosons will behave, i.e., when replacing fermionic with bosonic operators $c_i(c_i^\dagger) \to b_i(b_i^\dagger)$. However, as mentioned above, non-interacting disordered bosons exhibit pathological behavior, since they simply condense into the lowest lying single particle wavefunction, which is generically a strongly localized state at the extreme of the Lifshitz tail of the density of states. To remedy this pathology, interactions must be included in the bosonic case. A particularly interesting case is that of *hard-core* bosons which locally repel each other infinitely strongly. This is very similar to the local constraints of free spinless fermions, which obey the Pauli exclusion principle. In both cases at most one particle can occupy a given lattice site. The models differ, however, due to the exchange statistics. In the case of hard core bosons, the local repulsion renders the system genuinely interacting, while 'hard core' fermions can of course be understood entirely by solving the single particle problem at all energies. The difference of quantum statistics is ultimately responsible for the fact that superfluids of bosons survive weak disorder in 2 spatial dimensions, whereas repulsive fermions are generically prone to localize and form insulators at low temperature. How precisely a disordered Bose glass turns into a delocalized superfluid, especially in low dimensions, is not understood in detail. Several questions as to the localization of excitations in the Bose glass, the existence of bosonic mobility edges, or a finite temperature "many-body delocalization" are also under debate and serve as a motivation for the present analysis, which provides a small step towards a better understanding of some of those issues.

Physical realizations of hard core bosons arise naturally in several contexts: Apart from the obvious example of strongly repulsive cold bosonic atoms, hard core bosons emerge in correlated materials with a strong local negative U attraction where all electron sites are either empty or host two electrons of opposite spin. Naturally, such singlets form hard core bosons. A minimal description in the presence of disorder is given by the Hamiltonian

$$H_{\mathrm{hcb}} = -\sum_i \epsilon_i n_i - \sum_{\langle i,j \rangle} t_{ij} \left(b_i^\dagger b_j + b_j^\dagger b_i \right), \tag{4.2}$$

where interactions are retained only in the form of a local hard core constraint. Such a Hamiltonian was also obtained in an approximate description of strongly disordered superconductors by Ma and Lee [20], who generalized the BCS wavefunction to be constructed out of doubly occupied or empty single particle wavefunctions. Each such orbital forms an Anderson pseudospin, i.e., a hard core boson, which will be localized if the disorder is strong. The Ma-Lee model allows one to describe approximately the superfluid-to-insulator transition in strongly disordered systems with predominant attractive interactions. Recently this approach has been extended to take into account fractality of the paired single particle states [74, 75], which translates into unusual statistics of the pair hopping elements t occurring in (4.2).

The thermodynamics of the Hamiltonian (4.2) was studied extensively with quantum Monte Carlo techniques in the past [45] as a model for the disorder driven

superfluid-insulator transition. Recently the model was revisited from the perspective of localization of excitations in the insulating regime [29, 52]. Interestingly, clear signs of the quantum statistics, i.e. differences between fermions and hard core bosons, appear already deep in the insulating regime [51]: In $d > 1$ one finds that low energy excitations of hard core bosons delocalize more readily than fermions when subjected to the same disorder potential [51]. A more important difference is the fact that the wavefunctions of localized excitations react in an opposite sense to a magnetic field: While fermionic excitations tend to become more delocalized due to the suppression of negative interference of alternative tunneling paths, bosonic wavefunctions tend to contract under a magnetic field. This leads to strong, opposite magnetoresistance in the low temperature transport of such insulators.

4.1.1 Disordered spin models

The Hamitonian Eq. (4.2) of disordered hardcore bosons is equivalent to a XY ferromagnet $s = 1/2$ spins in a random transverse field, using the isomporhism $b_i^\dagger = \sigma_i^- = \frac{1}{2}(\sigma_i^x - i\sigma_i^y)$, $b_i = \sigma_i^+ = \frac{1}{2}(\sigma_i^x + i\sigma_i^y)$, $n_i = (\sigma_i^z + 1)/2$:

$$\begin{aligned} H_{\rm XY} &= -\sum_i \epsilon_i \sigma_i^z - J \sum_{\langle i,j \rangle} \left(\sigma_i^x \sigma_j^x + \sigma_i^y \sigma_j^y \right), \\ &= 2H_{\rm hcb} + \text{const.}, \end{aligned} \tag{4.3}$$

where we took the hopping/exchange $t_{ij} = J$ to be uniform. In (4.3) the operators $\sigma_i^{x,y,z}$ are Pauli matrices.

At zero temperature, this model exhibits a localized Bose glass phase (paramagnet) for $t, J \ll W$. In $d > 1$ dimensions, a superfluid (ferromagnetic) phase is expected for $t, J \gg W$, while in strictly one-dimensional chains, the system is known to be fully localized irrespective of the weakness of disorder.

We will contrast the model (4.3) with the closely related Ising model

$$H_{\rm Ising} = -\sum_i \epsilon_i \sigma_i^z - J \sum_{\langle i,j \rangle} \sigma_i^x \sigma_j^x. \tag{4.4}$$

While the hardcore boson model conserves particle number and possesses the related continuous $U(1)$ symmetry, the model (4.4) has only a discrete Ising symmetry $\sigma^x \to -\sigma^x$. For brevity we shall refer to the above models as the XY and Ising models, respectively. Below we will see how the two symmetries lead to differences in the localization properties of excitations in the localized phases.

4.1.2 Review of previous results

Many theoretical studies have focused on interacting bosons in one dimension, both at $T = 0$ and finite temperature. For the example of the interacting Bose gas, in the weak disorder strong interacting regime, a superfluid-Bose glass quantum phase transition occurs at a universal value of the Luttinger liquid parameter [7]. In the weak interacting

limit, where the Luttinger liquid description is not valid. By different approaches [76, 77, 78]. People show that there is also a Bose-glass to superfluid quantum phase transition, while the transition value is no longer universal [79]. At finite temperature, weakly interacting bosons gas exhibits a finite-temperature phase transition between fluid and insulator in the presence of disorder [80]. The transition temperature can be seen as the many-body analogue of the mobility edge which separates localized and delocalized states in the single particle Anderson transition.

In higher dimensions the disordered XY model can develop true long-range order. Quite a lot of numerical work has been done in this direction [45, 81, 82]. Phenomenological considerations of (4.3) have been presented in Ref. [52]. And later a mean-field analysis is available [28, 29] where the model (4.3) has been studied on a Cayley tree with large connectivity.

In this Chapter we revisit the models Eqs. (4.3) and (4.4) on general lattices deep in their insulating (disordered) phase, working to leading order in small hopping. We study the localization properties of excitations, by analyzing the life time of excitations due to an infinitesimal coupling to a bath at the boundaries of the sample, which allows us to characterize the exponential localization of bulk excitations. Comparing this perturbative approach to exact results for one-dimensional spin chains, we find exact agreement to leading order in hopping, and qualitative agreement in terms of the phenomenology. Especially, we find that both approaches predict that excitations are the more delocalized the lower the energy, at least in the lower part of the energy spectrum. In order to be able to approach the vicinity of the transition to a superfluid, we apply the formalism to a Cayley tree of large connectivity, where a perturbative approach is valid up to a parametrically small vicinity of the superfluid transition. However, in contrast to the analysis of Refs. [28, 29] where this problem was first studied, we find that in the spin models with either symmetry non-extensive excitations are localized in the insulating phase. In other words, in the considered models with uniform disorder potential, we do not find evidence for a mobility edge of bosonic excitations at finite energies. In particular, within the approximation to leading order in the hopping, the superfluidity of bosons appears as a delocalization phenomenon at zero energy, without preceding delocalization of excitations at low but finite energy.

4.2 Decay rate of local excitations

In this Section we study the decay of local excitations (spin flips) sufficiently deep within the disordered phases (i.e., the insulating Bose glass or the paramagnet) of the models (4.3) and (4.4), respectively. The transverse quantum fluctuations due to the exchange J (or hopping t) allow spin flips to propagate over some distance. However, within a localized regime, they die off exponentially at large distance. Following in spirit Anderson's approach to single particle localization, we characterize localization by the decay rate Γ of a local excitation, as induced by the coupling to a bath at the distant boundaries of the sample. In the localized phase Γ is exponentially small in the linear size of the system. A good measure for the localization radius ξ of such excitations is thus given by the decrease of $\log(\Gamma)$ with the distance R to the bound-

ary, which generally behaves as $\log \Gamma \approx -2R/\xi$. For delocalization, and thus energy diffusion, to occur in a many body context, typical decay rates must remain finite in the thermodynamic limit, as the system size tends to infinity, while the coupling to the bath is kept infinitesimal.

We study the models (4.3) and (4.4) on a general lattice Λ. We assume the system to be coupled infinitesimally to a zero temperature bath via the spins on a "boundary set" $\partial\Lambda$ of the lattice, which becomes infinite in the thermodynamic limit, too. Later on, to simplify the discussion, we will chose this subset to be the spatial boundary of the finite lattice Λ. [1] All boundary sites $l \in \Lambda$ are assumed to be coupled to independent, identical baths, described by a continuum of non-interacting harmonic oscillator modes $b_{\alpha,l}$ of energy ϵ_α and coupling strength λ_α:

$$H_{\rm b} = \sum_{l\in\partial\Lambda}\sum_{\alpha} \epsilon_\alpha b^\dagger_{\alpha,l} b_{\alpha,l}. \tag{4.5}$$

Such a bath is characterized by its spectral function

$$J_b(\epsilon) = \sum_\alpha \lambda_\alpha^2 \delta(\epsilon - \epsilon_\alpha). \tag{4.6}$$

For both the XY and Ising models we consider the following system-bath couplings:

$$\begin{aligned} H &= H_0 + H_{\rm s,b} + H_{\rm b}, \\ H_{\rm s,b} &= \sum_{l\in\partial\Lambda} \sigma^x_l \sum_\alpha \lambda_\alpha \left(b^\dagger_{\alpha,l} + b_{\alpha,l} \right), \end{aligned} \tag{4.7}$$

where $H_0 = H_{\rm XY,Ising}$ is the uncoupled spin Hamiltonian. Obviously, the details of the coupling to the bath are irrelevant for the determination of localization radii ξ of localized excitations, or to determine presence of delocalization.

In the limit $t \ll 1$, the ground state is well approximated by the product state

$$|{\rm GS}\rangle \approx \otimes_{i\in\Lambda} |\sigma^z_i = {\rm sign}(\epsilon_i)\rangle \ . \tag{4.8}$$

Let us now characterize the temporal decay of a local excitation close to the site $0 \in \Lambda$ in the bulk of the lattice. As a canonic example we will study the spin flip excitation $\sigma^x_0|{\rm GS}\rangle$. For $J = 0$ this creates the excited state

$$|E_0\rangle = \otimes_{i\in\Lambda} |\sigma^z_i = (1 - 2\delta_{0i}){\rm sign}(\epsilon_i)\rangle \ . \tag{4.9}$$

At finite J we denote by the same ket $|E_0\rangle$ the eigenstate, which evolves adiabatically from the excited state (at $J = 0$) and thus has largest overlap with the local spin flip excitation at small J. Our aim is to determine the life time of that eigenstate. It

[1] If one has only the purpose of distinguishing a localized from a delocalized phase, one might also choose to couple to a bath at every site, taking $\partial\Lambda = \Lambda$. In that case one usually just asks whether the thermodynamic limit and the limit of vanishing bath coupling commute (insulator) or not (delocalized phase). Here we mostly want to characterize the decay of localized excitations, for which a coupling at the boundary is more convenient.

is finite since the coupling to the bath induces decays to lower energy states, and in particular back to the ground state. As an explicit calculation below will confirm the life time can be evaluated simply by applying Fermi's Golden rule.

One should naturally ask whether the life time of spin flip excitations (which carry Ising or $U(1)$ charge) should be characteristic for the lifetime of other excited states that are created by local operators. Among the excitations that transform the same way under Ising or XY symmetry operations, one expects the localization length deep in the disordered phase, defined via the exponentially small inverse life time, to be the same function of energy as that of single spin flips. This is because the propagation to long distances proceeds furthest by making the minimal use of exchange couplings. At energies below the bandwidth this is always achieved by the shortest chains of exchange bonds between the location of excitation and the point of observation, which will be analyzed in detail below. For excitations with different symmetry, e.g. neutral ones like a pair of opposite spin flips, the localization is stronger in the regime of small J, since the matrix element to transfer such an excitation a distance R away decays as $\sim J^{2R}$, as compared to the amplitude $\sim J^R$ for single spin flips. However, we do not know whether this property remains true all the way to the ordering transition, where the expansion in J starts to diverge, and an estimate of the relative importance of various propagation channels is very difficult, and presumably dependent on the details of the considered model. Throughout this paper we thus stay within regimes where the perturbative expansion in the small exchange J is controlled.

In order to make the above notions formally precise, we define the retarded spin correlator

$$G_{l,0}(t) \equiv -i\Theta(t)\, {}_b\langle \mathrm{GS}|[\sigma_l^x(t), \sigma_0^x]|\mathrm{GS}\rangle_b, \tag{4.10}$$

where $|\mathrm{GS}\rangle_b = |\mathrm{GS}\rangle \otimes |\mathrm{bath}\rangle$ denotes the ground state of the uncoupled system and bath, $|\mathrm{GS}\rangle$ being the ground state of H_I, $H_I|\mathrm{GS}\rangle = E_{\mathrm{GS}}|\mathrm{GS}\rangle$, and $A(t) = e^{-iHt}Ae^{iHt}$ are Heisenberg operators. In the following, we will analyze in particular local correlators, such as $G_{0,0}(t)$. It will be convenient to study these correlators in the frequency domain

$$G_{l,0}(\omega) = \int_{-\infty}^{\infty} dt \mathrm{e}^{i(\omega+i\eta)t} G_{l,0}(t), \tag{4.11}$$

with $\eta \to 0^+$. Introducing $\mathcal{U}(t) = \mathrm{e}^{iH_0t}\mathrm{e}^{-iHt}$, we can write

$$\begin{aligned} G_{0,0}(t) = & \\ & -i\Theta(t)\, {}_b\langle \mathrm{GS}|[\mathcal{U}^\dagger(t)\mathrm{e}^{iH_0t}\sigma_0^x\mathrm{e}^{-iH_0t}\mathcal{U}(t), \sigma_0^x]|\mathrm{GS}\rangle_b. \end{aligned} \tag{4.12}$$

We evaluate (4.12) perturbatively in the coupling to the bath, expanding $\mathcal{U}(t)$ in λ_α. To second order one has

$$\begin{aligned} \mathcal{U}(t) \;\simeq\; & 1 - i\int_0^t dt_1 H_{\mathrm{s,b}}(t_1) \\ & - \int_0^t dt_1 \int_0^{t_1} dt_2 H_{\mathrm{s,b}}(t_1) H_{\mathrm{s,b}}(t_2) + O(\lambda_\alpha^3), \end{aligned} \tag{4.13}$$

where $H_{\rm s,b}(t) = {\rm e}^{iH_0 t} H_{\rm s,b} {\rm e}^{-iH_0 t}$. Inserting into $G_{0,0}(\omega)$ we obtain the expansion

$$G_{0,0}(\omega) = G^{(0)}_{0,0}(\omega) + G^{(2)}_{0,0}(\omega) + o(\lambda_\alpha^2), \tag{4.14}$$

whereby the linear term in λ_α vanishes due to conservation of the parity of the total spin projection, $\sum_i \sigma_i^z$. The leading term is

$$G^{(0)}_{0,0}(\omega) = \sum_n \left(\frac{|\langle {\rm GS}|\sigma_0^x|E_n\rangle|^2}{\omega + E_{\rm GS} - E_n + i\eta} - \frac{|\langle E_n|\sigma_0^x|{\rm GS}\rangle|^2}{\omega + E_n - E_{\rm GS} + i\eta} \right), \tag{4.15}$$

where n runs over all eigenstates of H_I labeled by their energy E_n.

The second order term $G^{(2)}_{0,0}(\omega)$ has a relatively complicated structure for arbitrary ω. However, we are particularly interested in understanding the life time of excitations, i.e., the imaginary part of the poles that appear in the leading term $G^2_{0,0}(\omega)$. Therefore we focus on $\omega \approx E_n - E_{\rm GS}$, and extract only the most singular term in the imaginary part of $G^{(2)}_{0,0}(\omega \to E_n - E_{\rm GS})$, which evaluates to:

$$\begin{aligned} {\rm Im}\, G^{(2)}_{0,0}(\omega \to E_n - E_{GS}) &= -\pi \frac{|\langle {\rm GS}|\sigma_0^x|E_n\rangle|^2}{(\omega + E_{\rm GS} - E_n)^2} \\ &\times \sum_{l\in\partial\Lambda} \sum_{E_m<E_n} J_b(E_n - E_m) |\langle E_m|\sigma_l^x|E_n\rangle|^2 \\ &\times \left[1 + O(\omega + E_{\rm GS} - E_n)\right]. \end{aligned} \tag{4.16}$$

As the bath couplings and the spectral functions $J_b(\omega)$ are assumed to be very small, we can account for this imaginary part as a shift of the poles into the complex plane:

$$G_{0,0}(\omega) \approx \sum_n \frac{|\langle {\rm GS}|\sigma_0^x|E_n\rangle|^2}{\omega - (E_n - E_{\rm GS} - i\Gamma_n/2)}, \tag{4.17}$$

where, to quadratic oder in the bath coupling,

$$\begin{aligned} \Gamma_n &= 2\pi \sum_{l\in\partial\Lambda} J_b(E_n - E_{GS}) |\langle {\rm GS}|\sigma_l^x|E_n\rangle|^2 \\ &\quad + 2\pi \sum_{l\in\partial\Lambda} \sum_{E_{\rm GS}<E_m<E_n} J_b(E_n - E_m) |\langle E_m|\sigma_l^x|E_n\rangle|^2 \end{aligned}$$

is the decay rate of the excited state n under emission of a bath mode. This is easily recognized as the inverse life time expected from Fermi's Golden rule. We have dropped the real parts of the self-energies which shift the poles by small amounts proportional to the coupling to the bath.

Note that the rate Γ_n includes the decay to the ground state as well as to other excited states of lower energy. However, we will merely focus on the contribution from the decay to the ground state,

$$\Gamma_n^{(GS)} = 2\pi J_b(E_n - E_{GS}) \sum_{l\in\partial\Lambda} |\langle {\rm GS}|\sigma_l^x|E_n\rangle|^2. \tag{4.18}$$

This indeed suffices for our purposes, for two reasons: On one hand, if we are interested in the rate at which energy escapes the system, we should not consider decays to other excited states, since those retain part of the excitation energy within the system. On the other hand, the relevant contributions to the full inverse life time due to decays into excited states are comparable in magnitude to the contribution form the decay to the ground state. Therefore the latter furnishes enough information to determine the localization radius of the excitations in a deeply insulating regime.

As we explained before, we are interested in the dominant excited state $|E_n\rangle = |E_0\rangle$, for which, according to (4.18), we need to evaluate the matrix element

$$\langle \mathrm{GS}|\sigma_l^x|E_0\rangle \approx \langle \mathrm{GS}|\sigma_l^x|E_0\rangle\langle E_0|\sigma_0^x|\mathrm{GS}\rangle \equiv A_{l0}, \tag{4.19}$$

since $\langle E_0|\sigma_0^x|\mathrm{GS}\rangle = 1 - O(J^2)$. Note the asymmetry of l and 0 in the definition of this amplitude: $A_{l0} \neq A_{0l}$. The first index denotes the site where the excitation probed, which is centered at site 0, while l is the site at which the excitation is probed.

From a Lehmann representation of the retarded Green's function (4.10) it becomes clear that A_{l0} is simply one of its residues:

$$\begin{aligned} G_{l,0}(\omega) &= \int_{-\infty}^{\infty} -i\Theta(t)\langle \mathrm{GS}|\left[\sigma_l^x(t), \sigma_0^x\right]|\mathrm{GS}\rangle e^{i(\omega+i\eta)}dt \\ &= \sum_n \langle E_n|\sigma_0^x|\mathrm{GS}\rangle\langle \mathrm{GS}|\sigma_l^x|E_n\rangle \times \\ &\times \left[\frac{1}{\omega - (E_n - E_{\mathrm{GS}} - i\eta)} - \frac{1}{\omega + (E_n - E_{\mathrm{GS}} + i\eta)}\right]. \end{aligned}$$

Indeed, the pole at $\omega = E_0 - E_{GS}$ has the desired matrix element as residue,

$$A_{l0} = \lim_{\omega \to E_0 - E_{\mathrm{GS}}} [\omega - (E_0 - E_{\mathrm{GS}})] G_{l,0}(\omega). \tag{4.20}$$

This observation can be used to determine A_{l0} in perturbation theory in J in an efficient manner, by solving recursively the equation of motion for $G_{l,0}$ in a locator expansion. As we will discuss further below, the matrix elements A_{l0} are needed not only to calculate the decay rate to the ground state, but also to determine the onset of long range order.

The above derivation is easily adapted for the XY model, cf. Sec. 4.2.2.

4.2.1 Equations of motion - Ising model

Let us now evaluate the Green's function $G_{l,0}(t)$ to the leading order in the exchange J. We first split $G_{l,0}(t)$ into two parts

$$\begin{aligned} G_{l,0}(t) &= G_{l,0}^+(t) + G_{l,0}^-(t), \\ G_{l,0}^\pm(t) &= -i\Theta(t)\langle \mathrm{GS}|\left[\sigma_l^\pm(t), \sigma_0^x\right]|\mathrm{GS}\rangle, \end{aligned} \tag{4.21}$$

which satisfy simpler equations of motion,

$$i\frac{dG_{l,0}^\pm(t)}{dt} = \delta(t)\langle\left[\sigma_l^\pm(t), \sigma_0^x\right]\rangle - i\Theta(t)\langle\left[i\dot{\sigma}_l^\pm(t), \sigma_0^x\right]\rangle. \tag{4.22}$$

The spin flip operators $\sigma_l^{\pm}(t)$ satisfy Heisenberg equations. For the Ising model, they read

$$i\dot{\sigma}_l^{\pm}(t) = \left[\sigma_l^{\pm}, H_0\right] = \pm 2\epsilon_l \sigma_l^{\pm}(t) \mp J\sigma_l^z(t) \sum_{j\in\partial l} \sigma_j^x(t). \tag{4.23}$$

The sum is over the set ∂l of nearest-neighbors of site l. To leading order in J, we can restrict ourselves to the neighbors j which are closer to the site 0 than l, since other terms lead to contributions of higher order in J. Furthermore, when evaluating the expectation value in the last term of Eq. (4.22), we can decouple the average over $\sigma_l^z(t)$ from the other operators,

$$\langle \sigma_l^z(t)\sigma_j^x ...\rangle = \langle \sigma_l^z(t)\rangle \langle \sigma_j^x ...\rangle \tag{4.24}$$

and use $\langle \sigma_l^z(t)\rangle = \mathrm{sign}(\epsilon_l) + O(J^2)$. Corrections to this approximation lead again to higher powers of J. However, they can be determined systematically by an extension of the present approach [83]. To the leading order, the recursion relations for the Green's functions, after Fourier transform, become

$$(2\epsilon_l \mp \omega) G_{l,0}^{\pm} = J\,\mathrm{sign}(\epsilon_l) \sum_{j\in\partial l} G_{j,0}(\omega). \tag{4.25}$$

Solving for $G_{l,0}(\omega)$ from Eq. (4.21) we obtain the recursion relation

$$G_{l,0}(\omega) = \sum_{j\in\partial l} J\,\mathrm{sign}(\epsilon_l) \frac{4\epsilon_l}{(2\epsilon_l)^2 - \omega^2} G_{j,0}(\omega), \tag{4.26}$$

which is exact to leading order in J. Upon iterating the recursion until we reach the site 0, we obtain the leading order of the Green's function as a sum over all shortest paths from l to 0 (of length $L = \mathrm{d}ist(l,0)$, the Hamming distance on the lattice between l and 0)

$$G_{l,0}(\omega) \approx \sum_{\mathcal{P}=\{j_0=0,..,j_L=l\}} \prod_{p=1}^{L=\mathrm{dist}(l,0)} \frac{4J|\epsilon_{j_p}|}{(2\epsilon_{j_p})^2 - \omega^2} G_{0,0}(\omega).$$

Notice that $G_{0,0}(\omega \to E_0 - E_{\mathrm{GS}}) \approx \frac{1}{\omega + E_{\mathrm{GS}} - E_0}$. Therefore, the sought residue of the corresponding pole in $G_{l,0}(\omega)$ around $\omega = E_0 - E_{\mathrm{GS}} = 2|\epsilon_0| + O(J^2)$ is

$$\begin{aligned} A_{l0} &= \left.\frac{G_{l,0}(\omega)}{G_{0,0}(\omega)}\right|_{\omega=2|\epsilon_0|} \\ &= \sum_{\mathcal{P}=\{j_0=0,..,j_L=l\}} \prod_{p=1}^{L} \frac{J|\epsilon_{j_p}|}{\epsilon_{j_p}^2 - \epsilon_0^2}, \end{aligned} \tag{4.27}$$

to the leading order in J.

4.2.2 Equations of motion - XY model

It is straightforward to repeat the same steps for the XY model. Without loss of generality, we suppose that the flipped spin sits on a site 0 with $\epsilon_0 \geq 0$ and thus essentially points up in the ground state. We aim at the matrix element of the operator σ_l^x between the ground state and the excited eigenstate $|E_0\rangle = \sigma_0^-|\mathrm{G}S\rangle$ (up to corrections of order $O(J^2)$),

$$\langle \mathrm{GS}|\sigma_l^x|E_0\rangle \approx \langle \mathrm{GS}|\sigma_l^+|E_0\rangle\langle E_0|\sigma_0^-|\mathrm{GS}\rangle \equiv A_{l0}. \tag{4.28}$$

We thus define the relevant Green's function as

$$G_{l,0}^{XY}(t) \equiv -i\Theta(t)\langle \mathrm{GS}|[\sigma_l^+(t), \sigma_0^-]|\mathrm{GS}\rangle. \tag{4.29}$$

Employing the Lehmann representation and solving recursively the equations of motion in powers of J, allows us to extract the matrix element of interest

$$\begin{aligned} A_{l0} &= \left.\frac{G_{l,0}^{\mathrm{XY}}(\omega)}{G_{0,0}^{\mathrm{XY}}(\omega)}\right|_{\omega=2|\epsilon_0|} \\ &= \sum_{\mathcal{P}=\{j_0=0,..,j_L=l\}} \prod_{p=1}^{L} \frac{J\mathrm{sign}(\epsilon_{j_p})}{\epsilon_{j_p} - |\epsilon_0|}, \end{aligned} \tag{4.30}$$

to the leading order in powers of J.

Notice the difference between Eqs. (4.30) and (4.27), which arises due to the different symmetries of the two models. Indeed, in the Ising model, by a gauge transformation, one can always choose $\epsilon_i > 0$, and therefore the physical correlators can only be functions of $|\epsilon_j|$. However, the same is not true for the XY model. Furthermore, the XY model the total spin $\sum_i \sigma_i^z$ (or the number of hard-core bosons) is conserved. In contrast, the Ising model only preserves its parity, which allows for more quantum fluctuations. The difference shows at finite excitation energies $\omega = 2|\epsilon_0|$, but disappears at low energies, $\epsilon_0 \to 0$ within the leading order approximation.

4.2.3 Comparison with non-interacting particles (fermions)

The result (4.30) was derived in Ref. [51] for hard core bosons. Using the correspondence $J \to t$, one obtains, up to subleading corrections,

$$\langle \mathrm{GS}|b_l^\dagger|E_0\rangle = A_{l0},$$

where in this case we denote by

$$|E_0\rangle = b_0|\mathrm{G}S\rangle + O(t)$$

the excited state with a boson removed from site 0.

Note that it has nearly the same form as the analogous sum for non-interacting fermions [1], which can be obtained from a recursive solution of the Schrödinger equation, but is also easily rederived in the same fashion as for bosons. The fermion result

differs only by the absence of the sign factors in the numerator $sign(\epsilon)$. This is easy to understand physically: Consider a loop formed by two shortest paths between two different sites. Taking the first path in forward direction and the second path back, a ring exchange of particles is performed, since in the process each particle is moving to the next negative energy site ahead of it on the loop. The corresponding amplitude for bosons and fermions should differ by an extra sign factor, if there is an odd number of particles on the loop (in the ground state). This results precisely in the extra factor $\prod_{j\in loop} \mathrm{sign}(\epsilon_j)$ which makes bosons distinct from fermions.

One should note that for non-interacting fermions the recursion relation for the Green's function is exact and does not require the decoupling of the correlation function obtained from taking a time derivative to obtain a closed recursion relation. Therefore the full Green's function can be expressed formally exactly as a sum over *all* paths, with amplitudes being products of the locators $t/(\epsilon_i - \omega)$, analogous to Eq. (4.30) without signs. In contrast, for hard core bosons this simple form is exact only for contributions from non-intersecting paths, with each link contributing a single factor of J. Loop corrections take a more involved form and require an extension of the equation of motion techniques used above [83].

4.3 One-dimensional case: chains

In order to better appreciate certain features of higher dimensional cases, it turns out to be useful to review some properties of one-dimensional chains, which are known due to their exact solvability due to exact mappings to free fermions [84], bosonization techniques [7] and approaches via strong randomness renormalization group [85, 86]. The latter was indeed developped for random transverse field Ising chains, while it is not well controlled for the XY case, since the RG does not flow to infinite randomness.

It is well-established that the random transverse field XY model, or hard core bosons in strictly 1 dimension does not exhibit a quantum phase transition, but only possesses the paramagnetic (insulating) phase. This can easily be seen from after a Jordan-Wigner transformation, which maps the hard core bosons to free fermions, which are always localized, even if the disorder potential is very weak. In bosonization language hard core bosons in weak disorder are described by a Luttinger liquid with Luttinger parameter $K = 1$. The interaction shave to be rendered sufficiently soft core to increase K above $K_c = 3/2$ to allow for a superfluid phase in sufficiently weak disorder [7, 87].

In contrast, the random transverse field Ising chain does undergo a para-to-ferromagnetic quantum phase transition, which is captured by strong disorder fixed point [85]. Some of its properties will be recalled below, to the extent that they are relevant to our discussion for higher dimenions.

We consider the strictly one-dimensional random transverse field Ising model

$$H = -\sum_j \epsilon_j \sigma_j^z - J \sum_j \sigma_j^x \sigma_{j+1}^x. \tag{4.31}$$

As mentioned above, by a gauge transformation, we can choose $\epsilon_i > 0$. Following the

transformations and notations of Ref. cite3ddisoerderedhardcorebosons, we introduce free fermions by the Jordan-Wigner transformation

$$c_j = \sigma_j^- e^{i\pi \sum_{k<j} \sigma_k^+ \sigma_k^-}, \quad c_j^\dagger = \sigma_j^+ e^{-i\pi \sum_{k<j} \sigma_k^+ \sigma_k^-}. \tag{4.32}$$

They satisfy the canonical anti-commutation relations

$$\{c_j^\dagger, c_k\} = \delta_{jk}, \quad \{c_j^\dagger, c_k^\dagger\} = \{c_j, c_k\} = 0. \tag{4.33}$$

In terms of fermionic degrees of freedom, the model (4.31) can be written as

$$H = \sum_{jk} \begin{pmatrix} c_j^\dagger & c_j \end{pmatrix} \mathcal{H}_{jk} \begin{pmatrix} c_k \\ c_k^\dagger \end{pmatrix}, \tag{4.34}$$

where

$$\mathcal{H}_{jk} = \frac{1}{2} \begin{pmatrix} \mathcal{D}_{jk} + \mathcal{D}_{jk}^\dagger & \mathcal{D}_{jk} - \mathcal{D}_{jk}^\dagger \\ \mathcal{D}_{jk}^\dagger - \mathcal{D}_{jk} & -\mathcal{D}_{jk} - \mathcal{D}_{jk}^\dagger \end{pmatrix}, \tag{4.35}$$

and $\mathcal{D}$ is the matrix defined as

$$\mathcal{D}_{jk} = -\epsilon_j \delta_{jk} - J\delta_{j,k-1}. \tag{4.36}$$

It is useful to perform a unitary transformation

$$(i\gamma_j^1, \gamma_j^2) = (c_j^\dagger, c_j)U, \tag{4.37}$$

with

$$U = \frac{1}{\sqrt{2}} \begin{pmatrix} 1 & 1 \\ -1 & 1 \end{pmatrix}. \tag{4.38}$$

The operators $\gamma_j^{1(2)}$ are Majorana fermions corresponding to the real (imaginary) parts of $c_j^\dagger$. In terms of those the Hamiltonian takes the form

$$H = \sum_{jk} \begin{pmatrix} i\gamma_j^1 & \gamma_j^2 \end{pmatrix} \widetilde{\mathcal{H}}_{jk} \begin{pmatrix} -i\gamma_k^1 \\ \gamma_k^2 \end{pmatrix}, \tag{4.39}$$

where

$$\widetilde{\mathcal{H}} = U^{-1}\mathcal{H}U = \begin{pmatrix} 0 & \mathcal{D} \\ \mathcal{D}^\dagger & 0 \end{pmatrix}, \tag{4.40}$$

which makes explicit the chiral symmetry of the problem. Indeed, the classification of Altland and Zirnbauer [88], the single particle Hamiltonian $\widetilde{\mathcal{H}}$ belongs to the chiral class BDI [86, 82]: $\widetilde{\mathcal{H}}$ is real, and there exists a matrix Σ^3,

$$\Sigma^3 = \begin{pmatrix} 1 & 0 \\ 0 & -1 \end{pmatrix}, \tag{4.41}$$

such that

$$\Sigma^3 \widetilde{\mathcal{H}} \Sigma^3 = -\widetilde{\mathcal{H}}. \tag{4.42}$$

4.3.1 Transfer matrix approach

For a chain of the length L, a $2L \times 2L$ unitary matrix V diagonalizes $\widetilde{\mathcal{H}}$,

$$V\widetilde{\mathcal{H}}V^{-1} = \mathrm{d}iag(\omega_1, ..., \omega_{2L}), \tag{4.43}$$

which implies that its n'th column vector $(\psi^1_{n,i}, \psi^2_{n,i})$ satisfies the Schrödinger equation

$$\begin{pmatrix} 0 & \mathcal{D} \\ \mathcal{D}^\dagger & 0 \end{pmatrix} \begin{pmatrix} \psi^1_n \\ \psi^2_n \end{pmatrix} = \omega_n \begin{pmatrix} \psi^1_n \\ \psi^2_n \end{pmatrix}. \tag{4.44}$$

The corresponding operators

$$d_n = \sum_{i=1}^{L} \left[\psi^1_{n,i}(-i\gamma^1_i) + \psi^2_{n,i}\gamma^2_i\right] \tag{4.45}$$

and their conjugates satisfy canonical anticommutation relations. They annihilate fermionic degrees of freedom of energy ω_n, $[H, d_n] = -\omega_n d_n$.

In the lattice basis, Eq. (4.44) takes the explicit form

$$\sum_j \mathcal{D}_{ij}\psi^2_j = \omega\psi^1_i, \tag{4.46}$$

$$\sum_j \mathcal{D}^\dagger_{ij}\psi^1_j = \omega\psi^2_i, \tag{4.47}$$

where from here on we drop the mode index n. Noting that in these sums j is restricted to the values $i-1, i$ or $i+1$, we find

$$\mathcal{D}_{ii+1}\psi^2_{i+1} = \omega\psi^1_i - \mathcal{D}_{ii}\psi^2_i - \mathcal{D}_{ii-1}\psi^2_{i-1}, \tag{4.48}$$

$$\mathcal{D}^\dagger_{ii+1}\psi^1_{i+1} = \omega\psi^2_i - \mathcal{D}^\dagger_{ii}\psi^1_i - \mathcal{D}^\dagger_{ii-1}\psi^1_{i-1}. \tag{4.49}$$

Using Eq. (4.36) and the fact that $\mathcal{D}_{i,i-1} = \mathcal{D}^\dagger_{ii+1} = 0$, this can be rewritten in the form of a recursive relation [84, 85]

$$\begin{pmatrix} \psi^1_{i+1} \\ \psi^2_{i+1} \end{pmatrix} = T_i(\omega) \begin{pmatrix} \psi^1_i \\ \psi^2_i \end{pmatrix}, \tag{4.50}$$

where the transfer-matrix $T_i(\omega)$ is given by

$$T_i(\omega) \;=\; \begin{pmatrix} -\frac{J}{\epsilon_{i+1}}\left(1 - \frac{\omega^2}{J^2}\right) & -\frac{\omega\epsilon_i}{J\epsilon_{i+1}} \\ -\frac{\omega}{J} & -\frac{\epsilon_i}{J} \end{pmatrix}. \tag{4.51}$$

4.3.2 Localization length

Except at the critical point all the mode functions ψ_i are exponentially localized. The typical localization length of these fermions, $\xi_{typ,f}$ can be extracted from the full

transfer matrix $\mathcal{M}(\omega) = T_L(\omega)...T_2(\omega)T_1(\omega)$, as its inverse of the largest Lyapunov exponent. This yields

$$\frac{1}{\xi_{typ,f}(\omega)} = \lim_{L\to\infty} \frac{1}{2L} \log[\max(\lambda_1, \lambda_2)], \tag{4.52}$$

where λ_1, λ_2 are the two eigenvalues of $\mathcal{M}^T(\omega)\mathcal{M}(\omega)$.

In the limit of zero energy, $\omega \to 0$, the two blocks of the transfer matrix decouple, and one can immediately read off the typical localization length as [2]

$$\frac{1}{\xi_{typ,f}(0)} = \left|\overline{\log\left(\frac{\epsilon_i}{J}\right)}\right| \equiv \left|\log\left(\frac{J_c}{J_c - \Delta}\right)\right|. \tag{4.53}$$

Here the overbar denotes the disorder average over the random onsite energies ϵ_i. J_c denotes the value of the critical exchange coupling, where $\xi_{typ,f}$ diverges at $\omega = 0$. J_c is given by the condition [85] $0 = \overline{\log(\epsilon_i/J_c)}$. $\Delta \equiv J_c - J$ is a measure of the detuning from criticality.

From Eq. (4.53) one can see that near the critical point, the *typical* low energy degrees of freedom delocalize as $\xi_{typ,f}(0) \sim \Delta^{-\nu}$ with $\nu = 1$. However, spatially averaged correlation functions decay more slowly with a faster diverging *average* correlation length [85], $\xi_{av,f}(0) \sim \Delta^{-2}$. This arises because such averages are dominated by rare regions with favorable disorder configuration.

Note that the typical localization length defined in (4.52) is a smooth function of energy ω. We studied the energy dependence using the transfer-matrix (4.51) and evaluating $1/\xi_{typ,f}(\omega)$ numerically for a box-distributed disorder. At the critical point, we find a logarithmically diverging localization length, $\xi_{typ,f}(\omega) \sim |\log(\omega)|$, cf. Fig. 4.1, which is consistent with the activated scaling predicted by the strong randomness renormalization [85].

Away from criticality, the localization length is finite at $\omega = 0$, but it behaves non-analytically at small ω

$$\xi^{-1}_{typ,f}(\omega) - \xi^{-1}_{typ,f}(0) \sim \omega^{\alpha}, \tag{4.54}$$

with $\alpha > 0$, cf. Fig. 4.2. We will discuss the origin of this power law and the exponent α in Sec. 4.3.4 below and compare it with exact results obtained in a continuum model. In the model with box-distributed disorder, upon increasing the energy to the fermionic band edge, we always found the localization length to decrease with increasing energy, independently of the distance to criticality.

4.3.3 Continuum limit

If the disorder is weak, the low energy physics can be captured by coarsegraining the lattice model and taking a continuum limit of $\widetilde{\mathcal{H}}$. After rewriting the matrix $\mathcal{D}$ from (4.36) as

$$\mathcal{D}_{jk} = -J(\delta_{j,k-1} - \delta_{jk}) + (\epsilon_j - J)\delta_{jk}, \tag{4.55}$$

[2] Strictly speaking, there are no normalizable eigenmodes with exactly $\omega_n = 0$. However, there are modes with energies that are exponentially small in the system size, and for those the value given in (4.53) still applies.

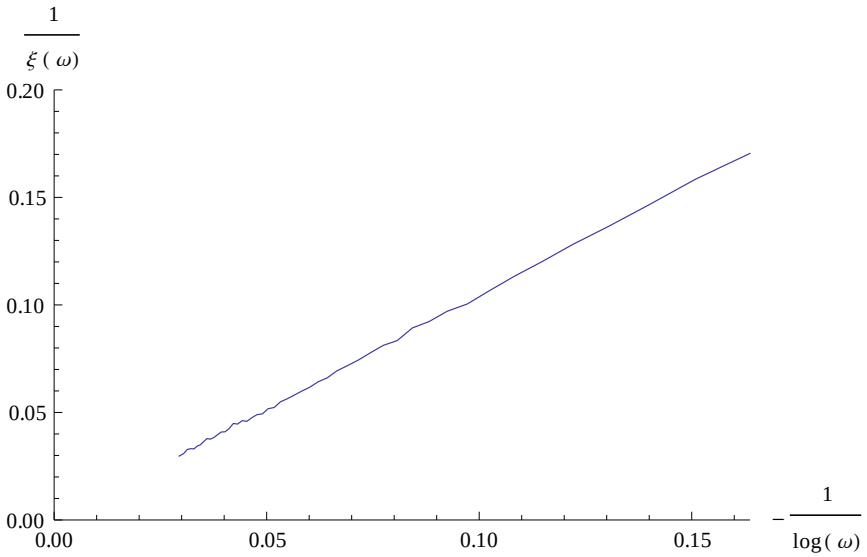

Figure 4.1: The numerically evaluated Lyapunov exponents of the Jordan-Wigner fermions, Eq. (4.53) at the critical point of the Ising spin chain, $J = J_c$. The localization length shows activated scaling $\xi^{-1}(\omega) \propto 1/|\log(\omega)|$.

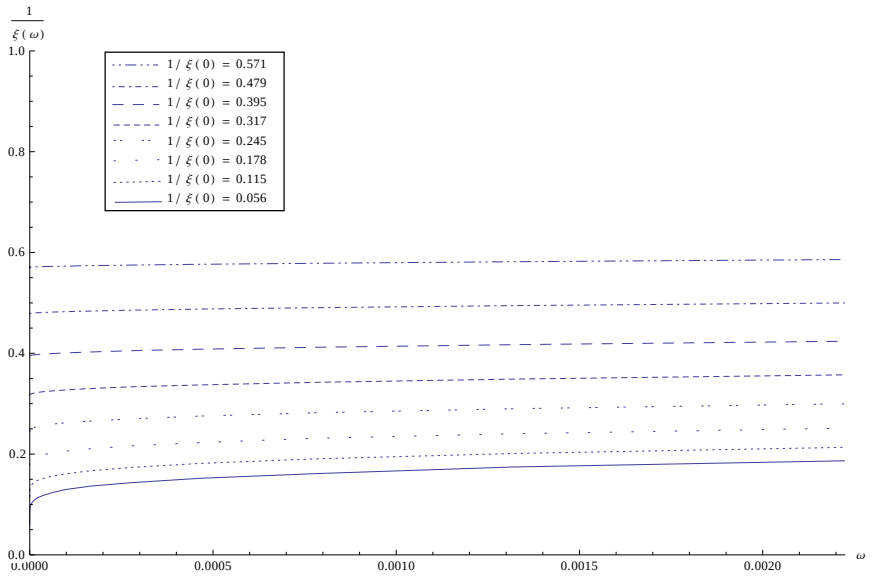

Figure 4.2: The numerically evaluated Lyapunov exponent of Jordan-Wigner fermions of the spin chain as a function of energy. The disorder is strong, and box-distributed. Data is shown for the paramagnetic regime ($J < J_c$) off criticality. The inverse localization length at zero energy, $1/\xi(0)$, serves as a measure for the distance from the critical point. At small ω, in the localization length $\xi_{typ,f}$ always *decreases* as a power law with increasing ω.

the continuum limit of $\widetilde{\mathcal{H}}$ can be taken as (with lattice spacing set to unity)

$$\mathcal{D}_c = J\left[-\frac{d}{dx} + \phi(x)\right]. \tag{4.56}$$

The random potential is given by

$$\phi(x) = \frac{\epsilon_j - J}{J}, \tag{4.57}$$

where the continuous variable x corresponds to the (coarse-grained) position j.

In the case where $\phi(x)$ is a Gaussian white noise potential of unit variance, the problem was solved exactly using supersymmetric quantum mechanics. [89, 90, 91] The continuum version of Eq. (4.44) is equivalent to the Schrödinger equation for ψ_2 with the supersymmetric Hamiltonian

$$\begin{aligned} H_c\psi_2 &\equiv \mathcal{D}_c^\dagger \mathcal{D}_c \psi_2 \\ &= \left[-\frac{d^2}{dx^2} + \phi^2(x) + \phi'(x)\right]\psi_2 = \omega^2\psi_2, \end{aligned} \tag{4.58}$$

whose spectrum is positive by construction (here and in the remainder of this section we set $J = 1$). In Ref. [90] the Lyapunov exponents (inverse localization length) of the eigenfunctions of the continuum Hamiltonian (4.58), was obtained in closed form as

$$\xi^{-1}_{typ,f}(\omega) = -\omega\frac{dM_\mu(\omega)/d\omega}{M_\mu(\omega)}, \tag{4.59}$$

where $M_\mu = \sqrt{J_\mu^2 + N_\mu^2}$, J_μ and N_μ being Bessel functions of order μ of the first and second kind, respectively. The index μ of the Bessel functions is the expectation value

$$\mu = \overline{\phi(x)}, \tag{4.60}$$

which matches with the definition of Δ, Eq. (4.53), in the vicinity of criticality.

Evaluating the expression (4.59) at the critical point, $\mu \to 0$, one obtains a logarithmic (activated) scaling at small ω,

$$\xi^{-1}_{typ,f}(\omega) = \frac{1}{|\log(\omega)|} + O(1/|\log(\omega)|^2) \quad (\mu = 0), \tag{4.61}$$

similarly as we find above for the discrete, strong disorder case. Close to the critical point, the formula (4.59) predicts the non-analytic behavior

$$\begin{aligned} &\xi^{-1}_{typ,f}(0) = \mu, \\ &\xi^{-1}_{typ,f}(\omega) - \xi^{-1}_{typ,f}(0) = A_\mu\omega^{2\mu}[1 + o(\omega)], \\ &A_\mu = 2\mu\frac{2^{-2\mu}}{\Gamma(\mu+1)^2}\frac{\pi\mu}{\tan(\pi\mu)}. \end{aligned} \tag{4.62}$$

This, too, is in qualitative agreement with the power law behavior we found numerically for strongly disordered chains.

4.3.4 Non-analyticity of $\xi(\omega)$ from rare events

The origin the power laws Eqs. (4.54,4.62) can be understood from an analysis of the transfer matrix, which will also make clear what kind of rare events lead to the non-analytic structure of $\xi(\omega)$. Let us consider the paramagnetic phase where $\overline{\epsilon_i} > J$. From Eq. (4.51), it is clear that the Lyapunov exponent (the growth rate of the norm of the matrix) at $\omega = 0$ is given by the product of the elements T_{22}. For $0 < \omega \ll J$, the norm of the transfer matrix is still mostly dominated by a product of factors T_{22}, but occasionally rare stretches along the chain may occur in which $\overline{\epsilon_i} < J$. If such a rare fluctuation is strong enough it can compensate for the small factor $\sim \omega^2$ associated with switching from the $2-2$ channel to the $1-1$ channel, and thus increases the Lyapunov exponent beyond its $\omega = 0$ value. The increase of ξ^{-1} is proportional to the spatial density of such rare fluctuations.

The probability for the product of a long stretch of length ℓ,

$$X = \prod_{j=i}^{i+\ell-1} \frac{|\epsilon_j|}{J}, \tag{4.63}$$

to be smaller than $\omega \ll 1$ can be estimated as

$$P(X < \omega) \approx \exp\left[-\frac{(|\log\omega| + \ell v)^2}{4\ell D}\right], \tag{4.64}$$

neglecting pre-exponential factors. Here

$$v = \overline{\log(\epsilon_i/J)}, \tag{4.65}$$

$$D = \frac{1}{2}\left(\overline{[\log(\epsilon_i/J)]^2} - v^2\right), \tag{4.66}$$

This follows from the consideration that $\log X$ is essentially a random walk with diffusion constant D and drift v, and applying the central limit theorem. For $|\log(\omega)| \gg 1$ this probability is maximized for stretches of length $\ell = |\log(\omega)|/v$, which occur with probability

$$P(X < \omega) \sim \Delta\xi^{-1}(\omega) \propto \exp\left[-|\log(\omega)|\frac{v}{D}\right] = \omega^{v/D}. \tag{4.67}$$

which predicts the exponent $\alpha = v/D$, in accordance with the exact result in the continuum, Eq. (4.62), where $v \to \mu$, $D \to 1/2$ and thus $\alpha \to 2\mu$.

The above shows that the leading, nonanalytic correction to the localization length is due to rare regions which favor the opposite phase (ordered or disordered) of the chain. It appears that low energy excitations are less backscattered from such regions than excitations at higher energy.

While the above argument makes a robust prediction of the exponent in (4.54,4.62), the prefactor A_μ in Eq. (4.62) is certainly much more sensitive to details of the disorder distribution. From the numerical evaluation of the Lyapunov exponents in the strongly disordered spin chains we found A_μ to be always positive, independently of the distance to criticality. In other words, the localization length at $\omega = 0$ is found

to be always greater than $\xi_{typ,f}(\omega > 0)$ at higher energies. However, in the exactly solvable continuum model such a behavior is found only for $\mu < 1/2$, cf. (4.62), while further away from criticality the prefactor changes sign. In that regime the cases of strong discrete disorder and weakly disordered continuum model have no a priori reason to yield qualitatively similar results. Nonetheless, the qualitative agreement of the trend of $\xi_{typ,f}(\omega)$ at low ω, close enough to criticality, suggests that $\xi_{typ,f}(0)$ is a local maximum, independently of the specific disorder, as long as one is close enough to the critical point.

4.3.5 Implications for spin systems

The relevance of the above results for correlation functions of spins in the Ising chain is limited to some extent. Indeed, spin correlation functions, which contain the information of localization properties of local spin excitations, are difficult to extract from the fermion representation, because of the nonlocal relation between spin and fermion operators. Nevertheless, one may expect that the localization length of fermion Green's functions will also control the spatial decay of spin correlations, at least at low enough energies.

In particular it is interesting to compare the exact result for the free fermions to our leading order results for the spin problem in general. Applying the locator expansion to the spin chain, and defining the localization length via the spin correlation function as [51]

$$\xi_s^{-1}(\omega) = -\lim_{l\to\infty} \frac{\overline{\log(|G_{l,0}(\omega)/G_{0,0}(\omega)|)}}{|l|}, \tag{4.68}$$

we find from Eq. (4.27) the expression

$$\xi_s^{-1}(\omega) = -\lim_{l\to\infty} \frac{1}{l}\sum_{j=1}^{l} \overline{\log\left[\frac{4J|\epsilon_j|}{(2\epsilon_j)^2-\omega^2}\right]}, \tag{4.69}$$

to the leading order in J. Remarkably, at zero frequency $\omega = 0$, Eqs. (4.53) and (4.69) yield the same result, implying that the leading order locator expansion is actually exact in this case. The reason for this phenomenon is that in Eq. (4.44), awhen $\omega = 0$, the fermion modes ψ^1 and ψ^2 decouple and satisfy independent equations, which are easily solved by forward integration, where no loop corrections arise. [3]

At finite ω, the locator expansion captures correctly the qualitative feature that $\xi_s^{-1}(\omega)$ decreases with increasing energy, however it misses the non-analytic corrections from rare events, discussed above. However, these rare events play a rather special role in one dimension, since rare regions of oppositely biased disorder cannot be avoided by an excitation. The associated backscattering tends to localize higher energy excitations. We should also point out that the non-analyticity of the localization at the

[3] However, in finite samples there are no fermionic modes at strictly $\omega = 0$, however there are eigenmodes at ω which are exponentially small in the system size, whose localization properties can be obtained by setting $\omega \to 0$.

critical point, as well as its divergence at the critical point, come along with an accompanying Dyson singularity in the density of fermionic states [90], very similarly as in tight-binding chains with off-diagonal disorder [86, 89, 92]. Both occur thanks to the BDI symmetry of the fermionic problem.

At this point it is not clear whether any of these features carry over to spin systems in higher dimensions. Indeed, for $d > 1$, the type of rare events identified above should play a much less important role, since such regions may be circumvented. At the same time, a new important factor comes into play, which is absent in one dimension: the interference between alternative favorable forward directed paths. As was shown in Ref. [**?**] their interplay also tends to localize higher energy excitations more. This is a simple consequence of the fact that the interference of paths in Eqs. (4.27,4.30) is maximally constructive at vanishing excitation energy $\epsilon_0 = 0$, while negative scattering amplitudes start to spoil this perfect interference at finite ϵ_0. Qualitatively similar effects are achieved by a magnetic field acting on charged bosons, which endows the various paths with different Aharonov-Bohm phases, which also degrade the perfect interference. The resulting magnetoresistance was discussed in detail in Ref. [93]. The above arguments rely a priori on the lowest order expansion in the exchange J, which we believe to capture the essential features of localization in $d > 1$ within the strongly localized regime. Subleading effects due to loop corrections have been studied in Ref. [83].

4.4 Approaching delocalization: Boson and spin models on highly connected Cayley tree

In an attempt approach the delocalization or ordering transition, we choose to apply our formalism to a situation where the expansion in hopping is expected to remain applicable even close to the phase transition. A priori one expects this to be the case in high dimensions, where loop corrections can be expected to be relatively unimportant. An extreme case where loops are absent altogether is the Cayley tree. Motivated by the related studies in Refs. [28, 29] we consider Cayley trees of large branching number K which locally resemble cubic lattices in $d = (K + 1)/2$ dimensions. The related Anderson model of non interacting fermions on such trees can be exactly solved due to the absence of loops [60]. Since it is known that in this case the delocalization transition happens when the hopping is still parametrically small, $t \sim 1/K \log(K)$ as $K \to \infty$, one may hope that a leading order expansion in the hopping may well capture the approach to the transition. Such an approach was proposed in Refs. [28, 29], where the localization properties of intensive low energy excitations in the disordered phase were studied. The authors claimed that in the disordered regime, close enough to criticality an intensive mobility edge ω_c exists, and that upon approaching criticality ω_c decreases to zero and vanishes simultaneously with the onset of long range order. Similar scenario had been proposed in Refs. [94, 52]. Here we revisit this question, using the leading order locator expansion formula (4.27,4.30), which differ from the expressions postulated in Refs. [28, 29].

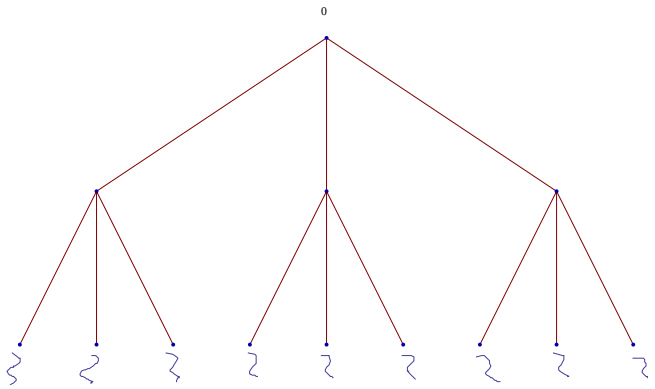

Figure 4.3: Cayley tree with branching number $K = 3$. 0 labels the root site. The depth of the tree, i.e., the distance from the root to a boundary site is L ($L = 2$ in this figure). The wavy lines represent the coupling of the boundary spins to independent baths.

Let us now analyze the spin models (4.3, 4.4) on a Cayley tree with a root site 0, branching number K and depth L, cf. Fig. 4.3. We will be interested in two distinct aspects: (i) the propagation of long range order ("surface magnetization"), (ii) the localization properties of local excitations at the root, as a function of the associated energy $\approx \epsilon_0$.

Anticipating that the delocalization transition appears when the exchange is of order $J \sim 1/K \log(K)$, as for single particle hopping, we introduce the notation $J \equiv \frac{g}{K}$, and we rely on the smallness of the parameter J close to criticality to restrict ourselves to leading order perturbation theory in J. This will give indeed a reliable estimation of localization properties up to a narrow critical window close to the phase transition, where subleading terms should be included, as we will discuss further below.

4.4.1 SI transition from insulating phase

The disorder-induced quantum phase transition in the models (4.3, 4.4) can be approached from the ordered or the disordered side. The route from the symmetry broken side was pioneered by Ioffe, Mézard and Feigelman [28, 29], where self-consistent equations for cavity mean fields (local order parameters) were analyzed and solved. This inhomogeneous mean field approach was further exploited by Monthus and Garel [95], both in finite dimensions and on the Cayley trees, finding that strong randomness physics governs the excitations in these disordered systems.

These works pointed out the close relationship between magnetic correlation functions at large distances and the physics of directed polymers in random media, which was recently beautifully demonstrated to be reflected in experimentally measured distributions of the local tunneling gap, which assumes a Tracy-Widom form in two spatial dimensions [96]. The mapping between between bosonic correlation functions and directed polymers is rendered exact on the insulating side $J \ll 1$ where the correlation functions can be argued to be well represented by the lowest order expansion in the

exchange [51, 93]. By restricting to the leading order the expansion of order parameter correlations in the ordered phase, or of two point functions like G_{l0} in the localized phase, one obtains the same estimate for the critical point $J_c = g_c/K$ where long range correlations set in. However, it is difficult to assess the quality of the mean field approximation, and to improve systematically beyond it, which would be desirable especially in low dimensions. In contrast, the expansion in the localized phase higher order corrections is amenable to a systematic expansion in powers of J, and thus may be a simpler route of attack towards the criticality.

In this section we approach the ordering transition from the insulating phase. We define the surface susceptibility

$$\chi_s \equiv \sum_{l\in\partial\Lambda} \frac{G_{l,0}(0)}{G_{0,0}(0)}, \tag{4.70}$$

where the sum is over all paths from the root site 0 to any of the boundary spins l, and we included the normalization by $G_{0,0}(0)$ for convenience. In the insulating phase, all $G_{l,0}$ decay rapidly, such that large number of boundary sites cannot offset the smallness of this susceptibility. Upon increasing the exchange coupling, g, the ordering transition (in typical realizations of disorder) occurs when the *typical* value of χ_s is of order $O(1)$. In finite dimensions this criterion is equivalent to asking that $-\log[G_{l,0}]$ does not grow linearly with the distance from the bulk site 0 to a boundary site l. However, on the Cayley tree, where there are exponentially many (K^L) boundary sites, the criterion must be applied to the whole sum, and cannot always be reduced to a criterion on typical or dominant paths on the tree.

The above criterion is valid on general lattices. However, in finite dimensions, the Green's functions $G_{l,0}$ are very hard to study analytically, especially close to the phase transition. On a Cayley tree with large branching number K a simplification occurs. First of all, there is only one shortest path connecting any two points, and thus there is only a single term contributing to the leading order locator expansion of $G_{l,0}$. Subleading terms are not very important when K is large, since paths with extra excursions on side paths are formally penalized by an extra factor of $\lesssim g_c^2/K$ (which is dominated by exchange processes with the most favorable neighboring sites). This argument is however known to be a bit too naive. Indeed, from the analogous single particle problem [1, 60], it is known that these self-energy corrections regularize resonances from very small denominators and modify the numerical prefactor A in the large K scaling $g_c = A/(K \log K)$, as compared to the so-called "Anderson upper limit" estimate, in which self-energies are neglected. Similar effects are of course present in the many body case as well.

Keeping this caveat in mind, we nevertheless restrict ourselves to the leading order perturbation theory and use the leading terms Eqs. (4.27,4.30) to evaluate $G_{l,0}$,

$$\chi_s = \sum_{l\in\partial\Lambda} \prod_{i\in\mathcal{P}_l} \frac{g/K}{|\epsilon_i|}, \tag{4.71}$$

where $\mathcal{P}_l$ is the unique path from the root to the boundary site l. This certainly captures well the behavior deep in the insulator, but as argued above, also rather close

to the ordering transition if the limit of large $K \gg 1$ is taken. We recall that to this leading order the two point functions at $\omega = 0$ are the same in the XY and the Ising model. Thus, we are lead to the same estimate of the critical coupling g_c, while it is expected that the inclusion of subleading terms will split these two values.

As we mentioned previously, one arrives at essentially the same conclusion from cavity mean field equations applied to the ordered side, by linearizing them in the exchange coupling and assuming transverse expectation values to be negligible close to the second order phase transition. Within that approach one notices that (assuming a preferred direction of symmetry breaking in the XY-plane) the local order parameter susceptibility is $1/\epsilon_i$ in both models. This immediately leads to the conclusion that the order parameter susceptibility ($\omega = 0$) at large distances is a product of such terms, as the expression Eq. (4.71) for the deeply insulating side - independent of the symmetry of the order parameter.

The near coincidence of the critical values g_c in the two models appears less obvious when reasoning from the disordered side. Naively, one might think that the additional exchange term $J\sigma_i^y\sigma_j^y$ in the XY model leads to enhanced fluctuations as compared to the Ising model. However, this effect is almost exactly compensated by the fact that the XY symmetry (conservation of hard core bosons) restricts the quantum fluctuations more strongly than the Ising symmetry.

The evaluation of the typical susceptibility follows from the exact mapping of the leading order expression for the surface susceptibility to the problem of a directed polymer on the Cayley tree. The latter was solved exactly by Derrida and Spohn [97], and their result was applied to the present context in Refs. [29, 28]. The susceptibility itself is a strongly fluctuating random variable, which depends on the disorder realization. However, its logarithm is a self-averaging quantity. Upon re-exponentiation one obtains the *typical* value, which is characterized by the logarithmic disorder average [97, 29, 28]

$$\lim_{L\to\infty} \frac{1}{L}\overline{\log \chi_s} \equiv \log\left(\frac{g}{K}\right) + \min_{x\in[0,1]} f(x), \tag{4.72}$$

where the function $f(x)$ is defined by

$$f(x) = \frac{1}{x}\log\left[K\int_{-1}^{1}\frac{1}{\mid \epsilon \mid^x}\frac{d\epsilon}{2}\right]. \tag{4.73}$$

Let us denote by x_c the argument at which $f(x)$ takes its minimum on the interval $x \in [0, 1]$. If $x_c < 1$, the associated directed polymer problem is in its low temperature frozen phase whose thermodynamics is essentially dominated by a single path on the tree. More precisely, the partition sum over paths that go to the boundary is dominated by a set of configurations, which all stay together and split only at a short distance before reaching the boundary. Thereby, that last distance does not scale with L in the limit $L \to \infty$. In spin glass terminology, the dominating paths have "mutual overlap" tending to 1 in the thermodynamic limit.This situation corresponds to a phase of broken replica symmetry (RSB) for the directed polymer. In the language of onsetting long range order in the spin model this translates into the statement that (in leading order approximation in the exchange) the surface susceptibility is dominated essentially

by a single path. If instead one finds $x_c = 1$, the dominant contribution to χ_s, or to the partition function of the equivalent polymer problem, comes from exponentially many configurations.

Within the approximation of leading order in the hopping one finds that the ordering transition occurs when [29],

$$0 = \log\left(\frac{g_c}{K}\right) + f(x_c), \tag{4.74}$$

which corresponds to the vanishing of the free energy density of the directed polymer. This has the solution [29]

$$g_c \exp\left(\frac{1}{e g_c}\right) = K, \quad x_c = 1 - e g_c. \tag{4.75}$$

or, in the limit of large K,

$$g_c \approx \frac{1}{e \log(K)}. \tag{4.76}$$

It is worth noting that the Eqs. (4.72,6.10), which determine the critical point, and the critical value g_c are identical to those obtained by Abou-Chacra et al [60]. for the delocalization of non-interacting particles, within the so-called Anderson upper limit approximation. The latter consists in dropping self-energy corrections, which is equivalent to the leading order approximation in hopping [1]. The coincidence of these results is not very surprising, since the localization properties of fermions and hard core bosons are very similar on the Cayley tree. In fact, to leading order in hopping, one considers only forward scattering processes, and since the Cayley tree does not contain loops, the quantum statistics of the particles is irrelevant to that order. Similarly, to leading order in the hopping, the dependence of localization properties on frequency will not differ between fermions and hard core bosons, as we will see in the following subsection.

Since $x_c \approx 1 - 1/\log(K) < 1$, the above result might suggest that transverse order sets in along essentially the best path to the boundary, which dominates the response to a symmetry breaking field applied there. Accordingly, one may expect a highly inhomogeneous condensate, which lives on an extremely sparse fraction of the tree, which does not even grow exponentially with L. However, since x_c is parametrically close to 1, and since it is known that subleading corrections in the fermion delocalization problem increase the value of x_c by a similar correction, the leading order estimate for x_c does not allow us to conclude about the precise structure of the onsetting long range order on the Cayley tree. However, it is nevertheless expected that the onsetting condensate is highly inhomogeneous on the Cayley tree.

4.4.2 Decay rates in the insulating phase for the XY model

Let us now turn to the localization properties in the insulating phase ($g < g_c$), where the locator expansion is best controlled. We are interested in particular in determining

whether there exists an intensive mobility edge, i.e., an energy of order $O(1)$ which separates localized from delocalized excitations in the many body system.

In order study the decay process of a local excitation on the root 0, we couple our system to zero temperature baths via the spins at the boundary of the Cayley tree, cf. Fig. 4.3. In terms of the general formalism of Sec. s:decay, we take take the Cayley tree as the lattice Λ, and its leaves as the boundary set $\partial\Lambda$. On a Cayley tree, there is only one shortest path between the root site 0 and any boundary site l. This simplifies the analysis of decay rates very significantly, since to leading order no interferences need to be taken into account. Notice that by taking K to be large, this leading order approximation is parametrically controlled in the insulating phase apart from a parametrically narrow region close to criticality where subleading corrections pa role, as discussed in the previous subsection. This is so, because large K disfavors subleading corrections in g/K, which arise from paths with transverse excursions. We therefore restrict again to the leading order approximation and evaluate the decay rate of a local excitation with energy $\omega \simeq 2\epsilon_0$ as

$$\Gamma_0(\omega) = \sum_{l\in\partial\Lambda} \prod_{i\in\mathcal{P}_l} \left[\frac{2g/K}{2\epsilon_i - \omega}\right]^2 J_b(\omega). \tag{4.77}$$

As before, the sum is over all shortest paths (of length L) from the root 0 to boundary sites l, and $\prod_{i\in\mathcal{P}_l}$ is the product along a path $\mathcal{P}_l$. As in the case of the zero-frequency susceptibility, the decay rate Γ_0 can be seen as the partition function for a directed polymer in a disorder potential on the tree, the locators taking the role of local Boltzmann weights.

The typical value Γ_0 at fixed frequency ω is best characterized by its mean spatial rate of decrease,

$$\begin{aligned} \gamma_{\mathrm{XY}}(\omega) &\equiv -\lim_{L\to\infty} \frac{1}{L} \overline{\log\left[\frac{\Gamma_0(\omega)}{J_b(\omega)}\right]} \\ &= -\left(\log\left(\frac{g}{K}\right) + \min_{x\in[0,1]} f_\omega(x)\right), \end{aligned} \tag{4.78}$$

where the function $f_\omega(x)$ is defined by

$$f_\omega(x) = \frac{1}{2x} \log\left(K \int_{-1}^{1} \frac{1}{|\,\epsilon - \omega/2\,|^{2x}} \frac{d\epsilon}{2}\right). \tag{4.79}$$

Notice that due to the assumed symmetry of the onsite disorder distribution, we have $f_{-\omega}(x) = f_\omega(x)$, so it suffices to study $\omega > 0$. Suppose again that $f_\omega(x)$ takes its minimum on the interval $[0,1]$ at $x = x_c$. Due to the small denominators arising from sites with $\epsilon_i \to 0$, (4.79) is well-defined only for $x < 1/2$ and thus x_c must be less than $1/2$. We note, however, that this restriction does not apply when the resonant levels are regularized, to account for effects of (subleading) self-energy corrections. This as is well-known from the case of free fermions.

$\gamma_{\mathrm{XY}}(\omega)$ controls the decay or growth of $\Gamma_0(\omega)$ with distance to the boundary. Clearly, as long as $\gamma_{\mathrm{XY}}(\omega) > 0$, the typical value of $\Gamma_0(\omega)$ is exponentially small as

$L \to \infty$, which implies that an excitation of energy ω is localized and does not decay into the bath in the thermodynamic limit $L \to \infty$. Instead, the delocalization of an excitation with energy ω occurs at the point where

$$0 = \gamma_{\rm XY}(\omega) = \log\left(\frac{g}{K}\right) + \min_{x\in[0,1]} f_\omega(x). \tag{4.80}$$

By minimizing the function $f_\omega(x)$ with respect to x, one obtains the two simultaneous conditions

$$1 = \frac{K}{2}\left(\frac{g}{K}\right)^{2x_\omega} \int_{-1}^{1} \frac{1}{|\epsilon - \omega/2|^{2x_\omega}} d\epsilon, \tag{4.81}$$

$$\log\left(\frac{g}{K}\right) = \frac{K}{2}\left(\frac{g}{K}\right)^{2x_\omega} \int_{-1}^{1} \frac{\log(|\epsilon - \omega/2|)}{|\epsilon - \omega/2|^{2x_\omega}} d\epsilon. \tag{4.82}$$

However, one finds that on the disordered side of the transition, $g < g_c$, there is no $\omega > 0$ such that the equations (4.81) and (4.82) are satisfied simultaneously. In other words, there is no critical energy (mobility edge) which separates localized states from delocalized states. Instead, all excitations with intensive energy are in fact localized in the quantum paramagnet (Bose insulator). Moreover, we find that in the whole localized phase $g < g_c$, $\gamma_{\rm XY}(\omega) > \gamma_{\rm XY}(0)$ for any $\omega \in [-1, 1]$. In Fig. 4.4 we illustrate this behavior at the critical point for both Ising and XY models. Ising excitations of energy ω are seen to localize slightly faster than similar excitations in the XY model. This might be seen as a weak analogue of what is expected from finite dimensions, where the Ising model in strong disorder is known to be governed by strong randomness fixed points at least in low enough dimensions ($d = 2, 3$) [98, 99, 100], with activated scaling, i.e. an inverse localization length $\xi^{-1}_{typ} = \gamma \sim |\log(\omega)|^\psi$. This behavior arises due to the discreteness of the spin symmetry. In contrast, XY models with continuous symmetry are expected to exhibit a power law scaling $\xi^{-1}_{typ} = \gamma \sim \omega^{-1/z}$ [101], which increases more slowly with frequency.

This result contradicts the one reported in Refs. [28, 29]. On a technical level, the difference arises because those authors restricted the on-site energies $\{\epsilon_i\}$ to be positive, postulating a matrix element of the form $\prod \left[\frac{2g/K}{2|\epsilon_i|-\omega}\right]^2$. However, this is only possible to impose for the Ising model. As we will discuss below, however, the Ising model requires a different matrix element in the formula (6.8). Conceptually, a similar error was present in the reasoning of Ref. [52], where it was argued that excitations close to the chemical potential should be more localized than at higher intensive energies, since the excitations behave like at a band edge of a single particle problem, since any local excitation cost a positive energy. However, this picture is incorrect since it neglects exchange effects of indistinguishable particles. Indeed, by the same reasoning one would conclude that the excitations of a fermionic Anderson insulator are the most localized at the Fermi level, which is obviously not true. Our findings on the Bethe lattice for the XY model are indeed identical, within the leading order approximation, to the localization properties of free fermions, as solved in Ref. [60]. If we consider

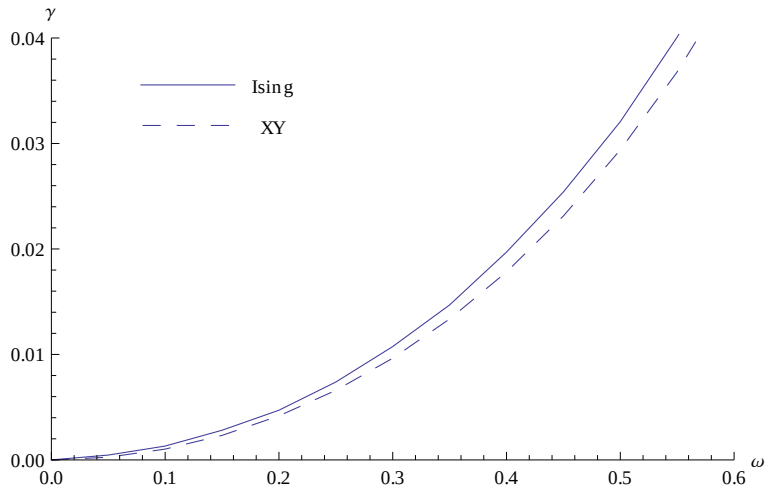

Figure 4.4: Spatial decay rate γ as a function of frequency ω for the XY model and the Ising model at the transition point. γ is positive for $\omega > 0$ and tends to zero as $\omega \to 0$. Note that $\gamma_{\rm XY} < \gamma_{\rm Ising}$, which suggests that at and close to the critical point local excitations with finite energy ω decay slightly faster in space in the Ising model as compared to the XY model.

a half filled lattice of hard core bosons, and uniform disorder, we indeed find the localization length to have a flat maximum at the band center, $\omega = 0$, as expected from the fermionic case. This is illustrated for the case of criticality in Fig. 4.4.

4.4.3 Decay rates in the disordered phase for the Ising model

Let us now analyze the Ising model in turn and contrast it with the XY model. The relevant matrix element $\langle {\rm GS}|\sigma_l^x|E_0\rangle$ for the Ising model is given by Eq. (4.27). Hence, the decay rate of a local excitation with energy ω at site 0 can be written as

$$\Gamma_0(\omega) = \sum_{l\in\partial\Lambda} \prod_{i\in\mathcal{P}_l} \left[\frac{\epsilon_i\, g/K}{\epsilon_i^2 - (\omega/2)^2}\right]^2 J_b(\omega). \tag{4.83}$$

As in the XY model, we obtain

$$\begin{aligned} \gamma_{\rm Ising}(\omega) &\equiv -\lim_{L\to\infty} \frac{1}{L}\overline{\log\left[\frac{\Gamma_0(\omega)}{J_b(\omega)}\right]} \\ &= -\left(\log\left(\frac{g}{K}\right) + \min_{x\in[0,1]} h_\omega(x)\right), \end{aligned} \tag{4.84}$$

where the function $h_\omega(x)$ is now given by

$$h_\omega(x) = \frac{1}{2x}\log\left(K\int_{-1}^{1}\left|\frac{\epsilon}{\epsilon^2-(\omega/2)^2}\right|^{2x}\frac{d\epsilon}{2}\right). \tag{4.85}$$

Delocalization at energy ω occurs again when $0 = \gamma_{Ising}(\omega)$. Exactly as in the XY model, one verifies that on the disordered side of the quantum phase transition, $g < g_c$, one has always $\gamma_{Ising}(\omega) > \gamma_{Ising}(0) > 0$ for $\omega \in [-1, 1]$, as shown in Fig. 4.4 at criticality. Note that this behavior, which we find here to leading order in the exchange coupling, is qualitatively similar to the exact results discussed for the Ising chain in Sec. 4.3, in that localization becomes stronger at higher intensive energies. The dependence on ω is however much less dramatic. This should be expected, since the events are much less important in the high dimensional situations.

4.4.4 On fractality

We should point out that both for the XY model and the Ising model, we find the minimum of the functions f_ω and h_ω are assumed at values of $x < 1/2$, and definitely $x < 1$. The same is known to happen more rigorously in the single particle case, where one can argue that upon taking self-energy corrections into account the effectively relevant value of x_c is $x_c = 1/2$ [60]. The fact that $x_c < 1$ indicates that the propagation of a local excitation of fixed energy follows essentially one selected path out of the exponentially many available ones.

Already in his seminal paper of 1958 Anderson had realized that the sum over fermionic paths, when approximated as a sum over uncorrelated terms, is dominated by the largest term in the sum (see Chapter II). In the exact solution of the localization problem of single particles on the Cayley tree, the above solution was found by a different route by Abou-Chacra et al. [60].

4.5 Discussion

We have shown that in both cases (XY and Ising models), there is no mobility edge in the insulating phase. This relies of course on our choice of a flat bare density of states. If the latter is not uniform, but increases with energy there is (quite trivially) a mobility edge. The same physics occurs in a less trivial manner in a glassy bosonic insulator where the onsite random potential ϵ_i is self-generated by random frustrated density-density interactions which form a Coulomb gap, thus generating a density of states which increases from the chemical potential [102].

4.6 Supplementary materials

As a non-trivial check of the result of the locator expansion Eq. (4.27), we calculate the matrix element $\langle \mathrm{GS}|\sigma_l^x|E_0\rangle$ for a three spin chain by standard pertubation theory. Suppose $\epsilon_i > 0$. Then $|\mathrm{GS}^{(0)}\rangle = |\uparrow\uparrow\uparrow\rangle$ and $|E_0^{(0)}\rangle = \sigma_0^-|\mathrm{GS}^{(0)}\rangle = |\downarrow\uparrow\uparrow\rangle$.

We now evaluate $\langle E_0|\sigma_2^x|\mathrm{GS}\rangle$ by standard perturbation theory. The Hamiltonian is

$$H = -\sum_{i=0,1} \epsilon_i \sigma_i^z - t\sum_{i=0}^{1} \sigma_i^x \sigma_{i+1}^x. \tag{4.86}$$

The perturbation term $H_I \equiv -t\sum_{i=0}^{1}\sigma_i^x\sigma_{i+1}^x$ and $H_I^{kl} \equiv \langle E_k^{(0)}|H_I|E_l^{(0)}\rangle$. The eigenstates adiabatically connected to $|E_{\rm GS}^{(0)}\rangle$ and the excited state $|E_0^{(0)}\rangle$ are

$$\begin{aligned}
|{\rm GS}\rangle &= |E_{\rm GS}^{(0)}\rangle - t\sum_{k\neq{\rm GS}}\frac{H_I^{{\rm GS}k}}{E_{\rm GS}^{(0)}-E_k^{(0)}}|E_k^{(0)}\rangle \\
&\quad +t^2\sum_{k\neq{\rm GS}}\sum_{l\neq{\rm GS}}\frac{H_I^{kl}H_I^{{\rm GS}l}}{(E_{\rm GS}^{(0)}-E_k^{(0)})(E_{\rm GS}^{(0)}-E_l^{(0)})}|E_k^{(0)}\rangle \\
&\quad -\frac{t^2}{2}\sum_{k\neq{\rm GS}}\frac{|H_I^{k{\rm GS}}|^2}{(E_{\rm GS}^{(0)}-E_k^{(0)})^2}|E_{\rm GS}^{(0)}\rangle + O(t^3) \\
&= |\uparrow\uparrow\uparrow\rangle - t\left(\frac{1}{-2\epsilon_0-2\epsilon_1}|\downarrow\downarrow\uparrow\rangle + \frac{1}{-2\epsilon_2-2\epsilon_1}|\uparrow\downarrow\downarrow\rangle\right) \\
&\quad +t^2\left[\left(\frac{1}{(-2\epsilon_0-2\epsilon_2)(-2\epsilon_0-2\epsilon_1)}\right.\right. \\
&\quad \left.+\frac{1}{(-2\epsilon_0-2\epsilon_2)(-2\epsilon_1-2\epsilon_2)}\right)|\downarrow\uparrow\downarrow\rangle \\
&\quad \left.-\frac{1}{2}\left(\frac{1}{(2\epsilon_0+2\epsilon_1)^2}+\frac{1}{(2\epsilon_2+2\epsilon_1)^2}\right)|\uparrow\uparrow\uparrow\rangle\right] + O(t^3) \\
&\equiv E|\uparrow\uparrow\uparrow\rangle + F|\downarrow\downarrow\uparrow\rangle + G|\uparrow\downarrow\downarrow\rangle + H|\downarrow\uparrow\downarrow\rangle \\
&\quad +O(t^3),
\end{aligned} \tag{4.87}$$

$$\begin{aligned}
|E_0\rangle &= |E_0^{(0)}\rangle - t\sum_{k\neq 0}\frac{H_I^{0k}}{E_0^{(0)}-E_k^{(0)}}|E_k^{(0)}\rangle \\
&\quad +t^2\sum_{k\neq 0}\sum_{l\neq 0}\frac{H_I^{kl}H_I^{0l}}{(E_0^{(0)}-E_k^{(0)})(E_0^{(0)}-E_l^{(0)})}|E_k^{(0)}\rangle \\
&\quad -\frac{t^2}{2}\sum_{k\neq 0}\frac{|H_I^{k0}|^2}{(E_0^{(0)}-E_k^{(0)})^2}|E_0^{(0)}\rangle + O(t^3) \\
&= |\downarrow\uparrow\uparrow\rangle - t\left(\frac{1}{2\epsilon_0-2\epsilon_1}|\uparrow\downarrow\uparrow\rangle + \frac{1}{-2\epsilon_2-2\epsilon_1}|\downarrow\downarrow\downarrow\rangle\right) \\
&\quad +t^2\left[\left(\frac{1}{(2\epsilon_0-2\epsilon_2)(2\epsilon_0-2\epsilon_1)}\right.\right. \\
&\quad \left.+\frac{1}{(2\epsilon_0-2\epsilon_2)(-2\epsilon_1-2\epsilon_2)}\right)|\uparrow\uparrow\downarrow\rangle \\
&\quad \left.-\frac{1}{2}\left(\frac{1}{(2\epsilon_0-2\epsilon_1)^2}+\frac{1}{(2\epsilon_1+2\epsilon_2)^2}\right)|\downarrow\uparrow\uparrow\rangle\right] + O(t^3) \\
&\equiv A|\downarrow\uparrow\uparrow\rangle + B|\uparrow\downarrow\uparrow\rangle + C|\downarrow\downarrow\downarrow\rangle + D|\uparrow\uparrow\downarrow\rangle \\
&\quad +O(t^3).
\end{aligned} \tag{4.88}$$

For the matrix element of the bath operator σ_2^x between thw excited and ground states we thus obtain

$$\begin{aligned} \langle E_0|\sigma_2^x|\mathrm{GS}\rangle &= AH + BG + CF + DE + O(t^3) \\ &= H + BG + CF + D + O(t^3). \end{aligned} \tag{4.89}$$

Combining the second term of H with BG and the second term of D with CF, the resulting 4 terms can be factorized into the form

$$\begin{aligned} \langle E_0|\sigma_2^x|\mathrm{GS}\rangle &= \left(\frac{t}{2\epsilon_1 - \omega} + \frac{t}{2\epsilon_1 + \omega}\right) \times \\ &\quad \left(\frac{t}{2\epsilon_2 - \omega} + \frac{t}{2\epsilon_2 + \omega}\right) + O(t^3). \end{aligned} \tag{4.90}$$

with $\omega = 2\epsilon_0$ being the excitation energy. This indeed coincides precisely with the result of the locator expansion, Eq. (4.27).

Chapter 5

Superglasses: coexistence of superfluid order and glassy order

In this Chapter I study the interplay of superfluidity and glassy ordering of hard core bosons with random, frustrating interactions. This is motivated by bosonic systems such as amorphous supersolid, disordered superconductors with preformed pairs and helium in porous media. I analyze the fully connected mean field version of this problem, which exhibits three low temperature phases, separated by two continuous phase transitions: an insulating, glassy phase with an amorphous frozen density pattern, a non-glassy superfluid phase and an intermediate phase, in which both types of order coexist. I elucidate the nature of the phase transitions, highlighting in particular the role of glassy correlations across the superfluid-insulator transition. The latter suppress superfluidity down to $T = 0$, due to the depletion of the low energy density of states, unlike in the standard BCS scenario. Further, I investigate the properties of the coexistence (superglass) phase. I find anticorrelations between the local order parameters and a non-monotonous superfluid order parameter as a function of T. The latter arises due to the weakening of the glassy correlation gap with increasing temperature. Implications of the mean field phenomenology for finite dimensional bosonic glasses with frustrating Coulomb interactions are discussed.

5.1 Model

We consider the fully connected model of hard-core bosons with random pairwise interactions between all bosons,

$$H = -\sum_{i<j} V_{ij} n_i n_j + \sum_i \epsilon_i n_i - \frac{t_b}{N} \sum_{i<j} \left(b_i^\dagger b_j + b_j^\dagger b_i \right). \tag{5.1}$$

Here, $n_i = b_i^\dagger b_i$ is the number operator on site i, and the hard core constraint limits n_i to assume values 0 or 1. $b_i(b_i^\dagger)$ denote the annihilation (creation) operators for a hard-core boson at site i. V_{ij} is a quenched disorder with Gaussian distribution of zero mean and variance V^2/N, ϵ_i describes a quenched disorder potential for the bosons, and t_b/N is the unfrustrated hopping strength between any pair of sites. The scaling

of the couplings with N is chosen so as to yield a non-trivial thermodynamic limit for $N \to \infty$.

In the absence of hopping, the model becomes classical and is equivalent to the Sherrington-Kirkpatrick spin glass (SK) model [63] in a random field. It is well-known that except for lowering the transition temperature, the random fields do not alter the low temperature properties of the glass phase. We thus restrict our attention mostly to a slightly simpler model proposed in Ref. [39], which corresponds to a special choice of the ϵ_i:

$$\begin{aligned} H &= -\sum_{i<j} V_{ij}(n_i - 1/2)(n_j - 1/2) \\ &\quad -\frac{t_b}{N}\sum_{i<j}\left(b_i^\dagger b_j + b_j^\dagger b_i\right). \end{aligned} \tag{5.2}$$

Similar fermionic mean field models have been studied in Refs. [103, 104]. The identification $2n_i - 1 = s_i^z \in \{\pm 1\}$, $b_i^\dagger = s_i^+, b_i = s_i^-$, allows us to map this model into a fully connected spin glass model with quantum fluctuations arising from non-random spin flip terms,

$$H = -\sum_{i<j} J_{ij} s_i^z s_j^z - \frac{t}{N}\sum_{i<j}\left(s_i^x s_j^x + s_i^y s_j^y\right), \tag{5.3}$$

with the simple dictionary

$$J_{ij} = \frac{V_{ij}}{4}, \quad t = \frac{t_b}{2}. \tag{5.4}$$

For $t = 0$, this Hamiltonian reduces to the SK model, which possesses a spin glass phase at low temperature, $T < T_g = J$. Without the Ising interactions, $J_{ij} = 0$, the Hamiltonian turns into the mean field XY model, which has a superfluid (or XY ferromagnetic) phase at low temperatures ($T < T_s = t$). In this paper we establish the phase diagram and study the properties of the bulk phases resulting from the competition of random density-density interactions and boson hopping (bosonic language) or equivalently random Ising interactions and ferromagnetic transverse coupling (spin language).

5.2 Free energy and self-consistent equations

5.2.1 General formalism

The disorder average of the free energy of the model (6.1) can be obtained using the replica method [71]

$$\langle \log Z \rangle_J = \lim_{n\to 0} \frac{\langle Z^n \rangle_J - 1}{n}, \tag{5.5}$$

where Z is the partition function and $\langle ... \rangle_J$ indicates an average over the couplings J_{ij}.

Following a method introduced by Bray and Moore [105] it is useful to represent the partition function as an imaginary time path integral:

$$
\begin{aligned}
Z^n &= \mathrm{Tr}\mathcal{T}\exp\Bigg\{\beta\int_0^1 d\tau\sum_{a=1}^{n}\sum_{i<j}\Bigg[J_{ij}s_{ia}^z(\tau)s_{ja}^z(\tau) \\
&\quad +\frac{t}{N}\Big(s_{ia}^x(\tau)s_{ja}^x(\tau)+s_{ia}^y(\tau)s_{ja}^y(\tau)\Big)\Bigg]\Bigg\},
\end{aligned}
\tag{5.6}
$$

where $\mathcal{T}$ orders the operators in decreasing order of their argument $\tau \in [0,1]$. This "time" argument of $s(\tau)$ merely serves us to define the time-ordering, while $s(\tau)$ denotes always the same Pauli matrix, independently of time.

Averaging over disorder and decoupling the spins on different sites using a Hubbard-Stratonovich transformation with the order parameter fields Q_{ab}, M_a^x, M_a^y, we obtain:

$$
\begin{aligned}
\langle Z^n\rangle_J &\propto \int\prod_a dQ_{aa}(\tau,\tau')\,dM_a^x(\tau)\,dM_a^y(\tau) \\
&\quad\times\prod_{a<b}dQ_{ab}(\tau,\tau')\exp\left(-N\mathcal{F}\right)
\end{aligned}
\tag{5.7}
$$

with

$$
\begin{aligned}
\mathcal{F} &= \frac{J^2\beta^2}{4}\int_0^1\int_0^1 d\tau d\tau' \\
&\quad\times\left[\sum_{a\neq b}Q_{ab}^2(\tau,\tau')+\sum_a Q_{aa}^2(\tau,\tau')\right] \\
&\quad+\frac{t\beta}{2}\int_0^1 d\tau\sum_a\left[M_a^x(\tau)^2+M_a^y(\tau)^2\right] \\
&\quad-\log\mathcal{Z},
\end{aligned}
\tag{5.8}
$$

$$
\mathcal{Z} = \mathrm{Tr}\mathcal{T}\exp\left(-S_{\text{eff}}\right),
\tag{5.9}
$$

$$
\begin{aligned}
S_{\text{eff}} &= -\frac{J^2\beta^2}{2}\int_0^1\int_0^1 d\tau d\tau' \\
&\quad\times\Bigg[\sum_{a\neq b}Q_{ab}(\tau,\tau')s_a^z(\tau)s_b^z(\tau') \\
&\quad+\sum_a Q_{aa}(\tau,\tau')s_a^z(\tau)s_a^z(\tau')\Bigg] \\
&\quad-t\beta\sum_a\int_0^1 d\tau\Big(M_a^x(\tau)s_a^x(\tau)+M_a^y(\tau)s_a^y(\tau)\Big).
\end{aligned}
\tag{5.10}
$$

In the limit $N \to \infty$, the functional integral (5.7) is dominated by the saddle point of the replicated free energy $\mathcal{F}$, which satisfies

$$\begin{aligned} 0 &= \frac{\delta \mathcal{F}}{\delta Q_{ab}(\tau,\tau')} \Rightarrow Q_{ab}(\tau,\tau') = \langle \mathcal{T} s_a^z(\tau) s_b^z(\tau') \rangle_{\text{eff}} \\ &= \langle s_a^z s_b^z \rangle_{\text{eff}} \equiv Q_{ab}, \qquad (5.11) \\ 0 &= \frac{\delta \mathcal{F}}{\delta Q_{aa}(\tau,\tau')} \Rightarrow Q_{aa}(\tau,\tau') = \langle \mathcal{T} s_a^z(\tau) s_a^z(\tau') \rangle_{\text{eff}} \\ &\equiv R(\tau,\tau'), \qquad (5.12) \\ 0 &= \frac{\delta \mathcal{F}}{\delta M_a^x(\tau)} \Rightarrow M_a^x(\tau) = \langle s_a^x(\tau) \rangle_{\text{eff}} \equiv M^x, \qquad (5.13) \\ 0 &= \frac{\delta \mathcal{F}}{\delta M_a^y(\tau)} \Rightarrow M_a^y(\tau) = \langle s_a^y(\tau) \rangle_{\text{eff}} \equiv M^y, \qquad (5.14) \end{aligned}$$

where $\langle ... \rangle_{\text{eff}}$ denotes the average with respect to the effective action S_{eff} of a single site. We have used that, as usual, the saddle point values of $Q_{a \neq b}$ and $M_a^{x,y}$ are independent of imaginary time, while $Q_{aa}(\tau,\tau')$ depends only on the imaginary time difference [119]. Furthermore, Q_{aa} and $M_a^{x,y}$ do not depend on the replica index a. For Q_{ab} we make the standard ultrametric ansatz, parametrized by a monotonous function $q(x)$ on the interval $x \in [0,1]$, which is well-known to describe successfully the SK model and other mean field glasses [?]. We are free to choose coordinates in the x, y plane such that the spontaneous magnetization $\vec{M}$ points in the x-direction, and thus we set $M^y = 0$.

Note that $M^x \neq 0$ signals the presence of transverse (XY) order of the spins, that is, superfluidity of the hard core bosons, which breaks the $U(1)$ symmetry spontaneously. On the other hand, a non-constant value of $Q_{a \neq b}$ implies the spontaneous breaking of the replica symmetry, and thus the presence of a glass phase with many metastable states and non-trivially broken ergodicity. As long as we do not consider random field disorder, the breaking of replica symmetry coincides with the breaking of the Ising symmetry and is signalled by a nonzero value of $Q_{a \neq b}$. We will see below that the $U(1)$ and the replica symmetries can be broken simultaneously in a what has been called a "superglass phase" in Refs. [39, 40].

To find the location of a (continuous) glass transition, we expand the free energy to second order in Q_{ab}. We find an instability towards replica symmetry breaking, and thus the emergence of a glassy density ordering of bosons, when

$$\begin{aligned} \beta J \int_0^1 \int_0^1 d\tau d\tau' \, \langle \mathcal{T} s_a^z(\tau) s_a^z(\tau') \rangle_{\text{eff}} &= \beta J \int_0^1 d\tau R(\tau) \\ &= 1, \qquad (5.15) \end{aligned}$$

or

$$J \chi^{\parallel} = 1, \qquad (5.16)$$

where $\chi^{\parallel} \equiv \chi_{zz}(\omega = 0)$ is the zero-frequency limit of the longitudinal susceptibility. This condition is of course to be evaluated at $Q_{a \neq b} = 0$.

On the other hand, a second order phase transition from the high temperature phase towards a superfluid state is indicated by the instability condition, which follows from $\partial^2 \mathcal{F}/\partial M^2 = 0$:

$$\beta t \int_0^1 \int_0^1 d\tau d\tau' \, \langle \mathcal{T} s_a^x(\tau) s_a^x(\tau') \rangle_{\text{eff}} = 1, \tag{5.17}$$

or

$$t\chi^\perp = 1, \tag{5.18}$$

where $\chi^\perp \equiv \chi_{xx}(\omega = 0)$ is the static transverse susceptibility. These expressions must be calculated in the non-superfluid phase where $M = 0$. In this regime the effective action S_{eff} is classical, which entails the further simplification $R(\tau) = 1$. This feature is due to the suppression of quantum fluctuations in the non-superfluid phase by factors of $1/N$, due to the scaling of the transverse coupling. It allows us to find the superfluid-insulator transition analytically, even at zero temperature, without solving a full quantum impurity problem. In particular, we immediately find that the transition from the disordered high temperature phase to a glassy phase is given by

$$T_g = J, \tag{5.19}$$

exactly as in the classical SK model. However, the glass transition line will be modified if it is preceded by a superfluid transition at higher temperature.

5.2.2 Solution of the saddle point equations

A full solution of the saddle point equations involves the solution of the problem of interacting replica as well as the evaluation of dynamical correlation functions with the effective action S_{eff}, if $M \neq 0$ and the replica symmetry is broken as well.

Here we describe what steps an exact solution involves, and then discuss the approximations we will use to study parts of the phase diagram, especially the bulk of the superglass phase.

To describe a non-glassy superfluid phase, the replica structure is trivial, and one needs to solve the self-consistency equations

$$M = \langle s^x \rangle_{\text{eff}}, \quad R(\tau) = \langle \mathcal{T} s^z(\tau) s^z(0) \rangle_{\text{eff}}, \tag{5.20}$$

with effective action

$$\begin{aligned} S_{\text{eff}} &= -\frac{\beta^2 J^2}{2} \int_0^1 \int_0^1 d\tau d\tau' s^z(\tau) R(\tau - \tau') s^z(\tau') \\ &\quad -\beta t M \int_0^1 d\tau s^x(\tau). \end{aligned} \tag{5.21}$$

These can be solved using techniques as used in dynamical mean field theory [106].

In a glassy phase the replica structure has to be taken into account. Assuming the standard ultrametric structure of the saddle-point matrix Q_{ab}, the above single-replica scheme has to be generalized to include a self-consistent distribution of frozen longitudinal fields $P(y)$ acting on a given replica. This captures the distribution of random frozen fields y_i created by the exchange of sites i with the frozen magnetization pattern with a spin glass state [107]. In practice this requires the simultaneous solution of

$$\begin{aligned} m(y) &= \langle s^z \rangle_{S_{\rm eff}(y)}\,, \\ m_x(y) &= \langle s^x \rangle_{S_{\rm eff}(y)}\,, \\ M &= \int dy P(y) m_x(y), \\ R(\tau) &= \int dy P(y)\, \langle \mathcal{T} s^z(\tau) s^z(0) \rangle_{S_{\rm eff}(y)}\,, \end{aligned} \tag{5.22}$$

where the effective single replica action in a frozen field y reads

$$\begin{aligned} S_{\rm eff}(y) &= -\frac{\beta^2 J^2}{2} \int_0^1 \int_0^1 d\tau d\tau' \\ &\quad \times s^z(\tau) \left[R(\tau - \tau') - q_{\rm EA} \right] s^z(\tau') \\ &\quad -\beta t M \int_0^1 d\tau s^x(\tau) - \beta y \int_0^1 d\tau s^z(\tau). \end{aligned} \tag{5.23}$$

The Edwards-Anderson order parameter $q_{\rm EA}$ characterizes the glassy freezing in a pure state of the glass and is given by

$$q_{\rm EA} = q(x=1) = \int dy P(y) m^2(y). \tag{5.24}$$

As first derived by Sommers and Dupont [107], the frozen field distribution $P(y) \equiv P(y, x=1)$ is obtained from a self-consistent solution of the differential equations on the interval $x \in [0,1]$

$$\dot{m}(y,x) = -\frac{\dot{q}(x)}{2} \left[m''(y,x) + 2x m(y,x) m'(y,x) \right], \tag{5.25}$$

$$\dot{P}(y,x) = \frac{\dot{q}(x)}{2} \left[P''(y,x) - 2x (m(y,x) P(y,x))' \right], \tag{5.26}$$

with

$$m(y, x=1) = m(y), \quad P(y, x=0) = \delta(y), \tag{5.27}$$

where dots and primes denote derivatives with respect to x and y, respectively. The solutions of these differential equations solve the saddle point equations of the replica

free energy(5.8) [107]. The overlap function $q(x)$, which parametrizes the ultrametric matrix Q_{ab} by the distance x between replica, must obey the self-consistency relation

$$q(x) = \int P(y,x) m(y,x)^2. \tag{5.28}$$

Notice that Eqs. (5.25) and (5.26) are the same as in a classical spin glass. The influence of quantum fluctuations enters through the boundary condition $m(y, x = 1) \equiv m(y)$, where $m(y)$ was defined in Eq. (5.22) These differential equations provide an elegant way of integrating out all spins except for one [108].

Once the above scheme has been solved self-consistently, site-averaged observables such as the longitudinal magnetization are given by

$$\begin{aligned} M^z \equiv \left\langle \frac{1}{N} \sum_i s_i^z \right\rangle &= \int dy P(y) \left\langle s^z \right\rangle_{S_{\rm eff}(y)} \\ &= \int dy P(y) m(y). \end{aligned} \tag{5.29}$$

The properties of the solution of these differential equations are well understood in several classical models exhibiting full replica symmetry breaking with continuous functions $q(x)$ [109, 110, 72, 111]. The full solution of mean field quantum glasses in the ergodicity broken has not been analyzed in the literature so far. However, an analysis of the transverse field SK model shows that most features of the low temperature solution of $q(x)$ carry over rather naturally to the quantum case [112]. A salient new feature in the quantum case is the fact that full replica symmetry breaking implies marginal stability of the whole glass phase, which in turn ensures the presence of gapless collective excitations. The latter is very similar to what was found, e.g., in the threshold states of quantum p-spin models [113], or in the quantum dynamics of elastic manifolds, approximated with a replica symmetry breaking variational approach [114].

5.2.3 Alternative derivation by a cavity approach

The replica-diagonal part of the above scheme will become easier to understand, if we derive it in a cavity framework [115] similarly to the derivation of the quantum analog of Thouless-Anderson-Palmer equations by Biroli and Cugliandolo [113]. From a cumulant expansion in the couplings involving site o it is easy to obtain the following effective action for the site o:

$$\begin{aligned} S_o^{\rm eff} &= -\frac{\beta^2}{2} \int_0^1 \int_0^1 d\tau d\tau' \\ &\quad \times s_o^z(\tau) \left[\sum_i J_{oi}^2 \left\langle s_i^z(\tau) s_i^z(\tau') \right\rangle_c^o \right] s_o^z(\tau') \\ &\quad -\beta \int_0^1 d\tau \left(h_o^z(\tau) s_o^z(\tau) + h^x(\tau) s_o^x(\tau) \right). \end{aligned} \tag{5.30}$$

Here

$$h_o^z(\tau) = \sum_i J_{oi} \langle s_i^z(\tau) \rangle^o = \sum_i J_{oi} \langle s_i^z \rangle^o \tag{5.31}$$

is the site-dependent longitudinal field, which does not depend on time, however. The index o denotes a "cavity average", i.e. an average over the action of the system, in which the site o has been removed. The subscript c indicates a connected correlator. The effective transverse field,

$$\begin{aligned} h^x(\tau) &= \frac{t}{N} \sum_i \langle s_i^x(\tau) \rangle^o = \frac{t}{N} \sum_i \langle s_i^x \rangle^o \\ &= \frac{t}{N} \sum_i \langle s_i^x \rangle = tM, \end{aligned} \tag{5.32}$$

does not fluctuate from site to site, and is independent of τ if we neglect subleading terms, which scale as inverse powers of N . Note that for large N

$$\sum_i J_{oi}^2 \langle s_i^z(\tau) s_i^z(\tau') \rangle_c^o \to J^2 \left[R(\tau - \tau') - q_{\mathrm{EA}} \right], \tag{5.33}$$

independently of the site o. The distribution of h_i^z over the sites i is the frozen field distribution,

$$P(y) = N^{-1} \sum_{i=1}^{N} \delta(y - h_i^z) \tag{5.34}$$

computed in the replica formalism. Thus we precisely recover the self-consistency problem for the replica diagonal, while the solution of the replica off-diagonal part furnishes the distribution $P(y)$.

For the study of the phase transition from the insulating glass phase into the superfluid, it will prove crucial to use the full low temperature solution of the SK model. However, in order to analyze properties of the mixed "superglass" phase we will restrict ourselves to a one-step approximation, which we discuss in the next section.

5.2.4 Static and one-step approximation

In order to avoid solving numerically a full self-consistent quantum problem as outlined in Eqs. (5.22) above, we will resort to the widely used static approximation. The latter consists in seeking a minimum of the free energy not with respect to the full function space $R(\tau)$ but, instead with respect to a constant value $R(\tau) \to R$.

A further approximation which we will use in the study of the quantum glassy phases is the one-step approximation for the structure of replica symmetry breaking. It is equivalent to assuming a step form of $q(x)$

$$q(x) = \Theta(x - x_1) Q_1 + \Theta(x_1 - x) Q_0 \tag{5.35}$$

and optimizing the free energy over x_1, Q_1, Q_0. This is expected to give qualitatively good results, especially at intermediate temperatures and close to the glass transition. Combined with the static approximation for the replica diagonal, short time part one obtains the free energy functional per spin:

$$\begin{aligned} \beta f &= \frac{\beta^2 J^2}{4}\left[(x_1-1)Q_1^2 - x_1 Q_0^2 + R^2\right] \\ &+\frac{\beta t}{2}M^2 - \frac{1}{x_1}\int Dy_0 \\ &\times \log \int Dy_1 \left[\int Dy_R 2\cosh(\beta\sqrt{h_y^2 + t^2 M^2})\right]^{x_1}, \end{aligned} \tag{5.36}$$

where $h_y = y_0 + y_1 + y_R$. Dy_0, Dy_1 and Dy_R are Gaussian measures: $Dy_0 = \frac{\exp\left(-\frac{y_0^2}{2Q_0J^2}\right)}{\sqrt{2\pi Q_0 J^2}}dy_0$, $Dy_1 = \frac{\exp\left(-\frac{y_1^2}{2(Q_1-Q_0)J^2}\right)}{\sqrt{2\pi(Q_1-Q_0)J^2}}dy_1$ and $Dy_R = \frac{\exp\left(-\frac{y_R^2}{2(R-Q_1)J^2}\right)}{\sqrt{2\pi(R-Q_1)J^2}}dy_R$.

Note that $Q_1 = q_{\rm EA}$ is the Edwards Anderson order parameter in the one step approximation, while Q_0 is the overlap between different spin glass states. We point out that the above free energy differs from the expression given in Ref. [39], where the static approximation was not carried out correctly. This error was at the origin of several strange features of the phase diagram reported there, such as a T-independent transition between superfluid and superglass and a J-independent superfluid transition.

5.2.5 1RSB free energy and self consistent equations

Here we rewrite the one-step self-consistency equations with the help of the local field distribution.

The effective partition function of a single spin is

$$\begin{aligned} Z_{\rm eff}(y) &= {\rm Tr}\mathcal{T}\exp\left(-S_{\rm eff}(y)\right) \\ &= {\rm Tr}\mathcal{T}\exp\left(\frac{\beta^2 J^2}{2}\int_0^1\int_0^1 d\tau d\tau' \right. \\ &\quad s^z(\tau)\left[R(\tau-\tau') - q_{\rm EA}\right]s^z(\tau') \\ &\quad \left. +\beta t M\int_0^1 d\tau s^x(\tau) + \beta y\int_0^1 d\tau s^z(\tau)\right). \end{aligned} \tag{5.37}$$

In the case of one-step replica symmetry breaking, the frozen field distribution within one pure state can be obtained by stepwise integration of the flow equations (5.25,5.26), yielding (cf. [71])

$$P(y) = \int Dy_0 \frac{\int Dy_1 \delta(y-(y_0+y_1)) Z_{\rm eff}^{x_1}(y_0+y_1)}{\int D\widetilde{y}_1 Z_{\rm eff}^{x_1}(y_0+\widetilde{y}_1)}, \tag{5.38}$$

where $D\widetilde{y}_1$ is a Gaussian measure like Dy_1 with variance $(Q_1-Q_0)J^2$.

Under the static approximation, Eq. (5.37) becomes

$$Z_{\rm eff}(y) = \int Dy_R Z_{\rm stat}(y + y_R), \tag{5.39}$$

where

$$Z_{\rm stat}(y) = 2\cosh(\beta\sqrt{y^2 + M^2t^2}). \tag{5.40}$$

One can interpret y_R as a random field, which is generated by the thermal fluctuations of the non-frozen part of the magnetization.

The longitudinal and transverse magnetizations of a spin in a frozen field y introduced in Eqs. (5.22) are easily seen to be given by

$$m(y) = \langle s^z \rangle_{S_{\rm eff}(y)} = \frac{1}{\beta}\frac{\partial}{\partial y}\log(Z_{\rm eff}(y)), \tag{5.41}$$

$$m_x(y) = \langle s^x \rangle_{S_{\rm eff}(y)} = \frac{1}{\beta}\frac{\partial}{\partial (tM)}\log(Z_{\rm eff}(y)). \tag{5.42}$$

The saddle point equations for the Edwards-Anderson parameter Q_1 and the superfluid order parameter M can now be expressed as:

$$Q_1 = \frac{1}{N}\sum_i \langle s_i^z \rangle^2 = \int dy P(y) m^2(y), \tag{5.43}$$

$$M = \frac{1}{N}\sum_i \langle s_i^x \rangle = \int dy P(y) m_x(y). \tag{5.44}$$

The saddle point equation for the parameter R reads

$$\beta(R - Q_1) = \int P(y)\chi^{\parallel}_{\rm loc}(y)dy, \tag{5.45}$$

which relates the static approximation of the connected s^z-correlator, $R - Q_1$, to the average local susceptibility

$$\chi^{\parallel}_{\rm loc}(y) = \frac{\partial m(y)}{\partial y}. \tag{5.46}$$

The saddle point equation for the Q_0 can be written in a similar way:

$$Q_0 = \int dy_0 P(y_0; x_1) m^2(y_0; x_1), \tag{5.47}$$

where

$$\begin{aligned} P(y_0; x_1) &= \frac{1}{\sqrt{2\pi Q_0 J^2}}\exp(-\frac{y_0^2}{2Q_0J^2}), \\ m(y_0; x_1) &= \frac{\int Dy_1 Z^{x_1}_{\rm eff}(y_0 + y_1) m(y_0 + y_1)}{\int D\widetilde{y}_1 Z^{x_1}_{\rm eff}(y_0 + \widetilde{y}_1)}, \end{aligned} \tag{5.48}$$

are discrete versions of the continuous functions $P(y,x), m(y,x)$ introduced above.

Optimizing the one-step free energy with respect to Q_1, M, R and Q_0 yields the saddle point equations Eqs. (5.43-5.47). To capture equilibrium states, we should further extremize with respect to the Parisi parameter x_1, i.e. $\frac{\partial f}{\partial x_1} = 0$, which yields the further condition

$$-\frac{\beta^2 J^2}{4}(Q_1^2 - Q_0^2)m^2 = \int Dy_0 \log \int Dy_1 Z_{\text{eff}}^{x_1}(y_0 + y_1)$$
$$-x_1 \int Dy_0 \frac{\int Dy_1 Z_{\text{eff}}^{x_1}(y_0 + y_1) \log Z_{\text{eff}}(y_0 + y_1)}{\int Dy_1 Z_{\text{eff}}^{x_1}(y_0 + y_1)}. \tag{5.49}$$

It is a useful check that upon imposing $Q_1 = Q_0$, the saddle point equations for Q_0 and Q_1 reduce to the same replica symmetric constraint. When $M = 0$, the local field distribution, the free energy and the saddle point equations reduce to those of the classical SK model, as it should be.

5.3 Phase diagram

Let us now study the phase diagram of our model (6.1). The gross features of the phase diagram we find are similar to the ones found in Refs. [39, 40]: The low temperature phase exhibits three phases: a non-glassy superfluid at small J/t, an insulating (non-super-fluid) glass phase at large J/t, and most interestingly, a phase in between with both glassy order and superfluidity. However, as mentioned before, we find a distinctly different behavior of the phase boundaries than Ref. citeGingras.

Moreover, we are able to analyze the limit $T \to 0$, whose properties were inaccessible in previous works [39, 40]. The latter is of particular interest in the context of the superfluid-insulator transition.

The findings of the mean field analysis are in qualitative agreement with Monte Carlo studies in finite dimensions at low but finite temperatures. The analytical approach allows for a detailed analysis of the properties of the mixed phase, and of the glass-to-superglass transition.

5.3.1 High temperature phase

The high temperature phase is simple to describe. Since $M = 0$, the system behaves identically to the paramagnetic phase of the classical SK model, and $R = 1$ holds exactly. In this regime the static approximation is of course exact.

At large enough J/t, the leading instability upon lowering the temperature is the classical glass transition at $T_g = J$, as mentioned earlier. However, at small values of J/t, the tendency to form a superfluid wins. The instability condition towards XY symmetry breaking,

$$t\chi^{\perp} = t\frac{\partial m_x(y=0)}{\partial h_x}\Big|_{h_x=0} = 1 \tag{5.50}$$

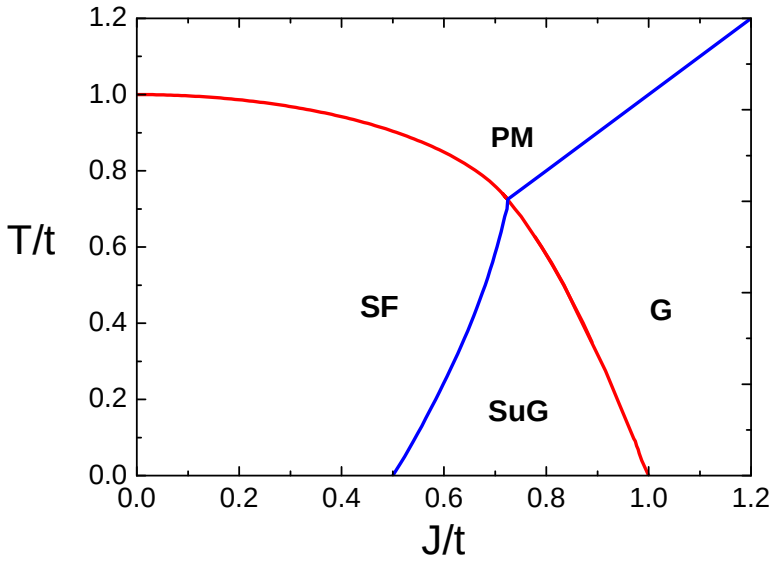

Figure 5.1: Phase diagram of glassy hard core bosons. At high temperature, the straight blue line $T = J$ indicates the classical SK glass transition line. The red solid line shows the superfluid phase boundary which is given by the instability condition (5.51). The two lines cross at the tricritical point $(T/t)_T = (J/t)_T = 0.7248$. At low temperature, the blue line shows the phase boundary of the glass within the superfluid phase, as evaluated within the static approximation, cf. (5.16). The glass transition at $T = 0$ occurs at $(J/t)_{g,\mathrm{stat}} = 1/2$. The red solid line indicates the location of the onset of superfluidity within the glass phase, as evaluated within the full breaking of the replica symmetry to the instability condition (5.63). The superfluid transition at $T = 0$ takes place at $(J/t)_s = 1.00$.

can be evaluated exactly. In this expression h_x is a uniform transverse field. The transverse susceptibility is easily calculated for the replicated Hamiltonian with a Hubbard-Stratonovich transformation of the quadratic term $R\int d\tau d\tau' s^z(\tau)s^z(\tau')$. This results in the instability criterion

$$\frac{1}{t} = \chi^{\perp} = \beta \frac{\int dh e^{-h^2/2J^2} \sinh(\beta h)/\beta h}{\int dh e^{-h^2/2J^2} \cosh \beta h}. \tag{5.51}$$

The glass transition and the superfluid transition line cross at the tricritical point

$$T_T = J_T = t_T \frac{\int dz e^{-z^2/2} \sinh(z)/z}{\int dz e^{-z^2/2} \cosh z} = 0.7248\, t_T. \tag{5.52}$$

The result (5.51) does not have the familiar looking form of an average local transverse susceptibility. However, it can indeed be recast in such a way. This furnishes us a better understanding of the interaction effects in the high temperature phase, and at the same time illuminates the nature of the static approximation in the superfluid phases.

Let us rederive the above result directly from the non-replicated Hamiltonian:

$$\begin{aligned} H &= -\frac{1}{2}\sum_{ij} J_{ij} s_i^z s_j^z - \frac{t}{2N}\sum_{ij}\left(s_i^x s_j^x + s_i^y s_j^y\right) \\ &\quad -\sum_i h_x s_i^x, \end{aligned} \tag{5.53}$$

where h_x is an infinitesimal field. In a given classical Ising configuration, the spin i sees an "instantaneous" local field $h_i^z = \sum_{j\neq i} J_{ij} s_j^z$, while the transverse coupling is negligible in the paramagnetic phase where $N^{-1}\sum_j \left\langle s_j^x \right\rangle = M = 0 = N^{-1}\sum_j \left\langle s_j^y \right\rangle$. Thus the transverse susceptibility can be calculated as a site and configuration average of the susceptibility of a single spin sitting in an instantaneous field h, $\chi^\perp(h) = \int_0^\beta d\tau \left\langle s^x(\tau) s^x(0)\right\rangle = \tanh(\beta h)/h$.

The thermal distribution of instantaneous local fields of the SK model has been well studied [116], and takes the rather simple form

$$P_{\text{inst}}(h) = \cosh(\beta h)\frac{\exp(-\frac{h^2}{2J^2} - \frac{\beta^2 J^2}{2})}{\sqrt{2\pi J^2}} \tag{5.54}$$

in the paramagnetic phase. Note that the instantaneous field distribution is not a simple Gaussian, but small fields are under-represented. This phenomenon is closely related to the suppression of small fields encountered in the cavity approach to Ising systems [115], and is a precursor effect of the opening of the pseudogap in glassy phases at low temperatures [72, 47, 111].

The total transverse susceptibility is obtained as an average of the local susceptibility $\chi(h)$ over $P_{\text{inst}}(h)$:

$$\begin{aligned} \chi^\perp &= \int dh P_{\text{inst}}(h)\chi^\perp(h) \\ &= e^{-\frac{\beta^2 J^2}{2}} \int dh \frac{e^{-\frac{h^2}{2J^2}}}{\sqrt{2\pi J^2}} \frac{\sinh \beta h}{h}, \end{aligned} \tag{5.55}$$

which indeed coincides with the replica result (5.51).

The static approximation for superfluid phases has a completely analogous effect. The approximation replaces the dynamically fluctuating exchange fields on the various sites by a random distribution of quasi static fields. The latter differs from the distribution of frozen fields (which is Gaussian at high T) by a random Gaussian smearing with variance $J^2(R - q_{\text{EA}})$, and a reweighing factor proportional to $\cosh(\beta h)$ which accounts for the fact that a small instantaneous fields is less likely to observe on a given site, as it implies a positive free energy fluctuation in the environment.

5.3.2 Onset of glassy order within the superfluid

The instability towards forming a glass occurs when $J\chi^\parallel = \beta J \int d\tau d\tau' R(\tau - \tau') = 1$. Within the superfluid phase it is difficult to calculate this susceptibility exactly, and

we thus first resort to the static approximation, $R(\tau - \tau') \to R$. The instability of the statically approximated free energy occurs when $J\beta R = 1$, βR being the static approximation for the longitudinal susceptibility $\chi^{\parallel}$. Within the non-glassy superfluid phase there are no frozen fields, $P(y) = \delta(y)$. Thus, from Eqs. (5.44-5.45), the two relevant saddle point equations read

$$M = m_x(y = 0), \tag{5.56}$$

$$\beta R = \chi^{\parallel}_{\rm loc}(y = 0), \tag{5.57}$$

where $m_x(y = 0)$ and $\chi^{\parallel}_{\rm loc}(y = 0)$ are to be evaluated from Eqs. (5.39-5.42) and (5.46).

They have a relatively simple low temperature limit. One verifies that it is self-consistent to assume that

$$\beta R = \chi^{\parallel} \to \frac{r}{t}, \quad M \to 1 - m\frac{T}{t}, \tag{5.58}$$

with finite numbers r, m, as $T \to 0$.

Injecting this into the above self-consistency equations, and evaluating the Gaussian integral over y_R in Eq. (5.39) around the stationary point, the equations simplify to:

$$r = 1 + \frac{J^2 r}{t^2 - J^2 r} + O(T/t), \tag{5.59}$$

$$m = \frac{J^2 r}{2(t^2 - rJ^2)} + O(T/t). \tag{5.60}$$

This yields the solution for the susceptibility $J\chi^{\parallel} = Jr/t = \frac{t}{2J}\left(1 + \sqrt{1 - 4\left(\frac{J}{t}\right)^2}\right)$.

The static approximation predicts the quantum glass transition to occur at the critical point

$$\left(\frac{J}{t}\right)_{g,{\rm stat}} = \frac{1}{2}, \qquad (T = 0) \tag{5.61}$$

where $J\chi^{\parallel} = 1$.

It is difficult to predict whether we over- or underestimate the phase boundary with the static approximation in the superfluid phase. This is because the approximation has two competing effects with respect to the onset of glassy order. On one hand, we approximate the dynamic longitudinal susceptibility by the static one. Since the latter is bigger, we tend to overestimate the stability of the glassy ordering of s^z. This effect is well-known from the SK model in a (constant) transverse field Γ [117, 118, 119]. On the other hand, the static approximation underestimates quantum fluctuations of s_x, at least at low T. Indeed we see above that at $T = 0$, the static approximation predicts maximal transverse order, $M = 1$, independently of the value of J/t, while it is easy to show that quantum fluctuations around the transverse ferromagnetic state

decrease the magnetization as $M = 1 - O((J/t)^2)$. The overestimate of M leads to an underestimate of the longitudinal susceptibility, and thus of the tendency to glassy order. In view of these competing tendencies, it is hard to predict on which side with respect to Eq. (5.61) the exact glass instability will be located.

However, there is a simple way to obtain an upper bound for the quantum critical point. In the superfluid phase our model (6.1) is very similar to the SK model in a constant transverse field Γ [118]. with the difference that the effective transverse field Mt is self-generated and has to be determined self-consistently. However, it is clear that the effective transverse field is always smaller than t. From quantum Monte Carlo results for the transverse field SK model, one knows that a quantum glass phase obtains for $J/\Gamma \geq 0.76$ [119]. This implies that the model studied in the present work must certainly be in a glassy phase if $J/t \geq 0.76$. The latter value is thus an upper bound for $(J/t)_g$. Approaching from large values of J/T we will find below in Eq. (6.2) that the non-superfluid glass phase becomes unstable towards superfluidity already at $(J/t)_s = 1.00$. Hence, we conclude that a phase with both superfluid and glassy order parameters exists for a substantial range of parameters covering at least the interval $0.76 \leq J/t \leq 1.00$.

5.3.3 Superfluid instability within the insulating glass phase

Our discussion of the phase boundaries will be complete, once we have addressed the superfluid instability with in the glass phase at large J/t. The instability condition reads

$$t \int dy P(y) \frac{\partial m_x(y)}{\partial h_x}\Big|_{h_x=0} = 1, \tag{5.62}$$

where $P(y)$ is the non-trivial distribution of frozen local fields in the classical glass phase of the SK model. The properties of $P(y)$ are well studied, and turn out to be crucial to understand the low temperature behavior of the phase boundary and the physics of the glassy superfluid-to-insulator quantum phase transition.

We recall that in the non-superfluid glass phase the static approximation is exact with $R = 1$, so that the instability criterion can be expressed in the form,

$$t \int dy P(y) \frac{\int Dy_R \sinh(\beta(y+y_R)) \frac{1}{y+y_R}}{\int Dy_R \cosh(\beta(y+y_R))} = 1, \tag{5.63}$$

where $Dy_R = \frac{1}{\sqrt{2\pi(1-q_{\rm EA})J^2}} \exp(-\frac{y_R^2}{2(1-q_{\rm EA})J^2})$. This condition can be expressed in terms of the instantaneous field distribution as

$$t \int dh P_{\rm inst}(h) \frac{\tanh(\beta h)}{h} = 1, \tag{5.64}$$

where

$$P_{\rm inst}(h) = \int P(y) dy \frac{\cosh \beta h}{\cosh \beta y} \frac{\exp\left(-\frac{\beta(h-y)^2}{2h_O} - \frac{\beta h_O}{2}\right)}{\sqrt{2\pi h_O/\beta}}. \tag{5.65}$$

is the instantaneous field distribution, which was first derived in Ref. [116]. The term $h_O = \beta J^2(1 - q_{\rm EA})$ is known as Onsager's back reaction. Eq. (5.64) can be recognized as a BCS-equation, where the instantaneous field distribution $P_{\rm inst}(h)$ takes the role of the density of states.

The temperature dependent local field distribution can be obtained from a numerical solution of the self-consistent set of full RSB equations (5.25-5.28), from which the phase boundary of the insulator-to-superfluid transition is deduced . This yields the solid [red] line in Fig. 5.1). For comparison we also evaluate the phase boundary within a one-step approximation, which works well at moderate temperatures. However, it fails badly at low T where a non-physical reentrance of the superfluid instability would be predicted, and the quantum phase transition at $T \to 0$ is completely missed.

We note in passing that the thermodynamics of the insulating phase is essentially classical because of the scaling of the transverse coupling as t/N. If instead t were random and scaled as $1/\sqrt{N}$, the glass phase would also exhibit quantum fluctuations and would not reduce to the purely classical SK model. In that case, the analysis of the transition would become much more complicated. However, even though the thermodynamics can be obtained by a purely classical saddle point computation, one should not conclude that excitations do not have any quantum dynamics.

At low temperatures, the most prominent feature of the local field distribution $P(y)$ is a linear pseudogap which opens at small fields. The latter is required to assure the stability of the glass phase [120, 121], in a very similar manner as the Efros-Shklovskii Coulomb gap arises in electron glasses with unscreened, long range $1/r$ interactions [48, 111]. More precisely, it is known that $P(y) = \alpha|y| + O(T)$ with $\alpha = 0.301$ for fields in the range $T \ll |y| \ll J$, while the distribution decays like a Gaussian for $|y| \gg J$. At zero temperature the pseudogap extends down to $y = 0$ (i.e., the chemical potential in the terminology of hardcore bosons), while at finite but low temperatures $T \ll J$, $P(y)$ assumes a scaling form $P(y) = Tp(y/T)$ with $P(0) = \text{const.}$ and $p(x \gg 1) = \alpha|x| + \text{const.}$ [111, 72].

This scaling form asserts that only a fraction of $(T/J)^2$ is thermally active. Therefore the Edwards-Anderson parameter tends to 1 as $1 - q_{\rm EA} \sim (T/J)^2$. Accordingly, as $T \to 0$ there is no difference between the distribution of frozen and instantaneous fields, $P_{\rm inst}(h)$, since no thermal fluctuations are left. In this limit the instability condition (5.63) for onset of superfluidity then takes the form:

$$t_s \int dy \frac{P(y; T = 0)}{|y|} = 1. \tag{5.66}$$

Using the above mentioned features of $P(y)$ at low T one can easily obtain a rough estimate for the superfluid-insulator transition point as $(J/t)_s \simeq 1.05 \pm 0.1$. However, since the precise value is also sensitive to the part of $P(y)$ at high fields, $y \geq J$, a full numerical evaluation of the condition (6.2) is necessary to obtain the exact location of the quantum critical point. Using high precision data for $P(y; T)$ at low T from Ref. [122], we find $(J/t)_s \simeq 1.00 \pm 0.01$.

We emphasize an important difference between the quantum phase transition we have found here and a standard BCS transition. The latter, in the presence of a constant low energy density of states always yields a finite T_c, even though it becomes

exponentially small in $1/t$ for small t. In our glassy system the situation is fundamentally different in that the frustrated interactions suppress the density of states around the chemical potential with $P(y \to 0) \to 0$. This quenches the tendency for superfluidity and allows for a superfluid-to-insulator transition at a finite value of t, even in the mean field limit of $N \to \infty$ which we consider here.

This has important consequences for the nature of excitations and transport properties across the superfluid-insulator transition. In particular, the transition to the Bose insulator is accompanied by the Anderson localization of lowest energy excitations, whereas higher energy excitations remain delocalized relatively far into the insulator [123]. We believe that the physics revealed by this mean field model is relevant for Coulomb frustrated bosonic systems which undergo a transition from a superfluid to a Bose glass state in finite dimensions. This will be discussed in detail elsewhere [124].

It is interesting to compare our mean field predictions for the phase diagram with the 3D quantum Monte Carlo (QMC) simulation results reported in Ref. [39]. The mean field predictions for the quantum critical points actually match the numerical results surprisingly well. The latter were done for the Hamiltonian

$$\begin{aligned} H &= -\sum_{\langle i,j \rangle} V'_{ij}(n_i - 1/2)(n_j - 1/2) \\ &\quad -t' \sum_{\langle i,j \rangle} \left(b_i^\dagger b_j + \text{h.c.} \right), \end{aligned} \tag{5.67}$$

with binary disorder, $V'_{ij} = \pm V'$ with equal probability. Contact with the mean field model (5.2) is made by replacing the coordination number with $N \to z = 6$ for the 3D cubic lattice, and taking a Gaussian disorder with the same variance, $V^2/z = V'^2$, as well as a hopping $t_b/z = t'$.

Recalling the dictionary (5.4), the mean field estimate of the superglass to glassy insulator quantum phase transition is

$$\begin{aligned} \left(\frac{V'}{t'} \right)_s^{\text{MF}} &= \left(\frac{V/\sqrt{z}}{t_b/z} \right)_s = \left(\frac{4J/\sqrt{z}}{2t/z} \right)_s \\ &= 2\sqrt{z} \left(\frac{J}{t} \right)_s \simeq 4.9 \approx \left(\frac{V'}{t'} \right)_s^{\text{QMC}} \backsimeq 5, \end{aligned} \tag{5.68}$$

which comes close to the extrapolation of QMC results to $T = 0$. The transition point between superglass and non-glassy superfluid is estimated from the static approximation as

$$\begin{aligned} \left(\frac{V'}{t'} \right)_g^{\text{MF}} &= 2\sqrt{z} \left(\frac{J}{t} \right)_{g,\text{stat}} \simeq 2.45 \\ &\approx \left(\frac{V'}{t'} \right)_g^{\text{QMC}} \backsimeq 3.2. \end{aligned} \tag{5.69}$$

This indicates that the static approximation overestimates the stability of the superglass phase, similarly as what is known from the mean field version of the transverse field Ising spin glass.

The mean field prediction (with static approximation) for the interaction-to-hopping ratio $(V'/t')_T$ at the tricritical point is rather good, too,

$$\left(\frac{V'}{t'}\right)_T^{\rm MF} = 2\sqrt{z}\left(\frac{J}{t}\right)_{T,{\rm stat}} \simeq 3.55$$
$$\approx \left(\frac{V'}{t'}\right)_T^{\rm QMC} \backsimeq 3.8. \tag{5.70}$$

While the tricritical ordering temperature is overestimated by a factor of 2 (similarly as in the classical Ising spin glass) [125]

$$\left(\frac{T}{t'}\right)_T^{\rm MF} = \frac{z}{2}\left(\frac{T}{t}\right)_T \simeq 2.2, \tag{5.71}$$
$$\left(\frac{T}{t'}\right)_T^{\rm QMC} \backsimeq 1.1. \tag{5.72}$$

5.3.4 Robustness of the phase diagram to random field disorder

In the previous sections we have seen that the model (6.1) possesses an intermediate phase which is simultaneously superfluid and glassy. We have determined the phase boundaries as instability lines, assuming second order phase transitions. Indeed it seems unlikely that any of the instabilities could be preempted by a first order transition. Since the superfluid to insulator transition at $(J/t)_s$ is of particular interest, we provide further arguments in this section that the parts of the phase diagram related to the phase boundary of the non-superfluid glass remain robust when disorder potentials, i.e. random fields ϵ_i of variance W^2, are restituted to the model. In particular we will show that glass and superfluid transition lines meet at a tricritical point at finite temperature T_T/J and $(J/t)_T$. Further we determine the superfluid instability of the glass phase at $T = 0$ and show that it always occurs at a larger ratio (J/t) than the tricritical point, $(J/t)_s > (J/t)_T$. This suggests that for any W the transition line between non-superfluid and superfluid glass is not reentrant as a function of temperature. The absence of reentrance in turn suggests that the quantum phase transition out of the insulating glass remains second order, independent of the strength of the disorder potential.

The Hamiltonian with a disorder potentials reads

$$H = -\sum_{i<j} J_{ij} s_i^z s_j^z - \frac{t}{N}\sum_{i<j}\left(s_i^x s_j^x + s_i^y s_j^y\right) + \sum_i \epsilon_i s_i^z. \tag{5.73}$$

The disorder potential breaks the Z_2 symmetry, therefore $Q_{a\neq b} \neq 0$ already in the high temperature phase, where it assumes a constant replica symmetric value Q_0. The glass phase occurs at the Almeida-Thouless instability, which is given by [111]:

$$\beta^2 J^2 \int dy \frac{P_W(y)}{\cosh^4(\beta y)} = 1, \tag{5.74}$$

where

$$P_W(y) = \frac{\exp\left(-\frac{y^2}{2(W^2+J^2Q_0)}\right)}{\sqrt{2\pi(W^2+J^2Q_0)}}, \tag{5.75}$$

and Q_0 satisfies the self-consistent equation

$$Q_0 = \int P_W(y)\tanh^2(\beta y)dy. \tag{5.76}$$

The instability towards the superfluid phase is instead determined by

$$1/t = \int dh P_{\rm inst}(h)\frac{\tanh(\beta h)}{h}, \tag{5.77}$$

where

$$\begin{aligned} P_{\rm inst}(h) &= \int dy P_W(y)\frac{\cosh\beta h}{\cosh\beta y} \\ &\quad \times \frac{\exp\left(-\frac{\beta(h-y)^2}{2h_O}-\frac{\beta h_O}{2}\right)}{\sqrt{2\pi h_O/\beta}}, \end{aligned} \tag{5.78}$$

with the Onsager field $h_O = \beta J^2(1-Q_0)$ [116, 111].

The glass and superfluid transition lines meet at a tricritical point at $(T/J)_T$ and $(J/t)_T$ which are to be evaluated from Eqs. (5.74-5.78).

In the limit $W/J \gg 1$, one finds the tricritical temperature $(T/J)_T = \frac{4}{3\sqrt{2\pi}}\frac{J}{W} + O(\frac{J^2}{W^2})$ and $\beta_T h_O \to 3/2$, as $W/J \to \infty$.

The superfluid transition at $T=0$ is given by the condition

$$(1/t)_s = \int dh \frac{P_{\rm inst}(h;T=0)}{|h|}. \tag{5.79}$$

In the limit $W/J \gg 1$, $P_{\rm inst}(h;T=0)$ is known to have a simple structure :

$$P_{\rm inst}(h;T=0) = \begin{cases} \alpha|h|/J^2, & |h| \ll h^\star, \\ \frac{\exp\left(\frac{-(h-\gamma J^2/W)^2}{2W^2}\right)}{\sqrt{2\pi W^2}}, & |h| \gg h^\star, \end{cases} \tag{5.80}$$

with a smooth crossover between the two limiting forms around $\frac{h^\star}{J} = \frac{1}{\alpha\sqrt{2\pi}}\frac{J}{W} + O(\frac{J^2}{W^2})$. The value of the constant $\gamma = O(1)$ can be estimated by the normalization condition $\int dh P_{\rm inst}(h;T=0) = 1$, but will be irrelevant below.

For $W/J \gg 1$, $(J/t)_s$ and $(J/t)_T$ both behave as $\frac{4}{\sqrt{2\pi}}\frac{\log(W/J)}{W/J}$ to leading order. Their difference scales like cJ/W. The coefficient c can be evaluated easily by rescaling the variables $\beta_T h = \hat{h}$ and $\beta_T y = \hat{y}$,

$$\begin{aligned} c &= \lim_{W/J\to\infty}\frac{W}{J}\left[(J/t)_s - (J/t)_T\right] \\ &= \sqrt{\frac{2}{3}}\int\frac{d\hat{h}}{\hat{h}}\left[\hat{p}(\hat{h};T=0) - f(\hat{h})\right], \end{aligned} \tag{5.81}$$

where

$$\hat{p}(\hat{h};T=0) \quad = \quad \lim_{W/J\to\infty}\sqrt{\frac{3}{2}}WP_{\rm inst}(\hat{h}/\beta_T;T=0) \tag{5.82}$$

and

$$f(\hat{h}) = \int \frac{d\hat{y}}{\sqrt{2\pi}}\frac{\sinh(\hat{h})}{\cosh(\hat{y})}\frac{\exp\left(\frac{-(\hat{h}-\hat{y})^2}{3}-\frac{3}{4}\right)}{\sqrt{2\pi}}, \tag{5.83}$$

and we have used $\beta_T h_O \to 3/2$. We approximate Eq. (5.80) by extending the formula all the way to $h^\star$ and neglecting the shift of field h and we get :

$$\hat{p}(\hat{h};T=0) \approx \begin{cases} \frac{2\alpha\hat{h}}{\sqrt{3\pi}}, & |\hat{h}| \le \frac{3}{4\alpha}, \\ \sqrt{\frac{3}{4\pi}}, & |\hat{h}| \ge \frac{3}{4\alpha}, \end{cases} \tag{5.84}$$

Evaluating Eq. (5.81) numerically, using the estimate Eq. (5.84) , one obtains $c = 0.231 > 0$, establishing that $(J/t)_s > (J/t)_T$ even in the presence of strong disorder. We point out that Eq. (5.84) overestimates Eq. (5.82), but this overestimation should be much smaller than $c = 0.231$.

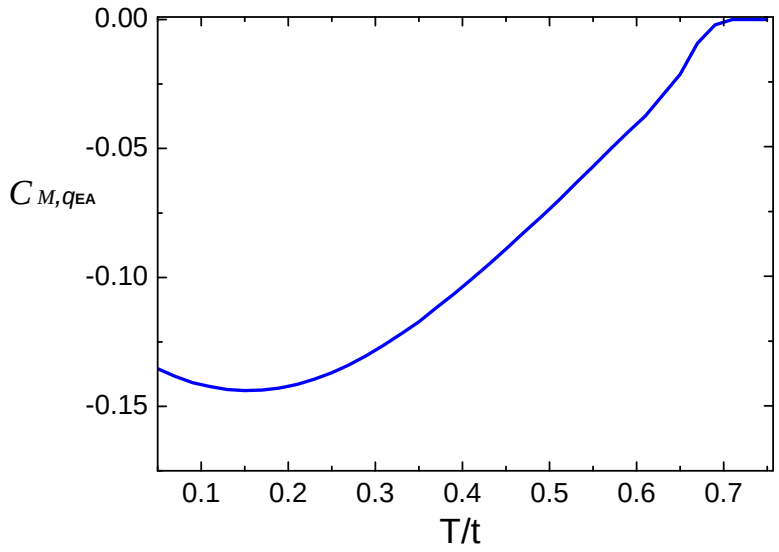

Figure 5.2: Cross-correlation between the local oder parameters for superfluidity and glassy order, respectively. The correlations are evaluated from Eq. (5.85) in the temperature range $0.05 < T/t < 0.75$ at fixed disorder $J/t = 0.724$, close to the ratio corresponding to the tricritical point. The local order parameters are anticorrelated, the maximal anticorrelation occurs at intermediate temperatures.

5.4 Properties of the super-glass phase

Having established the phase diagram of the model, we now focus on the properties of the bulk of the "superglass" phase. There the interplay between temperature, glassy order and superfluid order induce several interesting phenomena which potentially survive also in finite dimensional models of frustrated bosons. In the following, we investigate how the glassy and superfluid orders evolve with temperature, and how they are locally correlated.

5.4.1 Competition between glassy and superfluid order

While the effective transverse field $h_i^x = Mt$ is uniform for every site, the frozen longitudinal field, h_i^z depends on the site (and on the pure state in which the system is frozen). Therefore, the magnetization of the local spin s_i due to the local field $\overrightarrow{h_i} = (h_i^x, h_i^z)$ fluctuates from site to site. It is interesting to study the correlation of the local magnetization, whose components are the local order parameters of the glassy and the superfluid order, respectively. More precisely, we investigate the following correlation function:

$$\begin{aligned} C_{M,q_{\rm EA}} &\equiv \frac{\frac{1}{N}\sum_i \langle s_i^x\rangle \langle s_i^z\rangle^2 - (\frac{1}{N}\sum_i \langle s_i^x\rangle)(\frac{1}{N}\sum_i \langle s_i^z\rangle^2)}{(\frac{1}{N}\sum_i \langle s_i^x\rangle)(\frac{1}{N}\sum_i \langle s_i^z\rangle^2)} \\ &= \frac{\int dy P(y) m_x(y) m^2(y) - M q_{\rm EA}}{M q_{\rm EA}}. \end{aligned} \tag{5.85}$$

We have evaluated the correlation function (5.85) within the static 1-step RSB approximation in the center of the superglass phase ($J/t = 0.724$) as a function of temperature ($0.05 < T/t < 0.75$), see Fig. 5.2. Not surprisingly, the correlation is negative, since glassy and superfluid orders compete with each other. Indeed, one easily checks that for every pair of sites (i, j) it holds that if $\langle s_i^z\rangle^2 < \langle s_j^z\rangle^2$ then $\langle s_i^x\rangle > \langle s_j^x\rangle$. The maximal amplitude of the normalized correlation $C_{M,q_{\rm EA}}$ is only of order ≈ 0.1, suggesting that in the superfluid phase the non-uniformity of the two local order parameter fields is actually not very strong. It may be that the 1-step approximation underestimates these correlations a bit. The relative weakness of the anticorrelations might be the reason why they have not been noticed in the quantum Monte Carlo studies of Refs. [39, 40].

5.4.2 Non-monotonicity of the superfluid order

In the superglass phase, the glass order parameter $q_{\rm EA} = Q_1$ monotonously decreases with increasing temperature, as one should expect. However, surprisingly, the superfluid order parameter M exhibits non-monotonic behavior with a maximum at an intermediate crossover temperature T_m, as shown in Fig. 5.3. Below T_m, the superfluid order parameter M decreases, anomalously, when lowering the temperature. Above T_m, M decreases with increasing temperature as usual in a standard superfluid.

This phenomenon is related to the anti-correlation between glassy and superfluid order discussed in the previous section. While on one hand, thermal fluctuations tend

to diminish both glassy and superfluid order, there appears to be a low temperature regime $T < T_m$, where quantum fluctuations of the superfluid order are dominant. Due to the competition between the glassy and the superfluid order, the thermally induced decrease of the glassy order enhances the superfluid order. This effect dominates over the direct thermal effects on the superfluidity.

It seems natural that it is the superfluid order which undergoes such non-monotonic behavior, rather than the glassy order. Indeed, we expect the latter to react less sensitively to the diminution of quantum fluctuations due to decreasing transverse fields

We note that also the local order parameter correlations $C_{M,q_{\rm EA}}$ exhibit a non-monotonous behavior within our static 1-step approximation, as shown in Fig. 5.2. The absolute value of $C_{M,q_{\rm EA}}$ increases with temperature at very low temperatures, and decreases at higher temperatures. This can be seen again as a consequence of the non-monotonicity of the superfluid order. At fixed T, the larger h^x the stronger the normalized anticorrelation $C_{M,q_{\rm EA}}$. Since $h^x = tM$ initially increases with T, it is natural to expect an increasing $C_{M,q_{\rm EA}}$ until eventually thermal fluctuations become dominant and diminish $C_{M,q_{\rm EA}}$.

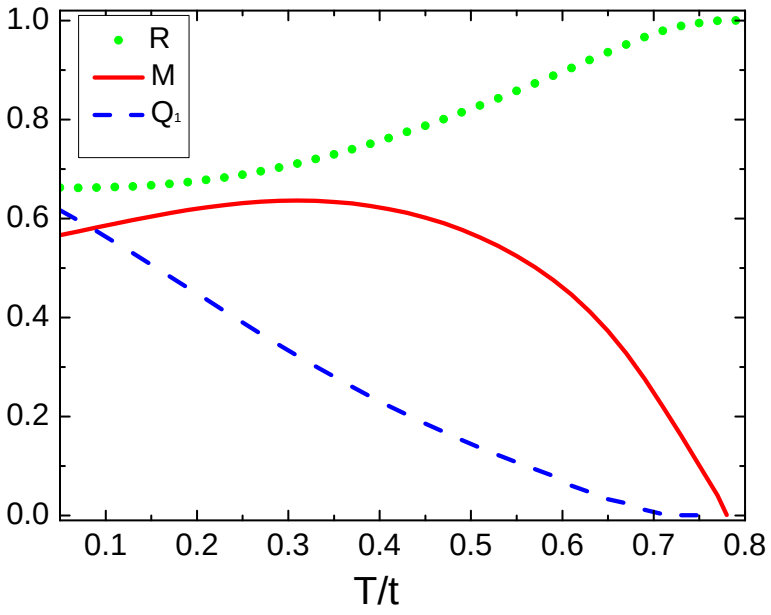

Figure 5.3: (color online) The order parameters in the superglass phase as a function of temperature $0.05 < T/t < 0.79$ at the fixed disorder $J/t = 0.724$. The blue dashed line indicates the Edwards-Anderson order parameter Q_1 (in 1-step approximation), which monotonously decreases with increasing temperature. The superfluid order parameter M (red solid line) exhibits non-monotonic behavior. The long time (static) on-site charge correlation R, (green dotted line) becomes 1 in the disordered high T phase.

5.5 Discussion

In this chapter we have analyzed a fully connected mean field model. The full connectivity is not a real limitation, however. Indeed, one can generalize the model to a highly connected Cayley tree. While this does not affect the thermodynamics of the model, this generalization allows for the study of localization and delocalization of excitations, since this model is endowed with a notion of distance. The analysis of localization properties is of particular interest in the vicinity of the superglass-to-insulating glass quantum phase transition, where the boson system collectively delocalizes into a superfluid at low energies. The nature of higher energy excitations in the insulator are crucially affected by the suppression of low energy states in the glass, leading to a non-trivial excitation spectrum at the glassy SI transition. The details of this analysis will be reported in the next Chapter.

What features of the mean field model should be expected to carry over to finite dimensions? In the present model we find a genuine insulating phase at $T = 0$, which suppresses the superfluidity, due to the strong self-generated on-site disorder within the glassy phase. A crucial ingredient for the suppression of superfluidity is the linear pseudogap within the glass phase. A very similar pseudogap is known to occur in disordered Coulomb interacting systems, where it is due to unscreened $1/r$ interactions between charged particles. This Coulomb gap may well be of importance in strongly disordered superconductors and play a significant role in the competition between glassy insulating behavior and superconductivity. In particular, in materials with strong negative U centers, one may think of preformed electron pairs constituting hard core bosons which interact with Coulomb repulsions [126]. The power law suppression of the low energy density of states makes it likely that the superfluid condensate is entirely destroyed once the hopping becomes too small. For short range interactions the density of states is merely reduced at low energy, but does not tend to zero. On a Cayley tree of very large connectivity this will always lead to delocalization, unless the hopping t is scaled down logarithmically with the connectivity. In finite dimensions, however, sufficiently strong disorder is known to suppress superfluidity [20], and thus one may expect that at sufficiently large ratios J/t, the disordered boson model will localize due to *spontaneously* created, frozen-in local fields. Such a conclusion may be suggestive from a straight extrapolation of the quantum Monte Carlo results of Ref. [39] to $T = 0$, but it seems difficult to exclude a scenario in which T_c becomes merely exponentially small with J/t. A more careful analysis will be necessary to settle this question in finite dimensional, short range interacting glasses.

As for the coexistence phase, the "superglass", the numerical data [39, 40] provides evidence that it exists also in finite dimensions. It would be interesting to confirm and quantify the local anticorrelation of order parameters in such simulations. From our mean field analysis one expects that the anticorrelation is in fact relatively weak. A further non-trivial prediction with measurable consequences is the non-monotonicity of the superfluid order parameter, which should translate into an equivalent non-monotonicity of the superfluid stiffness as a function of temperature. This non-monotonicity has its origin in the softening of the glassy order at low T, a feature which may potentially survive in finite dimensions, especially when the lattice connectivity is large, or the

interactions are not too short ranged. We should caution though that we obtained this effect by employing a static approximation and a replica symmetry breaking at the one-step level only. However, we believe that it is a real feature of the model.

As discussed earlier, a number of experiments have already shown promising indications of possible coexistence of glassy order with superfluidity. We hope that our analysis will help to unambiguously identify such phases in experiments. Note that finding an experimental system exhibiting a glassy superfluid-insulator transition might also be of great interest to study the intricate interplay of interactions and disorder with respect to glassy ergodicity breaking, and quantum ergodicity breaking, i.e. Anderson localization.

Chapter 6

Frustrated Bose glasses and the mobility edge

In this Chapter I focus on the glassy superfluid-insulator (GSI) quantum phase transition of bosons in the presence of frustrating interactions. The transition occurs from an insulating Bose glass to a "superglass" with locally coexisting superfluid and density order. To obtain an exactly solvable limit, I study hard core bosons on a Bethe lattice of high connectivity, with random nearest neighbor interactions, which serves as a guide to interpret finite-dimensional problems with large coordination number. This is an extension of the fully connected model I studied in Chapter V. The reason for extending the fully connected model to a Bethe lattice is to study the transport properties of localized frustrated hard-core bosons. The frustrating interactions in the glass phase have important qualitative effects: The suppression in the density of states impedes the onset of superfluidity up to relatively strong values of the hopping. In the insulating phase, the localized excitations are separated from the delocalized excitations a mobility edge, which does not close upon approaching the GSI quantum critical point. This suggests that the superfluid establishing is not signed by the mobility edge for the single excitation tending down to zero as approaching the critical point but is a collective phase ordering phenomenon at zero temperature. The other interesting finding is that the emerging ordered state is fractal, but rather weak comparing to the non-glassy SI transition.

The phenomena observed in the superglass-to-insulator transition in this mean field limit may serve as good guide for more realistic, Coulomb-frustrated bosonic systems undergoing a transition from a superfluid to a Bose glass state in finite dimensions.

6.1 Model

We consider the situation where the disordered potential is self-generated by random, frustrated density-density interactions between hard-core bosons on nearest neighbors on a half-filled lattice,

$$H = -\sum_{\langle i,j\rangle} 4J_{ij}(n_i - 1/2)(n_j - 1/2) - \frac{t}{K}\sum_{\langle i,j\rangle}\left(b_i^\dagger b_j + b_j^\dagger b_i\right). \tag{6.1}$$

At low T, strong enough interactions induce a glassy, inhomogeneous density pattern $\langle n_i \rangle \neq 1/2$, which breaks the particle hole symmetry and entails an effective disorder potential for a propagating test boson. Here, $b_i(b_i^\dagger)$ are the annihilation (creation) operators for hard-core bosons at site i, and $b_i^\dagger b_i = n_i \in \{0,1\}$ is their occupation number. J_{ij} is a quenched, random interaction taken to be Gaussian distributed with $\overline{J_{ij}} = 0$ and $\overline{J_{ij}^2} = J^2/K$, while t/K is the homogeneous hopping amplitude on the links. We have scaled the couplings with the number K in such a way as to obtain a non-trivial limit when $K \to \infty$. The model (6.1) can be mapped to a $s = 1/2$ pseudo spin model via the standard relations $2n_i - 1 = s_i^z \in \{\pm 1\}, b_i^\dagger = s_i^+$ and $b_i = s_i^-$.

The model (6.1) was studied by Quantum Monte Carlo simulations [39] in 3d, and was found to have three phases at low temperature: an insulating glass phase for large J/t, a non-glassy superfluid phase for small J/t, and an intermediate phase, coined "superglass", which is characterized by the coexistence of both orders: superfluidity ($M \equiv \frac{1}{N}\sum_i \langle s_i^x \rangle > 0$) and glassy density freezing, as captured by the Edwards-Anderson parameter $q_{\rm EA} \equiv \frac{1}{N}\sum_i \langle s_i^z \rangle^2$. Note that they spontaneously break two different symmetries: M breaks the XY symmetry, while q_{EA} breaks the particle-hole symmetry (or spin rotations by π around any axis in the XY plane).

Many aspects of the phase diagram can be better understood analytically in the mean field limit of large connectivity $K \to \infty$. This applies quantitatively in high dimensions, but it also furnishes valuable insight for low dimensions, at the level of a non-trivial, glassy mean field theory [127]. The critical point and the glassy superfluid-to-insulator (SI) transition is analytically tractable because, in the large K limit, the insulating glass turns locally into a classical Sherrington-Kirkpatrick Ising spin glass, with thermodynamically irrelevant quantum fluctuations. Using this fact, one finds that superfluidity at $T = 0$ emerges from the insulating glass at the critical hopping [127]:

$$t_s^\infty \int d\epsilon \, \frac{\rho(\epsilon)}{|\epsilon|} = 1. \tag{6.2}$$

Here, $\rho(\epsilon) \equiv \frac{1}{N}\sum_i \delta(\epsilon - \epsilon_i)$, denotes the density of frozen Hartree fields $\epsilon_i \equiv \sum_{j \in \partial i} J_{ij} \langle s_j^z \rangle$, arising from the non-zero density in the glass phase, ∂i being the set of neighbors of i. The most prominent feature of $\rho(\epsilon)$ is a linear pseudogap [66, 107] at low energies, which extends down to $\epsilon = 0$ at $T = 0$:

$$\rho(|\epsilon| \ll J) \approx c_K + \alpha \frac{|\epsilon|}{J^2}, \tag{6.3}$$

where the constant c_K vanishes as $1/\sqrt{K}$, and $\alpha \approx 0.31$. The exact quantum critical point (the glassy SI transition) is predicted by mean field theory [127] at $t_s^\infty \approx 1.00J$, in remarkably good agreement with the $T \to 0$ extrapolations of the numerical data in 3d [39].

We emphasize an important difference between the above transition, and the case of hard core bosons hopping in a disorder potential with *uniform* distribution $\tilde{\rho}(\epsilon_i)$. While the latter is always superfluid at $T = 0$ in the limit $K \to \infty$ (albeit with exponentially small T_c for small t), the self-generated disorder in the glass is able to

quench superfluidity completely for $t < t_s$, which traces back to the linear vanishing of $\rho(\epsilon \to 0)$ [1] .

In order to analyze the dynamics and/or localization of low energy excitations within the insulating glass phase, it is useful to introduce an effective low energy Hamiltonian which may capture few spin excitations on top of the ground state of model (6.1),

$$H_{eff} = -\sum_i \epsilon_i s_i^z - \frac{t}{K} \sum_{\langle i,j \rangle} \left(s_i^+ s_j^- + s_j^+ s_i^- \right) . \tag{6.4}$$

Here, the interaction term has been approximated via a mean field decoupling, which is justified in the large K limit, apart from the neglect of parametrically suppressed dephasing effects due to fluctuations in ϵ_i. For the same reason we may also neglect correlations among the frozen fields ϵ_i on different sites, approximating them as identically distributed variables with distribution (6.3).

Note that H_{eff} takes the same form as the model introduced by Ma and Lee [20]. This model was recently revisited [52, 29, 28, 128] from the point of view of the dynamics of low energy excitations, and the onset of superfluidity. The analysis of Ref. [51, 128] strongly suggests that for a uniformly distributed disorder, $\tilde{\rho}(\epsilon)$, and half filling, all low energy excitations in the insulating state at $T = 0$ are localized. In particular this implied that superfluidity arises through a delocalization process which is *initiated* at the lowest energies, instead of being brought about by a finite mobility edge in the insulator descending to the chemical potential at the critical point.

The glassy SI transition, is amenable to a similar kind of analysis, with remarkably different phenomenology, however. Even though at first sight the physics seems more intricate and complex in this case, the solution and the emerging phenomena are in fact cleaner, and render the distinction between mobility edges and bosonic condensation clearer. In the following we will analyze in turn the response to a symmetry breaking field at the boundary, i.e., the surface magnetization, and the propagation ([de-]localization) of finite energy excitations. As we will see the two phenomena are physically quite distinct and affected rather differently by the glassy pseudogap. For both calculations we will consider large but finite K. Furthermore, we will neglect the presence of loops in our lattice, which amounts to approximating the lattice as a Cayley tree of connectivity $K \equiv K' + 1$ and depth $L \to \infty$. While this approximation comes with certain unphysical features, such as the exponentially growing number of sites at a given distance, it reveals several interesting features, whose analogs in finite dimension will be pointed out.

6.2 GSI transition

Consider a spin on site 0 (the root of the Cayley tree Λ) and its linear response to an infinitesimal transverse field h_x applied on the boundary spins $l \in \partial\Lambda$. When K

[1] At finite K, the hard core bosons without nearest neighbor interactions undergo a SI transition as well, but at logarithmically smaller hopping, $\tilde{t}_s \sim 1/\log(K)$, which renders the limit $K \to \infty$ more cumbersome.

is large one may linearize the response in the leading order in the XY couplings t/K, and obtains the total surface susceptibility as [29]

$$\chi = \sum_{l \in \partial\Lambda} \prod_{i \in \mathcal{P}_l} \left[\frac{t}{K} \chi_i \right], \tag{6.5}$$

where $\chi_i \equiv \partial \langle s_i^x \rangle / \partial h_{i,x}$ is the local transverse susceptibility [127]. The sum runs over all surface spins l, $\mathcal{P}_i$ being the unique direct path from site 0 to the site l at distance L, and the products are over all sites on $\mathcal{P}_l$. At $T = 0$, $\chi_i = \chi_{\epsilon_i} = 1/|\epsilon_i|$. The sum (6.5) can be interpreted as the partition function of a directed polymer rooted at site 0 and running radially to the surface [28, 29], the exact solution to which has been given by Derrida and Spohn [97]. In the quantum disordered phase, χ decays exponentially as $L \to \infty$. Superfluid order sets in when the *typical* surface susceptibility starts to diverge, i.e., when [97]

$$\begin{aligned} 0 = \lim_{L\to\infty} \frac{1}{L} \overline{\log \chi} &= \min_{x\in[0,1]} \frac{1}{x} \log \left\{ K \overline{\left[\frac{t}{K} \chi_\epsilon \right]^x} \right\} \\ &\equiv \log(t/K) + \min_{x\in[0,1]} f(x). \end{aligned} \tag{6.6}$$

The bar denotes average over $\rho(\epsilon)$, and $f(x)$ is defined as

$$f(x) = \frac{1}{x} \log \left[K \int d\epsilon\, \rho(\epsilon) \chi_\epsilon^x \right] = \frac{1}{x} \log \left[K \int d\epsilon\, \frac{\rho(\epsilon)}{|\epsilon|^x} \right].$$

For $K \to \infty$, the minimum is assumed at $x_c \to 1$, and one readily retrieves the condition (6.2). At finite K, using the form (6.3) for the local field distribution, one finds that the minimum is assumed at

$$x_c = 1 - O(K^{-1/4} \log^{-1/2} K), \tag{6.7}$$

concomitant with a tiny decrease in t_s. The value of x_c has the following important physical significance: $1 - x_c$ is the weight of the most favorable path [2] contributing to χ. $1/(1 - x_c)$ can be taken as an estimate of the number of macroscopically different paths that actually contribute to the susceptibility. $x_c < 1$ implies that the response is dominated by a few paths only, despite the exponential number of boundary sites. This phenomenon is referred to as freezing (or replica symmetry breaking) in the context of directed polymers. In the present context it signals that the emerging condensate is concentrated on an extremely small subset of the available lattice [29, 28]. In finite dimensions, the analog of this phenomenon is to be sought in the *fractality* of the emerging condensate. The latter is indeed to be expected as the phase transition is known to be a kind of percolation phenomenon [98].

It is very interesting to compare these results with the case of uniform disorder as considered in Refs. [28, 29, 128]. In that case, one finds $1/(1 - x_c) \sim \log K$ at the

[2] See Ref. [97]. More precisely it is the contribution of a bunch of paths with mutual "overlap" that tends to 1 in the thermodynamic limit.

critical point, which is parametrically smaller than the $1/(1-x_c) \sim K^{1/4}\log^{1/2} K$ in the case of a pseudogapped $\rho(\epsilon)$. This has a natural interpretation. The concentration of disordered wavefunctions on a small number of paths, which was already noticed in Anderson's seminal paper on localization [1], is a result of resonances, i.e., small denominators in products like in (6.5). A pseudogap in the distribution of local energies reduces the probability for such resonances for the establishment of phase coherence at zero frequency. On the Cayley tree this is reflected by the enhanced value of $1/(1-x_c)$. In finite dimensions, we expect instead a decreased tendency to concentrate on highly optimized paths, and thus we conjecture that the emerging condensate to have an increased fractal dimension as compared to a non-glassy SI transition. It is worthwhile to point out that if $\rho(\epsilon \to 0)$ vanished exactly, as it happens in systems with long range Coulomb interactions, the same approximations as above would yield $x_c = 1$, suppressing the concentration on paths even more strongly than the rounded pseudogap (6.3). However, we should also caution that the above analysis relies on the leading approximation in the hopping, while close to the transition subleading corrections become important, and could modify (in fact, increase) the effective number of paths that contribute to the χ. However, we believe that the qualitative conclusion, that a pseudogap tends to decrease the fractality, will remain unchanged.

6.3 Localization of excitations in the glassy insulator

Let us now turn our attention to transport properties in the insulating phase, $t < t_s$, and examine the relation between condensate formation and delocalization of excitations. Consider a spin flip (boson insertion) on site 0 and let us determine whether such a local excitation of finite energy can propagate to the boundary or remains localized. The answer depends in fact on the injected energy. Indeed at higher energies there exist many sites with similar frozen fields, which can hybridize with each other via the hopping term. In contrast, at low energies such hybridizations are suppressed by the pseudogap, which we will show to localize low energy excitations. Accordingly, there must be a mobility edge, which separates the low energy localized spectrum from the continuum at higher energies.

Excitations are delocalized if they can decay due to an infinitesimal coupling to a bath coupled to the boundary of the system. On a Cayley tree, to leading order in the parametrically small hopping t/K, the possible decay channels are given by the shortest paths connecting the site 0 to boundary sites. Since in these leading order processes no bosons are exchanged, their quantum statistics does not matter [**?**] and the problem becomes identical to a (fermionic) single particle delocalization on the Cayley tree, which was solved in Ref. [60] The decay rate of a local excitation on site 0 back to the ground state is given by Fermi's golden rule [128]

$$\Gamma(\omega) = \sum_{l\in\partial\Lambda} \prod_{i\in\mathcal{P}_l} \left[\frac{t/K}{\epsilon_i - \omega/2}\right]^2 J(\omega), \tag{6.8}$$

where $\omega = 2\epsilon_0$ is the energy of the excitation, and $J(\omega)$ is the spectral function of the baths coupling to the individual boundary spins. In complete analogy to (6.5), one

finds the typical decay rate

$$\gamma(\omega) \equiv \lim_{L\to\infty} \frac{1}{L}\overline{\log \Gamma(\omega)} = \log(t/K) + \min_{x\in[0,1]} f_\omega(x), \tag{6.9}$$

where the function $f_\omega(x)$ is given by

$$f_\omega(x) = \frac{1}{2x}\log\left[K\int \frac{\rho_\Delta(\epsilon)}{|\,\epsilon-\omega/2\,|^{2x}}d\epsilon\right]. \tag{6.10}$$

The notation ρ_Δ indicates that, following Anderson's prescription [1], resonant energies with $|\epsilon_i - \omega/2| < \Delta \sim K^{-2}$ should be excluded from the integral [3] . Indeed, these small denominators are compensated by anomalously large self-energy correction on the next site on the path.

Delocalization of excitations at energy ω occurs when $\gamma(\omega_c) = 0$, which defines the mobility edge $\omega_c(t)$. It is determined by the two conditions

$$1 = K\left(\frac{t}{K}\right)^{2x}\int \frac{\rho_\Delta(\epsilon)}{|\epsilon-\omega/2|^{2x}}d\epsilon, \tag{6.11}$$

$$\log\left(\frac{t}{K}\right) = \frac{\int \frac{\rho_\Delta(\epsilon)}{|\epsilon-\omega/2|^{2x}}\log(|\epsilon-\omega/2|)d\epsilon}{\int \frac{\rho_\Delta(\epsilon)}{|\epsilon-\omega/2|^{2x}}d\epsilon}. \tag{6.12}$$

In the large K limit one finds that the mobility edge scales like $\omega_c = 2\hat{\omega}/\log K$ and f_ω assumes its minimum at $x_c = 1/2 + z/\log K$ ($z = (2x-1)\log K$).

For the density of states $\rho(\epsilon)$ which satisfies that $\rho(\epsilon \ll J) \sim \alpha|\epsilon|/J^2$ and $\rho(\epsilon \gg J) \to 0$, with these rescalings the $K\to\infty$ limit of Eq. (6.11) turns into

$$1 \;=\; te^{-z}\left[\int d\epsilon\frac{\rho(\epsilon)}{|\epsilon|} + \frac{2\alpha}{J^2}\frac{\hat{\omega}}{z}(e^{2z}-1)\right] \tag{6.13}$$

or, upon using (6.2),

$$\frac{t_s^\infty}{t} = e^{-z} + \frac{4\alpha t_s^\infty\hat{\omega}}{J^2}\frac{\sinh(z)}{z}. \tag{6.14}$$

The minimum condition (6.12) translates into

$$\frac{t_s^\infty}{t} = \frac{4\alpha t_s^\infty\hat{\omega}}{J^2}\left(\frac{e^z}{z} - \frac{\sinh(z)}{z}\right). \tag{6.15}$$

Eqs. (6.14,6.15) determine $\hat{\omega}$ and z. At the SI transition where $t/t_s^\infty \to 1$, we find the explicit solution $z = 1.2785$ as the root of $z = 1 + e^{-z}$, while

$$\omega_c = \frac{2\hat{\omega}}{\log K} = \frac{(z-1)J^2}{\alpha t_s^\infty\,\log K} \approx \frac{z-1}{\alpha\,\log K}J. \tag{6.16}$$

[3] The proportionality factor c in $\Delta = c/K^2$ plays no role in the our asymptotic analysis $K\to\infty$.

Notice that the above equations do not depend on the details of $\rho(\epsilon)$ at small or large energies, but only on its linear slope α.

We thus come to the conclusion that a finite, if parametrically small, mobility edge $\omega_c \sim 1/\log(K)$ exists on the insulating side. Even though the hopping is irrelevant for thermodynamic properties, it does allow for the propagation of excitations above ω_c. The most striking aspect of our analysis, however, is that the mobility edge does not vanish upon approaching the SI transition $t \to t_s^\infty$, instead it tends to the finite value (6.16), implying a finite interval of discrete spectrum anywhere in the insulator. However, those excitations all acquire a finite life time simultaneously, once the system becomes superfluid and the delocalized Goldstone modes at lowest energies provide a bath for decay processes of higher energy excitations.

The presence of a finite, and rather low mobility edge of the frustrated bosonic system differs from the problem without glassy interactions, where controllable calculations so far could not indicate the delocalization of finite energy excitations at $T = 0$ [128]. In practice, frustrating interactions are of course to be expected. In particular, Coulomb interactions among charged bosons will lead to an Efros-Shklovskii Coulomb gap in the distribution of local potentials, which is expected to have similar qualitative effects as the pseudogap analyze in the large connectivity limit of short range interacting glasses here, namely: the increase of the fractal dimension of the inhomogeneous condensate in emerging charged superfluids, and the presence of a (low lying) mobility edge close to the chemical potential. The presence of such an intensive mobility edge implies that the glassy insulator adjacent to the superglass exhibits finite transport at all positive temperatures, even in the absence of a phonon bath. Indeed, the delocalized modes above ω_c have a finite probability of being occupied and may conduct charge either by themselves, or in case they are neutral, may serve as a weak, but finite bath which provides the necessary level broadening to allow for transitions between otherwise localized excitations, or by conducting. Both transport channels would be simply activated with an exponential factor containing the activation energy to the mobility edge (in the limit $T \to 0$). This may be a possible scenario for the activated transport which is often observed close to bosonic SI-transitions [53, 129, 52].

In conclusion, we have presented the solution of a hard-core boson model with strongly disordered frustrated density-density interactions on the Bethe lattice. We found that the glassy order shifts the SI transition at zero temperature, and reduces the sparseness of the emerging condensate. In the insulating phase, we found a finite mobility edge for excitations, which tends to a finite value at the SI transition. This shows that in general the superfluid transition should not be thought of as a condensation into modes at a pre-existing mobility edge, which dives down to zero at the transition, in contrast to similar scenario discussed in the literature [29, 52]. Instead the superfluid emerges as a collective phase ordering phenomenon at the chemical potential, which turns out to be rather distinct from a single particle delocalization phenomenon.

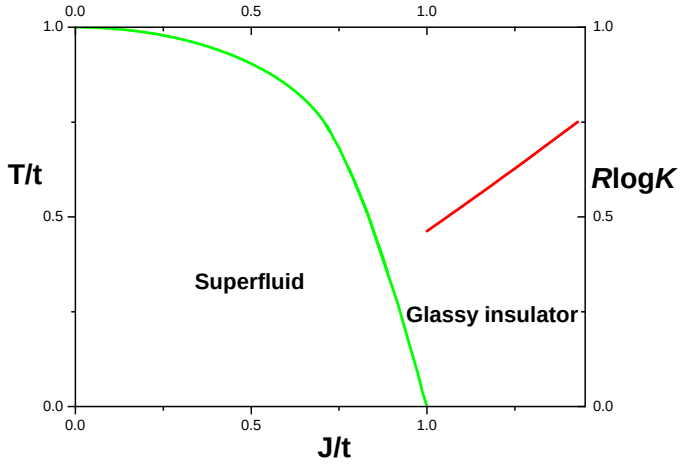

Figure 6.1: The green line shows the SI transition line. The red line is the mobility edge which separates the localized states (below) and the delocalized states (above). The mobility edge is located at parametrically small energies, $R = \omega_c \sim 1/\log K$.

Chapter 7

Conclusion

In this thesis I focus on the disorder-induced superfluid-insulator quantum phase transition, glassy insulators, and transport properties of localized interacting systems. My PhD work deals with superglasses, the superfluid-insulator transition and how it is affected by glassiness, as well as with transport properties of glassy insulators.

Here I summarize the main results I have obtained:

1) For a model of non-frustrated disordered hard-core bosons on a Cayley tree with large connectivity, I found that with a uniformly distributed disorder the excitations in the disordered phase (insulating phase) are all localized and there is no a boson mobility edge in the Bose glass.

2) For a fully connected model of random frustrated hard core bosons, I proved the existence of a superglass phase. I pointed out anticorrelations between the local order parameters, and a non-monotonicity of the superfluid order parameter as a function of temperature.

3) By extending this fully connected model to a Bethe lattice with finite but large connectivity, I was able to study the transport properties of a glassy bosonic insulator. I found that the glassy superfluid-insulator transition is significantly shifted to larger hopping due to the pseudo gap in the density of states of the glass state. Further I established that the glassy insulator has a finite mobility edge for bosonic excitations, which however not close upon approaching the SI transition point. Instead I found that the bosonic condensate emerges due to a collective delocalization at zero energy, which is unrelated to the delocalized modes that exist above the mobility edge in the insulator.

These results were obtained relying on large connectivity as a control parameter, where mean field theory (for the glass state) and a leading order approximation in the hopping (for transport) make an analytical study possible.

It is of course very important to understand how this connects to the physics in realistic, finite dimensional systems.

One aspect of realistic finite-dimensional systems is the presence of Coulomb interactions, which cannot be fully screened in insulators, and thus play a crucial role. The Coulomb interactions between localized carriers (electrons or pairs) are known to

create a Coulomb gap in the density of states, analogous to the pseudogap we discussed for frustrated bosons with short range interactions at large connectivity. It is natural to expect that the Coulomb gap may have similar physical effects on the physics of the insulator. For example, due to its suppression of the low-energy density of states, I expect that high energy excitations should be more delocalized than lower energy excitations. In dimensions $d \geq 3$ I therefore expect a mobility in the excitation spectrum of interacting systems, which tracks the chemical potential rather closely - a phenomenon which may have been observed in recent tunneling experiments on doped semiconductor systems close to the metal-insulator transition [130].

Another very interesting and challenging problem is to investigate the transport behavior near the SI quantum critical point, where the description in terms of elementary excitations breaks down and one has to take into account strong many body effects. many issues are still open: How does the bosonic statistics manifest itself at the SI transition (as opposed to a fermionic metal-insulator (MI) transition)? How does the Coulomb gap affect the nature of such delocalization transitions? Under which circumstances are there mobility edges in bosonic systems? Does it never happen that a bosonic delocalization transition is induced by a mobility edge touching the chemical potential upon approaching the critical point? A first step in this direction may consist in extending the bosonic locator expansion [51] and developing a systematic way to compute self-energy and other subleading corrections. This should shed more light on some of the questions I could not fully resolve within the approximations that restricted my analysis of localization properties to the leading order in hopping.

Bibliography

[1] P. W. Anderson, Phys. Rev. **109**, 1492 (1958).

[2] D. J. Thouless, Phys. Rep. C **13**, 93 (1974).

[3] Kramer, B., and A. MacKinnon, Rep. Prog. Phys. **56**, 1469 (1993).

[4] F. Evers and A. D. Mirlin, Rev. Mod. Phys. **80**, 1355 (2008).

[5] I. V. Gornyi, A. D. Mirlin, and D. G. Polyakov, Phys. Rev. Lett. **95**, 206603 (2005).

[6] D. M. Basko, I. L. Aleiner, and B. L. Altshuler, Ann. Phys. **321**, 1126 (2006).

[7] T. Giamarchi and H. J. Schulz, Phys. Rev. B **37**, 325 (1988).

[8] M. P. A. Fisher, P. B. Weichman, G. Grinstein, and D. S. Fisher, Phys. Rev. B **40**, 546 (1989).

[9] A. F. Hebard and M. A. Paalanen, Phys. Rev. Lett. **65**, 927 (1990); M. A. Paalanen, A. F. Hebard, and R. R. Ruel, Phys. Rev. Lett. **69**, 1604 (1992).

[10] B. Damski, J. Zakrzewski, L. Santos, P. Zoller, and M. Lewenstein, Phys. Rev. Lett. **91**, 080403 (2003).

[11] B. Deissler, M. Zaccanti, G. Roati, C. D'Errico, M. Fattori, M. Modugno, G. Modugno, and M. Inguscio, Nature Physics **6**, 354 - 358 (2010)

[12] B. Allard, T. Plisson, M. Holzmann, G. Salomon, A. Aspect, P. Bouyer, and T. Bourdel, Physical Review A **85** 033602 (2012).

[13] T. Giamarchi, Ch. Rüegg, and O. Tchernyshyov, Nat. Phys. **4**, 198 (2008).

[14] T. Nattermann and V. L. Pokrovsky, Phys. Rev. Lett. **100**, 060402 (2008).

[15] G. Roux, T. Barthel, I. P. McCulloch, C. Kollath, U. Schollwöck, and T. Giamarchi, Phys. Rev. A **78**, 023628 (2008).

[16] B. I. Shklovskii, Phys. Rev. B **76**, 224511 (2007).

[17] M. Mueller and B. I. Shklovskii, Phys. Rev. B **79**, 134504 (2009).

[18] P. Lugan, D. Clément, P. Bouyer, A. Aspect, M. Lewenstein, and L. Sanchez-Palencia, Phys. Rev. Lett. **98**, 170403 (2007).

[19] Anderson, P. W., J. Phys. Chem. Solids 11, **26** (1959).

[20] M. Ma and P. A. Lee, Phys. Rev. B **32**, 5658 (1985). M. Ma, B. I. Halperin, and P. A. Lee, Phys. Rev. B **34**, 3136 (1986).

[21] A. Goldman and N. Markovic, Phys. Today **51**, 39 (1998).

[22] Cao Lie-zhao, D. F. Brewer, C. Girit, E. N. Smith and J. D. Reppy, Phys. Rev. B **33**, 106 (1986).

[23] E. Kim and M. H. W. Chan, Science **305**, 1941 (2004). E. Kim and M. H. W. Chan, Nature **427**, 225 (2004).

[24] B. Hunt, E. Pratt, V. Gadagkar, M. Yamashita, A. V. Balatsky, and J. C. Davis, Science **324**, 632 (2009).

[25] V. Gurarie, L. Pollet, N. V. Prokof'ev, B. V. Svistunov, and M. Troyer, Phys. Rev. B **80**, 214519 (2009).

[26] Hertz, J. A., L. Fleishman, and P. W. Anderson, Phys. Rev. Lett. **43**, 942 (1979).

[27] V. Gurarie and J. T. Chalker, Phys. Rev. B **68**, 134207 (2003).

[28] M. V. Feigel'man, L. B. Ioffe, and M. Mézard, Phys. Rev. B **82**, 184534 (2010).

[29] L. B. Ioffe and M. Mézard, Phys. Rev. Lett. **105**, 037001 (2010).

[30] AnnSophieC.Rittner, J. D. Reppy, Phys. Rev. Lett. **97**, 165301 (2006).

[31] S. Balibar and F. Caupin, Journal of Physics: Condensed Matter **20**, 173201 (2008).

[32] M. Boninsegni, N. Prokof'ev, and B. Svistunov, Phys. Rev. Lett. **96**, 105301 (2006).

[33] B. Svistunov, Physica B **404**, 521 (2009).

[34] L. Dang, M. Boninsegni, and L. Pollet, Phys. Rev. B **79**, 214529 (2009).

[35] J. West, O. Syshchenko, J. Beamish, and M. H. W. Chan, Nature Phys. **5**, 598 (2009).

[36] B. Hunt, E. Pratt, V. Gadagkar, M. Yamashita, A. V. Balatsky, and J. C. Davis, Science **324**, 632 (2009).

[37] G. Biroli, C. Chamon, F. Zamponi, Phys. Rev. B **78**, 224306 (2008).

[38] G. Biroli, B. Clark, L. Foini, and F. Zamponi, Phys. Rev. B **83**, 094530 (2011).

[39] K. M. Tam, S. Geraedts, S. Inglis, M. J. P. Gingras, and R. G. Melko, Phys. Rev. Lett. **104**, 215301 (2010).

[40] G. Carleo, M. Tarzia, F. Zamponi, Phys. Rev. Lett. **103**, 215302 (2009).

[41] L. Foini, G. Semerjian, and F. Zamponi Phys. Rev. B **83**, 094513 (2011).

[42] D. Larson, Ying-Jer Kao arXiv:1202.3908 (2012).

[43] Markus Müller, Philipp Strack, and Subir Sachdev, Phys. Rev. A **86**, 023604 (2012).

[44] V. Dobrosavljević, D. Tanasković, and A. A. Pastor, Phys. Rev. Lett. **90**, 016402 (2003).

[45] W. Krauth, N. Trivedi, and D. Ceperley, Phys. Rev. Lett. **67**, 2307 (1991).

[46] J. H. Davies, P. A. Lee, T. M. Rice, Phys. Rev. Lett. **49**, 758 (1982).

[47] S. Pankov and V. Dobrosavljević, Phys. Rev. Lett. **94**, 046402 (2005).

[48] M. Müller and L. B. Ioffe, Phys. Rev. Lett. **93**, 256403 (2004).

[49] B. Deissler et al., Nature Physics **6**, 354 (2010).

[50] A. Leggett, Phys. Rev. Lett. **25**, 1543 (1970); G. Chester, Phys. Rev. A **2**, 256 (1970); A. F. Andreev and I. M. Lifshitz, Zh. Eksp. Teor. Fiz. **56**, 2057 (1969) [Sov. Phys. JETP **29**, 1107 (1969)]; H. Matsuda and T. Tsuneto, Prog. Theor. Phys. Suppl. **46**, 411 (1970).

[51] M. Müller, arXiv:1109.0245 (2011).

[52] M. Müller, Ann. Phys.(Berlin) **18**, 849 (2009).

[53] G. Sambandamurthy, L. W. Engel, A, Johansson, and D. Shahar, Phys. Rev. Lett. **92**, 107005 (2004).

[54] Imry, Y., 1996, Introduction to Mesoscopic Physics (Oxford University, London).

[55] A. L. Efros and B. I. Shklovskii, J. Phys. C: Solid State Phys. **8**, L49 (1975).

[56] E. Feenberg, Phys. Rev. **74**, 206 (1948).

[57] K. M. Watson, Phys. Rev. **105**, 1388 (1957).

[58] D. J. Thouless, J. Phys. C **3**, 1559 (1970).

[59] Notes on a course on Probability theory, M. Marsili, (2008).

[60] Abou-Chacra, R., P. W. Anderson, and D. J. Thouless, J. Phys. C **6**, 1734 (1973).

[61] Fischer, K. H., and J. A. Hertz, 1991, Spin Glasses (Cambridge University, Cambridge, England).

[62] K. Binder, and A. P. Young, Rev. Mod. Phys. **58**, 801-976 (1986).

[63] D. Sherrington and S. Kirkpatrick, Phys. Rev. Lett. **35**, 1792-1796 (1975).

[64] F. Zamponi, arXiv:1008.4844.

[65] B. Derrida, Phys. Rev. Lett. **45**, 79-82 (1980).

[66] D. J. Thouless, P. W. Anderson, and R. G. Palmer, Philos. Mag. **35**, 593 (1977).

[67] A. Georges and J. S. Yedidia, Journal of Physics A: Mathematical and General 24, 2173 (1991).

[68] A. J. Bray and M. A. Moore, Metastable states in spin glasses, J. Phys. C: Solid St. Phys. **13** (1980) L469.

[69] R. G. Palmer and C. M. Pond, J. Phys. F **9**, 1451 (1979).

[70] A. J. Bray and M. A. Moore J. Phys. C: Solid State Phys. **12** L441 (1979).

[71] M. Mézard, G. Parisi, and M. A. Virasoro, Spin-Glass Theory and Beyond, Lecture Notes in Physics Vol. 9 (World Scientific, Singapore, 1987).

[72] S. Pankov, Phys. Rev. Lett. **96**, 197204 (2006).

[73] K. Slevin and T. Ohtsuki, Phys. Rev. Lett. **82** (1999) 382

[74] M. V. Feigel'man, L. B. Ioffe, V. E. Kravtsov, and E. A. Yuzbashyan, Phys. Rev. Lett. **98**, 027001 (2007). M. V. Feigelman, L. B. Ioffe, V. E. Kravtsov, and E. Cuevas, Annals of Physics **325**, 1368 (2010).

[75] I. S. Burmistrov, I. V. Gornyi, and A. D. Mirlin, Phys. Rev. Lett. **108**, 017002 (2012).

[76] P. Lugan, D. Clément, P. Bouyer, A. Aspect, M. Lewenstein, and L. Sanchez-Palencia, Phys. Rev. Lett. **98**, 170403 (2007).

[77] G. M. Falco, T. Nattermann, and V. L. Pokrovsky, Phys. Rev. B **80**, 104515 (2009).

[78] E. Altman, A. Polkovnikov, G. Refael, and Y. Kafri, Phys. Rev. Lett. **93**, 150402 (2004).

[79] E. Altman, Y. Kafri, A. Polkovnikov, and G. Refael, Phys. Rev. B **81**, 174528 (2010).

[80] I. L. Aleiner, B. L. Altshuler and G. V. Shlyapnikov, Nature Physics **6**, 900-904 (2010).

[81] M. Makivić, N. Trivedi, and S. Ullah, Phys. Rev. Lett. **71**, 2307 (1993).

[82] V. Gurarie, L. Pollet, N. V. Prokof'ev, B. V. Svistunov, and M. Troyer, Phys. Rev. B **80**, 214519 (2009)

[83] V. Bapst and M. Müller, in preparation.

[84] R. Shankar and G. Murthy, Phys. Rev. B **36**, 536 (1987).

[85] D. S. Fisher, Phys. Rev. B **51**, 6411 (1995).

[86] L. Balents and M. P. A. Fisher, Phys. Rev. B **56**, 12970 (1997).

[87] T. Giamarchi, Quantum Physics in One Dimension (Oxford University, Oxford, 2004).

[88] M. Zirnbauer, J. Math. Phys. **37**, 4986 (1996).

[89] T. P. Eggarter and R. Riedinger, Phys. Rev. B **18**, 569 (1978).

[90] J. P. Bouchaud, A. Comtet, A. Georges and P. Le Doussal, Ann. Phys. (N.Y.) **201** 285 (1990).

[91] A. Comtet, J. Desbois, and C. Monthus, Ann. Phys. **239** 312 (1995).

[92] F. J. Dyson, Phys. Rev. **92**, 1331 (1953).

[93] A. Gangopadhyay, V. Galitski, M. Müller, arXiv:1210.3726 (2012).

[94] J. A. Hertz, L. Fleishman, and P. W. Anderson, Phys. Rev. Lett. **43**, 942 (1979).

[95] C. Monthus, T. Garel, J. Stat. Mech. (2012) P09016.

[96] G. Lemarié, A. Kamlapure, D. Bucheli, L. Benfatto, J. Lorenzana, G. Seibold, S. C. Ganguli, P. Raychaudhuri, and C. Castellani, arXiv:1208.3336 (2012).

[97] B. Derrida and H. Spohn, J. Stat. Phys. **51**, 817 (1988).

[98] O. Motrunich, S-C Mau, D. A. Huse, and D. S. Fisher, Phys. Rev. B **61**, 1160 (2000).

[99] I. A. KovÂńacs and F. IglÂńoi, Phys. Rev. B **82**, 054437 (2010).

[100] I. A. KovÂńacs and F. IglÂńoi, Phys. Rev. B **83**, 174207 (2011).

[101] T. Vojta, J. Phys. A **39**, R143 (2006).

[102] X. Yu and M. Müller, in preparation.

[103] A. A. Pastor and V. Dobrosavljević, Phys. Rev. Lett. **83**, 4642 (1999).

[104] D. Dalidovich and V. Dobrosavljević, Phys. Rev. B **66**, 081107 (2002).

[105] A.J. Bray and M.A. Moore, *J. Phys. C.: Solid St. Phys.*, **13** (1980), L655-60.

[106] A. Georges, G. Kotliar, W. Krauth, and M. Rozenberg, Rev. Mod. Phys. **68**, 13 (1996).

[107] H.-J. Sommers and W. Dupont, J. Phys, C **17**, 5785 (1984).

[108] B. Duplantier J. Phys. A: Math. Gen. **14**, 283 (1981).

[109] G. Parisi and G. Toulouse, J. Phys. (Paris), Lett. **41**, L361 (1980).

[110] A. Crisanti, T. Rizzo, Phys. Rev. E **65**, 046137 (2002)

[111] M. Müller, and S. Pankov, Phys. Rev. B **75**, 144201 (2007).

[112] A. Andreanov and M. Müller, Phys. Rev. Lett. **109**, 177201 (2012).

[113] G. Biroli and L. F. Cugliandolo, Phys. Rev. B **64**, 014206 (2001).

[114] T. Giamarchi, P. Le Doussal, Phys. Rev. B **52**, 1242-1270 (1995)

[115] M. Mézard, G. Parisi, and M. A. Virasoro, Europhys. Lett. **1**, 77 (1986).

[116] M. Thomsen, M. F. Thorpe, T. C. Choy, D. Sherrington, and H.-J. Sommers, Phys. Rev. B **33**, 1931 (1986).

[117] G. Büttner and K. D. Usadel, Phys. Rev. B **42**, 6385 (1990).

[118] J. Miller and D. A. Huse, Phys. Rev. Lett. **70**, 3147 (1993).

[119] M. J. Rozenberg and D. R. Grempel, Phys. Rev. Lett. **81**, 2550 (1998).

[120] D. J. Thouless, P. W. Anderson, and R. G. Palmer, Phil. Mag. **35**, 593 (1977).

[121] R. G. Palmer and C. M. Pond J. Phys. F: Met. Phys. **9**, 1451 (1979).

[122] A. Crisanti, L. Leuzzi, G. Parisi, T. Rizzo, Phys. Rev. B **70**, 064423 (2004).

[123] The notion of delocalization requires a straightforward extension of the present model to a lattice model, which is not fully connected but maintains a large coordination number N.

[124] X. Yu and M. Müller in preparation.

[125] K. Binder and A. P. Young, Rev. Mod. Phys. **58**, 801 (1986).

[126] J. Mitchell, A. Gangopadhyay, V. Galitski, and M. Müller, arXiv:1110.0074 (2011).

[127] X.Yu and M. Müller, Phys. Rev. B **85**, 104205 (2012).

[128] X.Yu and M. Müller, in preparation.

[129] M. D. Stewart, A. Yin, J. M. Xu, and J. M. Valles, Science **318**, 5854 (2007). H. Q. Nguyen et al., Phys. Rev. Lett. **103**, 157001 (2009).

[130] A. Richardella, P. Roushan, S. Mack, B. Zhou, D. A. Huse, D. D. Awschalom, and A. Yazdani, Science 327, 665 (2010).